

# **Green Motorway Vehicular Networks**

Adnan Muhtar

Submitted in accordance with the requirements for the degree of  
Doctor of Philosophy

The University of Leeds  
School of Electronic and Electrical Engineering  
September 2013

The candidate confirms that the work submitted is his/her own, except where work which has formed part of jointly-authored publications has been included. The contribution of the candidate and the other authors to this work has been explicitly indicated below. The candidate confirms that appropriate credit has been given within the thesis where reference has been made to the work of others.

This copy has been supplied on the understanding that it is copyright material and that no quotation from the thesis may be published without proper acknowledgement.

## Acknowledgments

I take this opportunity to express my gratitude to the people who have been instrumental in the successful completion of this thesis. I would like to show my sincere gratitude to my supervisor, Prof. Jaafar Elmirghani for his patience, motivation and immense knowledge. Without his vision, guidance and support, this thesis would not have materialized.

I am also thankful to Dr. Bilal Qazi and Dr. Samya Bhattacharya for their continuous support and guidance

I would also like to thank my parents, who have always supported, encouraged and believed in me.

Finally, I would like to thank my wife, Fatima Babaji for her love, kindness, support and great patience at all times.

## Abstract

The information age has pushed the requirement of data transfer to a vehicular frontier whereby the safety and comfort of drivers can significantly be enhanced by time critical communications in rural and urban areas. Safety along with the growing reliance on infotainment is driving the development of a dedicated vehicular network that spans an all-encompassing coverage area. Where safety critical and multimedia applications urge for stringent network requirements, the vehicular environment has posed several obstacles to researchers in meeting those demands. This burden is compounded by growing environmental concerns that have compelled the greening of information and communication technologies including vehicular communication networks.

As maintaining quality of service (QoS) for the intended applications is hindered by the dynamic nature of the vehicular environment, innovative protocols and architectures need to be devised and systematically analysed to meet the requirements. Furthermore gains in energy efficiency tend to be achieved by limiting equipment operation, and hence QoS performance. An optimal balance is therefore required to maximise energy savings with bounds on QoS. Furthermore renewable energy solutions provide a green and more flexible alternative power source but their variable nature must be studied to ensure they meet QoS requirements. Finally, with the

impracticality and expense of field tests the methodology of accurately studying vehicular networks presents a problem on its own.

This thesis designs studies and attempts to improve the QoS and energy performance of a motorway vehicular network by taking account of realistic traffic flows, packet sizes, physical layer characteristics, and wind speeds. The performance of routing protocols such as most forward and shortest hop schemes has been studied and optimised. A number of optimal hop lengths have been determined. Medium access protocols (MAC) such as fixed and dynamic channel allocation, 802.11p and the modified packet reservation protocols have been analysed. A novel micro/macro network architecture has been proposed to enhance energy efficiency by enabling sleep cycles and renewable energy use in road side units. Finally the reliability of wind renewable energy has been investigated.

## Table of contents

ACKNOWLEDGMENTS .....	I
ABSTRACT .....	II
TABLE OF CONTENTS .....	IV
LIST OF TABLES.....	VIII
LIST OF FIGURES.....	IX
LIST OF ABBREVIATIONS.....	XI
LIST OF SYMBOLS .....	XV
<b>1 INTRODUCTION.....</b>	<b>1</b>
1.1 RESEARCH OBJECTIVES.....	7
1.2 RESEARCH CONTRIBUTIONS .....	7
1.3 THESIS OVERVIEW.....	9
<b>2 VEHICULAR COMMUNICATION NETWORKS.....</b>	<b>11</b>
2.1 INTRODUCTION.....	11
2.2 APPLICATIONS.....	11
2.2.1 <i>Safety</i> .....	12
2.2.2 <i>Traffic Monitoring and Management</i> .....	14
2.2.3 <i>Infotainment</i> .....	15
2.3 NETWORK DESIGN CHALLENGES .....	15
2.4 VEHICULAR NETWORK ENVIRONMENTS.....	16
2.5 VEHICULAR NETWORK TECHNOLOGIES AND STANDARDS.....	17
2.5.1 <i>DSRC</i> .....	17
2.5.2 <i>Wireless Access in Vehicular Environment (WAVE)</i> .....	17
2.6 MEDIUM ACCESS CONTROL (MAC) PROTOCOLS .....	19

# Introduction

---

2.6.1 <i>Distributed versus Centralised Architectures</i> .....	20
2.6.2 <i>CSMA/CA</i> .....	21
2.6.3 <i>Reservation and Scheduling</i> .....	22
2.6.4 <i>Multiple Channel</i> .....	23
2.6.5 <i>Directional Antennas</i> .....	24
2.7     QUEUEING THEORY ANALYSIS.....	27
2.8     ENERGY EFFICIENCY IN VEHICULAR NETWORKS .....	28
2.8.1 <i>Energy Efficient MAC protocols</i> .....	29
2.8.2 <i>Energy Efficient Routing</i> .....	30
2.8.3 <i>Energy Saving in Road Side Units</i> .....	33
2.9     RENEWABLE ENERGY .....	36
2.10    GREEN NETWORK RELIABILITY .....	39
2.11    SIMULATING VEHICULAR COMMUNICATION NETWORKS.....	42
2.11.1 <i>Mobility Modeling</i> .....	43
2.11.2 <i>Motorway Vehicular Mobility Model and Simulation</i> .....	46
2.11.2.1. <i>Vehicular Traffic Traces</i> .....	47
2.11.2.2. <i>Vehicular Traffic Simulation</i> .....	53
2.12    SUMMARY.....	54
<b>3     ENERGY EFFICIENT ROUTING.....</b>	<b>55</b>
3.1    INTRODUCTION.....	55
3.2    PROPOSED SCENARIO .....	56
3.3    ENERGY MODEL .....	57
3.4    SIMULATION OF SHORTEST AND MOST FORWARD HOP SCHEMES .....	58
3.5    LINEAR PROGRAMMING OPTIMISATION MODEL .....	59
3.6    PERFORMANCE EVALUATION.....	61
3.7    ROUTE CONNECTIVITY .....	64
3.8    SUMMARY.....	67
<b>4     ENERGY PERFORMANCE OF 802.11 AND MPRMA.....</b>	<b>69</b>

## **Introduction**

---

4.1	INTRODUCTION.....	69
4.2	THE STUDIED SCENARIO .....	70
4.3	802.11P SIMULATOR DESIGN.....	71
4.4	MPRMA.....	74
4.5	MODELLING ENERGY CONSUMPTION.....	75
4.6	PERFORMANCE EVALUATION.....	77
4.7	SUMMARY.....	84
<b>5</b>	<b>ENERGY EFFICIENCY IN A MOTORWAY VEHICULAR NETWORK .....</b>	<b>86</b>
5.1	INTRODUCTION.....	86
5.2	PROPOSED SETUP .....	87
5.3	AVERAGE PACKET DELAY MINIMISATION AT THE CLUSTER HEADS .....	89
5.4	ANALYSIS OF PACKET ARRIVAL PROCESS AT THE RSU .....	93
5.5	ANALYTICAL MODEL OF AN RSU WITH SLEEP CYCLES.....	96
5.6	TRAFFIC SHAPING AT THE RSU .....	105
5.7	SIMULATION SETUP.....	108
5.8	PERFORMANCE EVALUATION.....	110
5.9	SUMMARY.....	113
<b>6</b>	<b>USING RENEWABLE ENERGY IN A MOTORWAY VEHICULAR V2R NETWORK.....</b>	<b>115</b>
6.1	INTRODUCTION.....	115
6.2	PROPOSED SCENARIO .....	116
6.3	WIND ENERGY ANALYSIS.....	117
6.4	SYSTEM MODEL AND QoS METRICS.....	119
6.5	SIMULATION .....	122
6.6	PERFORMANCE EVALUATION.....	124
6.7	BATTERY CAPACITY .....	131
6.8	SUMMARY.....	132
<b>7</b>	<b>RELIABILITY ANALYSIS FOR STANDALONE WIND POWERED RSUS.....</b>	<b>133</b>

## **Introduction**

---

7.1	INTRODUCTION.....	133
7.2	WIND SPEED PROFILE.....	133
7.3	WIND POWER.....	135
7.4	RELIABILITY ANALYSIS .....	140
7.5	PERFORMANCE EVALUATION.....	142
7.6	SUMMARY.....	149
<b>8</b>	<b>CONCLUSIONS AND FUTURE WORK.....</b>	<b>150</b>
8.1	SUMMARY.....	150
8.2	KEY FINDINGS .....	152
8.3	FUTURE WORK.....	154
	<b>REFERENCES.....</b>	<b>156</b>
	<b>APPENDIX A .....</b>	<b>164</b>
A.1	MODELLING THE PHYSICAL LAYER.....	164
A.2	PROPAGATION MODEL FOR V2R COMMUNICATIONS.....	165
A.3	PROPAGATION MODEL FOR V2V COMMUNICATIONS .....	168

## List of Tables

Table 3.1: System Parameters .....	61
Table 4.1: System communication parameters .....	75
Table 5.1: System Paramters .....	89
Table 5.2: RSU energy parameters .....	104
Table 5.3: Sleep count in an hour with and without traffic shaping. ....	110
Table 6.1: Wind Energy System Parameters .....	119
Table 7.1: Weibull parameters.....	134
Table 7.2: System Reliability .....	148

## List of Figures

Figure 2.1: Curve speed warning .....	13
Figure 2.2: Electronic emergency brakes .....	13
Figure 2.3: Platooning vehicles .....	14
Figure 2.4: Main facets of greening vehicular networks. ....	36
Figure 2.5: PDF of inter-arrival time .....	48
Figure 2.6: Vehicular flow per hour.....	49
Figure 2.7: Hourly Vehicular Flow and Density .....	50
Figure 2.8: PDF of vehicles' average speed in m/s .....	51
Figure 2.9: Vehicles' average speed in m/s.....	52
Figure 3.1: Multihop routing scenario .....	57
Figure 3.2: Average hops and hop lengths per hour .....	62
Figure 3.3: Energy consumption.....	63
Figure 3.4: Energy consumption with efficient transceiver. ....	64
Figure 3.5: CDF of inter-vehicle spacing .....	65
Figure 3.6: Probability of connectivity.....	67
Figure 4.1: MPRMA/802.11p Proposed Scenario. ....	71
Figure 4.2: 802.11p pseudo code.....	74
Figure 4.3: Packet loss ratio .....	78
Figure 4.4: Average access delay .....	79
Figure 4.5: Goodput.....	80
Figure 4.6: Total transmitting and receiving energy .....	81
Figure 4.7: Total listening energy .....	82
Figure 4.8: Energy and time ratio .....	83
Figure 4.9: Total network energy .....	84
Figure 5.1: Energy efficient RSU operation in a motor vehicular network....	88
Figure 5.2: Sleep pdf with delay minimisation. ....	91

Figure 5.3: Average packet delay with and without delay minimisation. ....	92
Figure 5.4: Packet blocking probability with and without delay minimisation.	
.....	93
Figure 5.5: Pdf of Inter-arrival time (IAT) of the packets at the RSU for min. no. of vehicles.....	95
Figure 5.6: Pdf of Inter-arrival time (IAT) of the packets at the RSU for avg. no. of vehicles.....	95
Figure 5.7: Pdf of Inter-arrival time (IAT) of the packets at the RSU for max. no. of vehicles.....	96
Figure 5.8: Queuing model for the RSU. ....	98
Figure 5.9: Embedded state diagram of the RSU (for K' = 4).....	99
Figure 5.10: Shaped sleep pdf with length-based traffic shaping.....	107
Figure 5.11: Shaped sleep pdf with time-based traffic shaping.....	108
Figure 5.12: Average packet delay with and without traffic shaping.....	111
Figure 5.13: Energy savings with and without traffic shaping.....	112
Figure 6.1: RSU with sleep cycles and renewable energy in a motorway V2R scenario. ....	117
Figure 6.2: Average wind over a day at Reading, UK. ....	119
Figure 6.3: Simulation flow chart. ....	124
Figure 6.4: Energy Required .....	127
Figure 6.5: Packet blocking probability.....	128
Figure 6.6: Average packet delay .....	129
Figure 6.7: Cumulate energy storage. ....	131
Figure 7.1: Weibull wind speed distribution .....	134
Figure 7.2: Fitted Power Curve for Wind Turbine. ....	136
Figure 7.3: MTTR and MTBF estimation from system UP/Down time.....	142
Figure 7.4: PDF of hourly energy surplus/deficit. ....	143
Figure 7.5: System outage reduction with increased battery capacity. ....	144
Figure 7.6: Hourly LOLP and EDNS with and without a battery. ....	145
Figure 7.7: Overall system reliability.....	146
Figure 7.8: MTBF survivor function. ....	147
Figure 7.9: MTTR Cumulative Probability.....	148
Figure A.1: Probability of outage ( $P_{out}$ ) for V2R systems.....	167

## List of Abbreviations

AASC	Adaptive Avoid Second-Collision
AC	Access Channel
ACK	Acknowledgment
AIFS	Arbitration Inter-Frame Space
AIR	Air information resource
AODV	Ad hoc On-Demand Vector
BEB	Binary Exponential Back-off
BS	Base Station
CCH	Control Channel
CDF	Cumulative Distribution Function
CFL	Compact Fluorescent Lamp
CH	Cluster Head
CSMA/CA	Carrier Sense Multiple Access/ Collision Avoidance
CTS	Clear to Send
CW	Contention Window
dB	Decibels
DCF	Distributed Coordinated Function
DCH	Double Cluster Head
DE-OLSR	Differential Evolution Optimised Link State Routing Protocol
DIDD	Double Increment Double Decrement

DIFS	Distributed Inter-frame Space
DOD	Depth of Discharge
DSRC	Dedicated Short Range Communications
DSRC-AA	DSRC-Asymmetric and Asynchronous
EDCA	Enhanced Distributed Channel Access
EENS	Expected Energy Not Supplied
EDNS	Expected Demand Not Served
EIR	Energy Index of Reliability
ELCC	Effective Load Carrying Capacity
FCR	Fast Collision Resolution
FOR	Forced Outage Rate
FRMA	Fast Reservation Multiple Access
FS	Free Space
GAF	Geographic Adaptive Fidelity
GaN	Aluminium Gallium Nitride
GPS	Global Positioning System
HGV	Heavy Goods Vehicle
IAT	Inter-Arrival Time
IID	Independent and Identically Distributed
ISP	Internet Service Provider
IVC	Inter-Vehicular Communications
IVS	Inter-Vehicular Systems
LOEE	Loss of Energy Expectation
LOLE	Loss of Load Expectation
LOLP	Loss of Load Probability
LOS	Line of Sight

LP	Linear Programming
MAC	Medium Access Control
MACA	Multiple Access with Collision Avoidance
MACA/PR	MACA/ Packet Reservation
MGM	Matrix Geometric Method
MILD	Multiplicative Increase and Linear Decrease
MILP	Mixed Integer Linear Programming
MIMO	Multiple Input and Multiple Output
MMF	Morgan Mercer Flodin
M-PRMA	Modified-Packet Reservation Multiple Access
MSC	Mobile Switching Centre
MTBF	Mean Time before Failure
MTTF	Mean Time to Failure
MTTR	Mean Time to Repair
MW	Mega Watts
NAV	Network Allocation Vector
NINT	Nearest Integer Function
OLSR	Optimised Link State Routing
PC	Point Coordination
PCF	Point Coordination Function
PDF	Probability Density Function
PLR	Packet Loss Ratio
PRMA	Packet Reservation Multiple Access
PSM	Power Save Mechanism
QoS	Quality of Service
rms	Root Mean Square

RRA	Reservation Random Access
RRA-ISA	RRA Independent Stations Algorithm
RSU	Road Side Unit
RTR	Ready to Receive
RTS	Ready to Send
SAPS	Small Autonomous Power Systems
SCF	Store Carry and Forward
SCH	Service Channel
SIFS	Short Inter-Frame Space
SINR	Signal to Interference plus Noise Ratio
SIR	Signal-to-Interference Ratio
SSWECS	Small Standalone Wind Energy Conversion Systems
TDD	Time Division Duplex
TDMA	Time Division Multiple Access
V2R	Vehicle-to-Roadside
V2V	Vehicle-to-Vehicle
VANET	Vehicular Ad hoc Network
VCN	Vehicular Communication Network
VSC	Vehicle Safety Communications
WAVE	Wireless Access in Vehicular Environments
WBSS	WAVE Basic Service Set
WSA	WAVE Service Advertisement
WSMP	WAVE Short Message Protocol

## List of Symbols

$C_p$	Coefficient of performance
$D_{max}$	Maximum delay in time based traffic shaping
$E_0$	Energy demand of the system over 24 hours
$E_s$	Transmission energy savings
$E_{WO}$	Wake up overhead energy
$E_{l\_BS}$	Listening energy consumption of base station
$E_{l\_Vehs}$	Listening energy consumption of vehicles
$E_{r\_BS}$	Reception energy consumption of base station
$E_{r\_Vehs}$	Reception energy consumption of vehicles
$E_{t\_BS}$	Transmission energy consumption of base station
$E_{t\_Vehs}$	Transmission energy consumption of vehicles
$K'$	Maximum buffer size
$K_{opt}^{gen}$	Optimal buffer size with Generally distributed service time
$K_{opt}^{mvk}$	Optimal buffer size with memory-less (negative exponential distributed) service time
$N_S$	Sleep count
$P_0$	Mean received power
$P_B$	Packet blocking probability
$P_H$	Packet header
$P_L$	Payload

$P_{MAX}$	Maximum operational power
$P_{Min}$	Minimum operational power
$P_{avg}$	Average wind power
$PktSize_i$	Size of the $i^{th}$ packet
$P_{lc}$	Power consumed in listening state
$P_{out}$	Probability of outage
$P_r(d)$	Mean received power at distance $d$
$P_r(d_{ref})$	Reference power
$P_{rc}$	Power consumed in receiving state
$P_{rc}$	Power utilised by a receiver
$P_s$	Average packet size
$P_t$	Transmit power
$P_{th}$	Receiver threshold power
$P_{th}$	Transmitter threshold power
$P_{tc}$	Total power consumed by the transmitter circuitry
$P_w$	Wind power
$\bar{S}$	Mean sleep duration
$T_{r\_BS}$	Total receiving time for base station
$T_{r\_N}$	Time taken to receive packets
$T_{t\_BS}$	Total transmitting time for base station
$T_{t\_N}$	Time taken to transmit packets
$\bar{V}$	Mean wind speed
$V_{cut-in}$	Cut in speed for wind turbine
$V_{cut-off}$	Cut off speed for wind turbine
$\bar{X}$	Mean packet size

$d'$	Maximum delay in length based traffic shaping
$d_b$	Break point distance
$d_r$	Data rate
$d_t$	Vehicle data generation rate
$d_v$	Vehicular Density
$e_a d^v$	Distance dependent amplifier energy
$e_e$	Electronic energy
$e_r$	Energy consumed in the reception of a packet
$e_{r\_bit}$	Reception energy per bit
$e_t$	Energy consumption in the transmission state
$e_{t\_bit}$	Transmission energy per bit
$f_j$	Probability of $j$ packet arrivals in the system within a sleep cycle
$h_b$	Base station antenna height
$h_v$	Vehicle antenna height
$n_i$	Number of packets in the RSU just after the $i^{th}$ embedded point
$q_0$	Probability of the system being empty after a sleep cycle completion
$q_k$	Probability of state $(k, 0)$
$r_0$	Probability of the system being empty after a service completion
$r_k$	Probability of state $(k, 1)$
$s_m$	Vehicular spacing in meters
$v_1$	First path loss exponent for single and two slope models

$\nu_2$	Second path loss exponent for a two slope model
$\alpha_j$	Probability of $j$ packet arrivals in service duration $t$
$\beta_k$	Ratio of the probability of the system having $k$ packets to the probability of the system being empty
$\mu_{l\_new}$	Mean of log-normal distribution
$\rho_c$	Carried load
$\sigma^2$	Time-average power of the received signal
$\sigma_d$	Shadow deviation
$\sigma_{d\_new}$	Standard deviation of log-normal distribution
$\sigma_{rms}$	Root mean square value of received signal
$\omega'$	Shifted origin of exponential distribution
$\phi_i$	$i^{th}$ embedded point (either a sleep cycle completion or a service completion)
$\text{erfc}(\cdot)$	Complementary error function
$V'$	Perturbation term for instantaneous wind speed
$A$	Cross-sectional area of wind turbine
$C$	Energy Capacity
$D$	Diameter
$D$	Mean time between successive embedded points
$K$	Rician factor
$L$	Energy Load
$M$	Vehicular density/ No of vehicles
$N$	Number of packets
$N$	Average number of packets in an RSU
$U$	Utilisation of the system

$V$	Instantaneous wind speed
$W$	Average packet delay
$X$	Gaussian random variable
$a$	Scale parameter of the Weibull distribution
$b$	Shape parameter of the Weibull distribution
$d$	Distance
$k$	Number of packets
$m$	Shape parameter, Gamma distribution
$q$	Vehicular flow
$s$	Free flow speed
$t$	Time duration
$v$	Speed
$\zeta(\cdot, \cdot)$	Riemann's zeta function
$\eta$	Goodput
$\lambda$	Packet arrival rate
$\mu$	Packet service rate
$\rho$	Offered load
$\varsigma$	Air density
$\sigma$	Standard deviation
$\varphi$	Scale parameter of Gamma distribution
$\psi(m)$	Euler psi function
$\omega$	Packet burst period
$\phi$	Shape parameter of Gamma distribution

## 1 Introduction

Telecommunications has reached a mobile frontier where users expect connectivity everywhere and even in highly dynamic vehicular environments. Vehicular communications have thus expanded to not only serve users within the city but across cities with technology traversing motorways to provide services through a new breed of networks with distinct characteristics and requirements. With the growing popularity of ‘connectivity on the move’, the transportation industry is realising an increasing number of applications that can make use of a dedicated vehicular network [1]. The emerging trends of ‘connected vehicles’ in the market [2], the sheer size of motorway and city road (transportation) networks with respect to both dimension (i.e. 31,600 miles in Great Britain in 2011 [3]) and users (31 million vehicles in the UK in 2009 [4]) with the envisaged applications for vehicular communication networks (VCNs) suggest a foreseeable growth that can be parallel if not higher than that of the current cellular network. Therefore, it is evident that some of the already existing and well researched operational challenges of cellular topology will also be inherited in vehicular networks with the added complexity of maintaining seamless connectivity with stringent quality of service (QoS) requirements in high vehicle mobility environments. The looming spectrum shortage will strain the support of existing exponential increase in bandwidth requirements and will probably rule out the use of incumbent cellular networks to support vehicular

communications. Extensive BS deployment to support ubiquitous vehicular network coverage is rendered impractical due to the difficulty of providing high data rates in large coverage zones at low costs.

The ever increasing capabilities of vehicles only make way for a wider range of possible applications requiring a dedicated network. It is envisaged that an intelligent vehicle will be equipped with an on-board computing and sensing device to report traffic conditions and accidents, a wireless communication device, and a GPS device enabling the vehicle to track its location/position [5]. Collision avoidance and cooperative driving are the most important safety related applications for vehicles and pedestrians in a vehicular environment whereas non-safety applications refer to internet access, multimedia (voice, video and data) streaming, entertainment and gaming all being planned for this dynamic environment [6]. Other vehicular applications include toll services, travel information support, parking, and congestion information [7].

The vehicular environment and the sheer size of both city and motorway road layouts call for innovative and distinct network designs to suit the vehicular scenario. Providing high speed (up to 54 Mbps) communication in such environments is extremely challenging due to significantly fast changing network topologies as vehicles move past one another in various directions. Vehicular communication can typically be (i) vehicle to vehicle (V2V) communication (VANET for example), (ii) vehicle to infrastructure (V2I) or roadside (V2R) communication, and (iii) Hybrid communication (combination of both). A final category of VCN known as intra-vehicular communication which denote data exchange within vehicles tend to be wired networks and will not form a part of this thesis. Since the majority of the

communication cases require Internet connectivity, the infrastructure such as base station (BS) or road side units / access points (AP), also known as road side unit (RSU) plays an important role in vehicular networks. Each case along with the intended applications brings about its own specific complications when building a robust network to provide a high level of QoS with stringent requirements.

As with traditional networks, comprehensive testing is required prior to deployment. The stringent QoS requirements for safety applications however, require even more rigorous tests than traditional networks. High user mobility covering significant distances distinguishes vehicular networks and the difficulties that may arise in deploying them, due to the environment in which they operate. These features render field tests impractical due to the costs and difficulty associated with covering a large network serving highly mobile users. This obstacle is the main impetus for dedicated vehicular network simulators which when coupled with realistic vehicular traces, can be used to accurately model the vehicular environment. Such a simulator will subsequently open a window for energy and performance measurements enabling tuning of new and existing protocols and schemes in order to achieve the desired QoS and lower overall energy consumption of the network.

The growth of VCNs comes at a critical point of time, when existing communication technologies are already consuming significant amounts of energy, and environmental concerns are increasingly gaining importance. The global push to reduce the carbon footprint has only amplified the challenges that must be addressed by VCNs. Although reducing the energy usage in the highly mobile vehicular communications scenario can benefit

from the progress in wireless networks' energy efficiency, paying particular attention to the requirements of vehicular networks can lead to innovative solutions which not only maintain QoS in this dynamic environment, but also save significant amounts of energy. The limited direction of vehicular flow especially in a motorway environment, for instance, provides a unique network topology that can assist in geographical network routing schemes through the use of cooperative relaying amongst nodes. Energy efficient routing schemes for a motorway vehicular scenario can provide network wide energy minimisation by delivering a packet from a source to the destination using the lowest amount of energy possible. Their aim is to reduce the power needed by all three functions of the transceiver (reception, transmission and processing) by minimising the amount of data that is replicated in the network and the propagation distances used when routing the packets.

In assuming VCNs will follow the footsteps of incumbent cellular networks with the aim of ubiquitous vehicular network coverage of road networks, a closer look at the energy issues faced by these networks can enable a forecast of where the main source of energy consumption will arise in VCNs. Base station energy consumption is notably significant in its contribution to the carbon footprint of communication networks. Amongst the core network, base stations, and mobile terminals which comprise the typical cellular network, BS components give the highest cost impact not only from an environmental perspective but also from the industries overall expenditures (OPEX) with respect to energy costs. The length of the M4 motorway presents a significant amount of BS placements and is used as an example motorway in this thesis due to the availability of vehicular traffic traces for

this motorway. To actualise ubiquitous coverage, considerable energy expenditure can be expected along with the costs of bringing power lines to the isolated suburban locations solely for vehicular communication purposes. In the case of base stations placed in off or unreliable electrical grid locations, the requirement for diesel generators to power them significantly increases the energy costs to 10 times the normal cost [8]. In 2008, 25 leading telecommunication companies initiated a program called “Green Power for Mobile” to aid the mobile industry in deploying renewable energy sources for base stations in developing countries [8]. With 35,908 green deployments to date these renewable sources including solar, wind and sustainable bio fuels are aimed at new and existing off-grid base stations. Reaching a target of 118,000 base stations will save an estimated 2.5 billion litres of fuel, cutting carbon emissions by up to 6.8 million tons. A similar initiative thus poses a viable low carbon solution to support vehicular communications in urban road networks.

A convergence of energy efficiency paradigms along with the need for vehicular applications forces us to take account of the power hungry nature of BS entities in cellular networks and minimise BS energy use in VCNs through a heterogeneous use of pico-cells served by RSUs within a macro cell that enable intermittent BS placement. The deployment of such cells offers high data rates and reduces the number of BSs required in the network while fulfilling a certain QoS level [9]. Furthermore these RSUs can utilise various sleep cycle strategies that are impractical for base station only scenarios due to the large number of operational tasks a BS has to perform continuously. Finally, the use of low power road side units enable the implementation of small standalone renewable energy systems that can

render large scale deployments more feasible by decreasing the size of the renewable power systems required. As the availability of vehicular communication systems becomes critical to deploy envisaged safety applications, the reliability of renewable energy sources requires extensive analysis. This analysis becomes especially important when using wind powered systems due to the intermittent nature of wind speed. This raises the need for determining the reliability and adequacy of wind power generation systems while taking the variable and stochastic nature of wind into account, along with the dynamic power demand of the motorway vehicular network.

The various obstacles, opportunities, and circumstances posed by the realization of a motorway VCN have subsequently led to the use of a dedicated vehicular mobility simulator to investigate the vehicular environment and its effects on communication protocols. We start with an analysis of energy consumption and connectivity of a range of routing schemes on a stretch of motorway where packets need to be relayed through V2V communications to a base station sink. Since the high mobility of vehicular networks along with stringent QoS requirements means only a few MAC protocols designed for traditional ad-hoc networks can be adapted to efficiently work in VANETs [15], a study of MAC protocols designed specifically for VANETS follows. The physical channel characteristics of the motorway scenario are taken into account in comparing the QoS and energy consumption of the 802.11p (contention based medium access control (MAC)) protocol with the power consumption of a slot based modified packet reservation multiple access (M-PRMA) protocol. Focus is then shifted to make RSUs energy efficient by introducing a number of sleep mechanisms

## **1.1 Research Objectives**

---

along with their queuing theory analysis. To maximise energy savings, traffic shaping techniques have been explored in conjunction with sleep mechanisms, (in contrast to the traditional use of these traffic shaping mechanisms for improving QoS). Finally carbon footprint offsetting is proposed through small standalone wind energy conversion systems. This led to a thorough statistical analysis of wind energy supply adequacy and reliability in a motorway vehicular network scenario.

### **1.1 Research Objectives**

The research objectives of this thesis were:

- To understand the performance of medium access control protocols and routing protocols in a highly mobile vehicular scenarios.
- To evaluate and understand the energy consumption of MAC and routing protocols in the motorway vehicular scenario.
- To achieve a low carbon footprint for VCNs
- To determine the viability and reliability of the use of renewable energy for motorway vehicular communication systems.

### **1.2 Research Contributions**

The author, in this thesis, has,

1. Developed an energy model to determine the energy consumption of MAC and routing protocols in a motorway vehicular scenario.
2. Compared the QoS and energy performance of a time division multiple access (TDMA) based protocol, namely M-PRMA protocol

## **1.2 Research Contributions**

---

with the IEEE 802.11p carrier sense multiple access (CSMA) protocol.

3. Used simulations and linear programming optimisation to evaluate the impact of relaying a packet through routing schemes at different experimentally measured vehicular densities and determined the probability of connectivity with the derived hop length.
4. Proposed a novel reactive sleep strategy to maximise energy savings at the RSU and developed an analytical model using G/G/1/K vacation queuing. Used two types of traffic shaping techniques (time and length based) to minimise adaptive sleep cycle overhead thereby maximising energy savings
5. Investigated for the first time the QoS performance and reliability analysis of standalone wind powered roadside units (RSUs) in a vehicular motorway network. Used real vehicular traffic profiles, reported data traffic measurements and reported wind measurements to analyse the performance in various test cases and suggested an operational scenario.

These contributions are supported by the following publications:

1. Kumar, W.; Muhtar, A.; Qazi, B.R.; Elmirghani, J.M.H, "Energy and QoS Evaluation for a V2R Network," Global Telecommunications Conference (GLOBECOM 2011), 2011 IEEE , pp.1,5, 5-9 Dec. 2011
2. Muhtar, A.; Qazi, B.R.; Bhattacharya, S; Elmirghani, J.M.H, "Greening Vehicular Networks with Standalone Wind Powered

RSUs: A Performance Case Study," International Conference on Communications (ICC), 2013.

### 1.3 Thesis Overview

Following the Introduction, the thesis is organised as follows:

**Chapter 2** provides an overview of VCNs including their applications, environments and standards. The current research trends and related works on MAC protocols, routing protocols, energy efficiency, and reliability are also discussed.

**Chapter 3** examines a range of routing schemes to determine the network wide energy effects of routing a packet using vehicle to vehicle (V2V) communication through a 5 km motorway stretch to a base station. A linear programming optimisation is carried out to find the optimum number of hops and optimum hop lengths at varying vehicular loads (dependent upon hourly traffic). The probability of connectivity is then determined for the hop lengths associated with all routing schemes and the optimum range.

**Chapter 4** studies the QoS and energy performance of carrier sense multiple access with collision avoidance based 802.11p scheme and a modified version of packet reservation multiple access (M-PRMA) scheme for a vehicle-to-roadside (V2R) network. A physical layer model for a V2R scenario has been incorporated to gain a more realistic representation of the communication layer and an energy model has been developed.

**Chapter 5** proposes a novel reactive sleep strategy for energy saving in RSUs of a motorway V2R network by using a micro-macro cellular topology. An analytical model is developed using G/G/1/K vacation queuing. Length

and time-based traffic shaping techniques are then used to minimise adaptive sleep cycle overheads thereby maximising energy savings.

**Chapter 6** investigates the performance of wind-powered standalone road side units (RSUs) in the vehicular motorway network. Using reported wind measurements, several test cases are analysed and an operational scenario is suggested along with a suitable battery size to support acceptable QoS for video related applications.

**Chapter 7** studies the reliability of RSUs supported by wind power through detailed reliability analysis with the use of probabilistic indices to define the performance of a standalone wind powered RSU on the M4 motorway. A thorough analysis of wind speed is followed by graphical and analytical methods of deriving wind power used for the reliability analysis. A battery size is then calculated and enhanced reliability illustrated.

**Chapter 8** concludes the thesis with key findings and explores how the work can be extended in the future.

---

## **2 Vehicular Communication Networks**

### **2.1 Introduction**

The ever increasing sophistication of vehicles allows many to have several computers and sensors to serve different parts of the car operation [2]. This sophistication along with traffic navigation, video and audio output, make the vehicle, as a mobile unit, possess computational power much greater than that of mobile phones in cellular networks. While mobile devices are limited to the amount of instantaneous energy usage requirements, sufficient energy generation and storage in vehicles provides the opportunity to support higher computational capabilities enabling more sophisticated on-board units when compared to other wireless access devices. With high node capabilities however comes a requirement to provide high quality services at low energy costs. Such requirements combined with the unique characteristics of the motorway environment make the design and deployment of vehicular networks quite challenging.

### **2.2 Applications**

Various papers have classified vehicular services and applications along with the networking needs to support them. While some authors [10] simply classify them as safety, and non-safety applications others [5] further divide the non-safety set into traffic management and monitoring applications, and

## 2.2 Applications

comfort applications. The main differentiator of the classes is the priority given to safety messages over non-safety data. While safety messages are time sensitive broadcasts that can be either event driven or periodic, non-safety applications are less strict on real time constraints and pose no threat to life if messages are delayed.

### **2.2.1 SAFETY**

Active road safety, being the primary drive for developing vehicular communication networks (VCN), has many envisaged applications to decrease the chances of road traffic collisions, destruction of property and most importantly the loss of life [5]. The vehicle safety communications (VSC) project carried out by a number of car manufactures identified up to 34 potential safety applications [11]. The safety application can be classified into four groups which are: intersection collision avoidance, public safety, sign extension, and information from other vehicles. Amongst them the highest benefit were deemed to be derived from the following scenarios:

**Traffic Signal Violation Warning:** Messages are broadcasted to all vehicles by road side units that detect a traffic signal violation.

**Curve Speed Warning:** Vehicles approaching a curve receive messages to signal they are approaching a curve. Furthermore the messages can provide the recommended speed for the curve and even induce the vehicle to start broadcasting its own emergency alert messages to trailing vehicles if it goes through the curve at excess speeds. Furthermore as vehicles transmit their speed and location to road side units (RSUs), RSUs can communicate hidden dangers such as a traffic jam to approaching vehicles. This example is depicted in Figure 2.1.

## 2.2 Applications

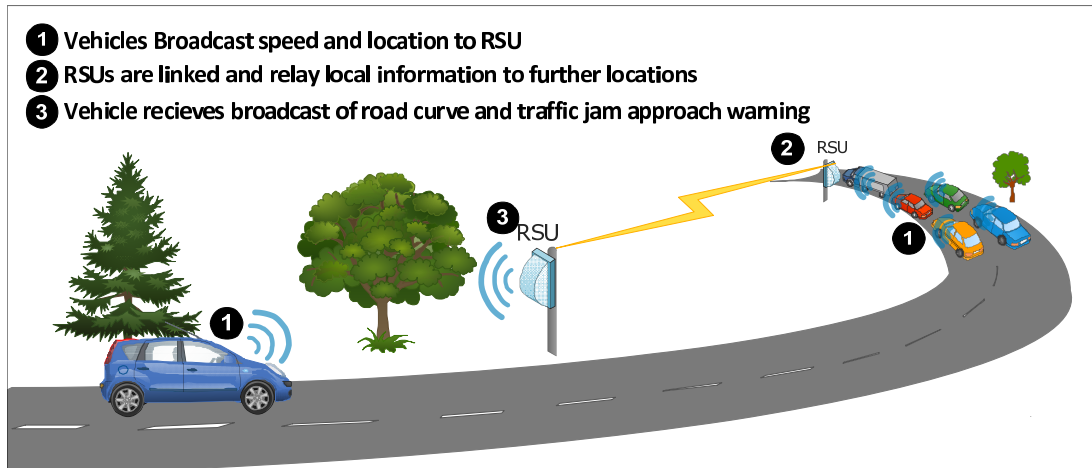


Figure 2.1: Curve speed warning

**Emergency Electronic Brake Lights:** A vehicle compelled to hard brake initiates a beacon message broadcast to alert vehicles behind it of the emergency situation. The messages can be relayed to vehicles further down the lane giving drivers a longer time to react and thus enabling drivers to decelerate on time to avoid collisions.

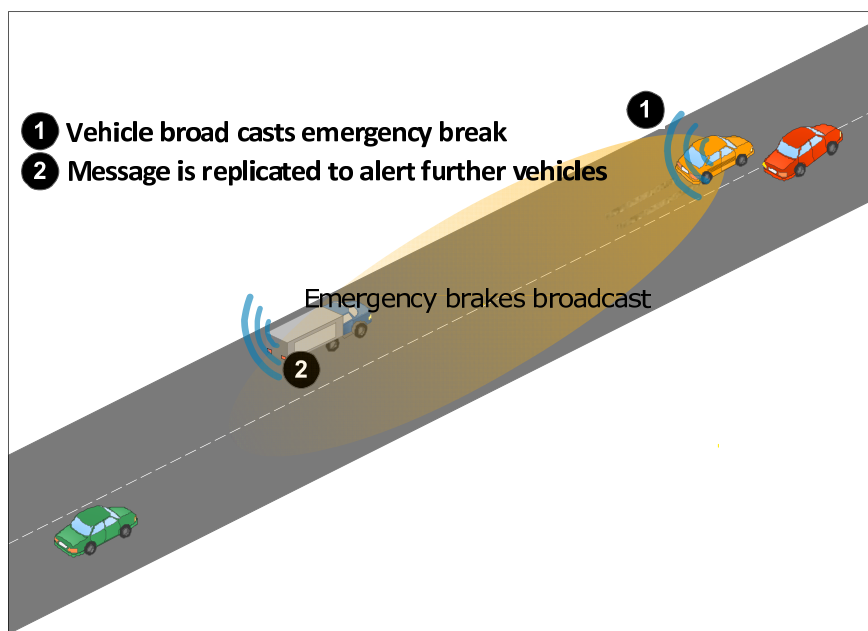


Figure 2.2: Electronic emergency brakes

**Pre-Crash Sensing:** In situations where vehicles and road side units through cooperation by periodic dissemination of messages determine a

## 2.2 Applications

---

crash is unavoidable, they initiate vehicular peripherals such as airbags, actuators, seatbelt tensioners and extendable bumpers to reduce the effects of the crash.

### 2.2.2 TRAFFIC MONITORING AND MANAGEMENT

The sharing of information between vehicles and with road side units can be used to facilitate traffic flow and lower traffic congestion, travel time, and thus fuel consumption. The aggregation and relay of data through multi-hop communications can enable a high level of cooperation between vehicles effectively leading to adaptive cruise control and ultimately, cooperative navigation and automated motorway systems [7]. Such systems can be used in platooning especially by trucking companies to decreasing fuel consumption and increase safety [12].

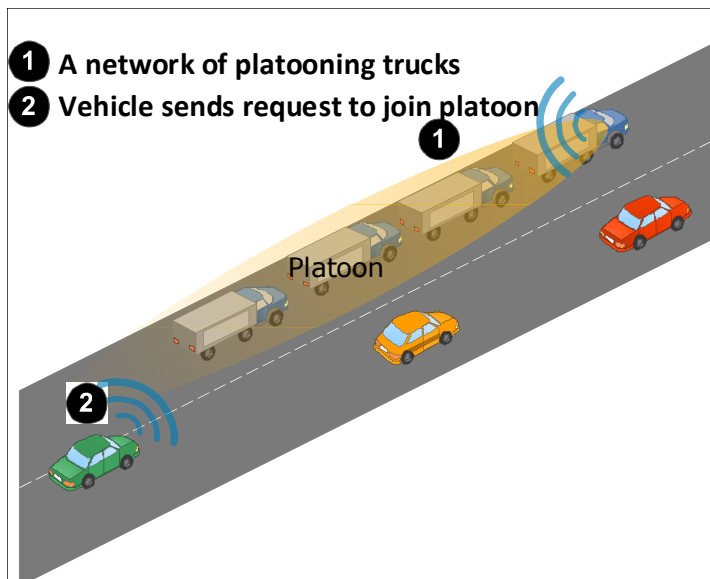


Figure 2.3: Platooning vehicles

### **2.2.3 INFOTAINMENT**

Comfort applications also known as infotainment can provide information and entertainment to the passengers. Though content sharing between vehicles is one notion to consider, the majority of the proposed applications rely on a certain amount of Internet connected road side units. These RSUs become the main source of information that can later be distributed amongst the vehicles [6]. Internet connectivity provides entertainment and multimedia content including streamed audio, video, and gaming along with information such as news, books, email synchronisation, and local information (i.e. hotels, restaurants, shopping centres, and gas stations) [7].

## **2.3 Network Design Challenges**

The high computational and sensing capabilities of smart vehicles can generate an unprecedented amount of data from each vehicle which ultimately leads to a requirement for high bandwidth and highly reliable communications to support the various leisure and road safety applications. With high bandwidth requirements that arise from the various new classes of data hungry vehicular applications, VCNs can end up demanding more bandwidth than that required by mobile nodes in cellular communications. This bandwidth requirement compounded by a need for time-critical broadcasts in safety applications such as cooperative collision warnings make the design of VCNs more challenging compared to other types of networks. In addition to the challenge of strict communication requirements, relative vehicular speeds that can reach up to 300 km/h [13] present mobility that surpasses that of ad-hoc and cellular networks. The high mobility of

vehicles is one of the main sources of difficulty for wireless vehicular networks [14]. It brings about dynamic network topologies with frequent partitions and disconnections arising from large inter-vehicle gaps. Such gaps in sparsely populated scenarios complicate the achievement of reliable routes for data relay. These disconnections also make it difficult to implement a medium access control (MAC) protocol for vehicular ad-hoc networks as vehicles pass one another at high speeds making medium contention even more challenging [15].

## **2.4 Vehicular Network Environments**

The road network itself is one of the major differences inherent in vehicular communications in comparison with all other types of networks. It presents major advantages and poses challenges when designing and deploying VCNs. The expected direction of travel on roads provides a predictable movement of vehicles that can be taken advantage of in the design of routing protocols and the selection of network architecture. The containment of vehicles within the roads provide network architectures that simplify network deployment by narrowing the required coverage area [13]. A significant drawback, however, lies in the relative coverage required to support the length and number of road networks in comparison to ad-hoc or even cellular networks. Ad-hoc and cellular networks have generally been deployed within a locality and with low mobility. Road networks on the other hand, will present a coverage requirement where city scenarios present a dense and localised network while motorway scenarios pose an extended network with fluctuating densities to be served with high bandwidth and high QoS [13].

## 2.5 Vehicular Network Technologies and Standards

### 2.5.1 DSRC

The Dedicated Short-Range Communication (DSRC) spectrum allocated by the U.S. Federal Communication Commission provides communications for vehicle to vehicle, and vehicle to roadside communications covering a range from 300 metres up to a maximum of 1000 metres. Primarily aimed at enhancing public safety and traffic flow, private services have been permitted to encourage DSRC adoption and development [16]. DSRC defines short to medium range radio communication based on the 802.11a Wireless LAN MAC, and physical layer specifications. It has been adjusted for low overhead operations in the DSRC spectrum, and is known as the 802.11p revision defining Wireless Access in Vehicular Environments (WAVE) [17]. DSRC operates in the 5.9 GHz of the radio spectrum divided into 10-MHz channels with a control channel (CCH) at 5885-5895-MHz dedicated to safety communications. While two more channels at the edges of the spectrum have been reserved for future safety critical applications with such messages given priority in all channels, the remaining service channels (SCH) are available for non-safety applications [18]. The DSRC in effect will complement cellular communications and provide high data transfer rates of 6-27 Mbps with minimal latency to serve vehicular applications.

### 2.5.2 WIRELESS ACCESS IN VEHICULAR ENVIRONMENT (WAVE)

The resulting allocation of the DSRC spectrum along with the definition of standards for DSRC is known as WAVE technology. The WAVE family of

standards have been developed based on the IEEE 802.11p to deal with the physical and MAC layers, with the IEEE 1609 standards stipulating higher-layer protocols [7].

### 2.5.2.1. IEEE 802.11P

IEEE 802.11p defines the physical layer and MAC protocol which enables IEEE 802.11 to work in a vehicular environment. The MAC protocol used by the WAVE stack is based on the IEEE 802.11 Distributed Coordination Function (DCF), which uses a Carrier Sense Multiple Access with Collision Avoidance (CSMA/CA) medium access (detailed in section 2.6.2). To maintain QoS for safety applications, the Enhanced Distributed Channel Access (EDCA) mechanism is used to coordinate medium access by using four different Access Categories (ACs) to group data traffic. The ACs thus provides internal contention before medium access in order to differentiate priorities and give safety messages precedence [16]. Furthermore, the WAVE MAC avoids additional latency arising from authentication and association methods in 802.11 by either using the control channel (CCH) to broadcast safety, and critical control messages, or using the CCH along with the SCHs in a multi-channel operation mode to create WAVE Basic Service Sets (WBSS) [17]. Time synchronisation in the latter (WBSS) scheme is achieved through WAVE Service Advertisement frames (WSA) transmitted in the CCH to state the service channels (SCH) that will be used in the next SCH interval. Both transmitter and receiver jump between CCHs and SCHs with receivers being notified of the next SCH intervals in the CCHs, and transmission taking place in the SCH intervals. Once data transmission

ends, the transmitter leaves the WBSS followed by the receiver when no more frames are being received.

### 2.5.2.2. IEEE 1609

- ***IEEE 1609.1 WAVE Resource Manager*** describes the application for services and interfaces of message formats and their read/write protocols between RSUs and the vehicles OBUS.
- ***IEEE 1609.2 WAVE Security Services*** defines the security and anonymity of message format processing and exchanges ensuring authenticity and confidentiality
- ***IEEE 1609.3 WAVE Networking Services*** provides the network and transport layer services using the WAVE Short Message Protocol (WSMP) for routing and the WAVE Basic Service Set (WBSS) for group addressing.
- ***IEEE 1609.4 WAVE Multichannel Operations*** Integrates tightly with the IEEE 802.11p to manage and coordinate usage of the 7 DSRC frequency bands.

## 2.6 Medium Access Control (MAC) Protocols

Given the limited bandwidth capacity of the wireless medium along with the continuous increase in users a key approach to maintain and improve the performance of wireless networks is by improving the way the wireless medium is used. A substantial amount of research has been focused on MAC protocols in order to enhance the efficiency of medium access [19]. This has led to significant improvements in key performance metrics such as packet access delay, jitter, throughput, fairness, support for multimedia,

stability, making wireless communication more robust against channel fading, and lowering power consumption. In effect, the focus on the MAC protocols has heightened the level of QoS enabling the support of a plethora of applications including multimedia and real-time along with the incumbent voice and data capabilities [20].

### **2.6.1 DISTRIBUTED VERSUS CENTRALISED ARCHITECTURES**

The operation of the MAC protocols is significantly affected by the network architecture. The two logical network classifications comprise of distributed and centralised medium access methods. As the name suggests the former has a distributed MAC while the latter maintains a centralised MAC. The distributed method also known as ad-hoc networks, functions in an arbitrary manner without a coordinator, thus maintenance and the possibility of network failure is not relegated to any single node. Communication is by direct connections between nodes or through multi-hop relays to reach the destination. The lack of coordination however limits ad-hoc networks to a single frequency band as there is no central administration to assign frequencies to nodes. This limitation forces nodes to access the medium one at a time. An attempt by more than one node to transmit results in a collision which is resolved based on specific MAC rules [20]. Centralised wireless networks on the other hand enable a central node to dictate how resources are divided and shared among nodes. Transmission between nodes is done through the base station with uplinks serving as last-hop links to the base station. Downlink can be broadcast to all nodes in the coverage area giving all nodes a good view of the network and thus eliminating the problem of hidden and exposed nodes. The coordination of centralised

networks gives way to more flexible MAC designs by allowing additional resource division methods as the base station can assign specific frequencies or codes to different nodes. Furthermore the centralised network architecture can use the arbitrary feature of medium access at certain stages when nodes communicate with the base station. Such mixing of coordinated and arbitrary medium access methods are known as hybrid protocols [21].

### **2.6.2 CSMA/CA**

MAC protocols are classified into various groups that define how they operate and/or the functions they provide. Primarily all ad-hoc MAC protocols use the ‘listen before talk’ and contention based carrier sense multiple access (CSMA) mechanism. The carrier sense indicates the requirement for the stations to listen to the medium to see if it is in use or has been reserved before transmission. Multiple access and collision avoidance is achieved by distributed coordinate function (DCF) medium access mechanism, acknowledgement frames and medium reservation. With DCF, transmission is delayed for a Distributed Inter-Frame space (DIFS) after stations sense the medium availability. Within this time stations compete for transmission by using a random back-off algorithm which selects a random value for further delay of transmission [22]. The random waiting times are based on backoff algorithms which uniformly select the waiting period from a value between 0 and a contention window (CW). The station that selects the shortest contention window waits for the period and transmits next. Several backoff algorithms have been presented to improve the throughput, delay, fairness and stability. A few which include the binary exponential back-off (BEB), double increment double decrement (DIDD), fast

collision resolution (FCR), multiplicative increase and linear decrease (MILD) and adaptive avoid second-collision (AASC) which work by altering the contention window; have been evaluated in [22]. The study exposes the weaknesses of current backoff algorithms and their unsuitability for multihop wireless networks. This makes 802.11 unsuitable for vehicular communications stipulating the need for a different standard which in turn resulted in the 802.11p WAVE MAC amendment.

### **2.6.3 RESERVATION AND SCHEDULING**

Amongst the contention based protocols, some enable a reservation mechanism whereby a node may set up some sort of reservation prior to transmission in order to get exclusive access to reserved bandwidth so that QoS can be provided for real-time traffic. The reservation based schemes use ‘request to send’ (RTS) signals and ‘clear to send’ (CTS) signals prior to data transmissions. Nodes overhearing these RTS-CTS control packets, defer transmission for a proposed duration that is contained in the RTS-CTS signals [35]. This allows for virtual carrier sensing known as network allocation vector (NAV) applied to the system. By updating the fields in the NAV using the proposed durations from the RTS-CTS the area covered by the transmission range of the sender and the receiver is effectively reserved for data transfer. The dynamic reservation scheme used in ad-hoc networks involves the use of (RTS/CTS) control packets to avoid collisions as used in multiple access with collision avoidance (MACA). By adding packet reservation the MACA/PR enables piggybacking reservations onto data packets in multi-hop networks. This way the entire path is reserved as the first packet makes the reservation for subsequent packets. Most reservation

protocols were proposed for QoS provisioning in ad-hoc networks but incur severe performance degradation in high mobility environments due to the disruption of reservations [23]. Centralised forms of reservation protocols such as the modified packet reservation protocol studied in Chapter 4 avoid the overheads associated with exchanging reservation tables since the base station broadcasts information on which node has a reservation. These schemes are based on hybrid access protocols that mix the contention aspect of ad-hoc networks with the coordinated aspect of centralised networks. Packet frames are divided into slots which nodes can contend for. In the second phase, the base station reserves uplink slots for successful contending nodes. Various centralised reservation protocols including packet reservation multiple access (PRMA), reservation random access independent stations algorithm (RRA-ISA), and fast reservation multiple access (FRMA) evaluated in [21] have been developed to fine-tune access rights for voice and data packets. Furthermore the energy and QoS performance of the M-PRMA is compared with a non-reservation CSMA scheme in Chapter 4.

### **2.6.4 MULTIPLE CHANNEL**

Multiple channel approaches attempt to reduce the probability of collisions as nodes increase in a network. The authors in [24] categorise multi-channel protocols into two categories; those that divide channels into a control and a data channel as seen in the IEEE 802.11p MAC protocol and others that use multiple-data-channels. The general idea for both categories is to maximise throughput by using more channels, reduce interference and allow simultaneous transmissions in the same regions, and support higher QoS.

The authors in [24] note the complications of multichannel when assigning different channels to different nodes in real time. The work in [25] highlights that the main issue to resolve is the bottleneck that occurs in the exchange of control information in single channel protocols, noting that even though multiple channels alleviate this bottleneck, the allotment of channels to nodes becomes an issue. The researchers in [25] therefore classify multi-channel protocols based on how the allotment of channels is performed. The four different ways include the use of a dedicated control channel, common hopping, split phase, and multiple arrangement methods. The dedicated control channel protocols use two radios, having one tuned to a control channel for sending and receiving control messages and the other radio tuned to any of the other data channels to transmit or receive. The common hopping multiple access approach has nodes that use a single radio and cycle through all channels synchronously as is done in the WAVE MAC, stopping on a channel as soon as they make an agreement to transmit. The split phase also uses a single radio but divides control and data exchange into two time periods in which all nodes must tune to the control period simultaneously to make transmission agreements. Multiple arrangement methods enable multiple nodes to make agreements on distinct channels. This approach works by having the receiver maintain a slow “home” hopping sequence and the transmitter finding this receiver.

### **2.6.5 DIRECTIONAL ANTENNAS**

MAC protocols specifically designed for use with directional antennas can be used to avoid collisions and increase the channel reuse in addition to increasing the range of transmissions. With omnidirectional antennas, only

two nodes can communicate in one area while all the remaining nodes within the same coverage area remain silent. Directional antennas enable nodes to transmit in specific directions by dividing the space around the terminal into  $N$  transmission angles of  $(360/N)$  degrees [15]. Nodes can therefore transmit or receive from selective directions avoiding interference that comes from unwanted directions thus increasing the signal to interference and noise ratio (SINR). Furthermore the higher gain of directional antennas will allow nodes to communicate with nodes further away thus delivering messages in fewer hops [26]. Various schemes have been proposed which may employ multiple antennas facing different directions or a single antenna that can be rotated. Such systems can present a significant advantage in the motorway environment especially in scenarios where packets need to be routed in a single direction towards a sink entity as investigated in Chapter 5. Some protocols rely on nodes being location aware with the aid of GPS so that silenced regions can be detected and avoided allowing simultaneous communication in a close locality by silencing or rotating antennas to avoid interference. Other schemes simply employ an omnidirectional use of handshaking signals to discern the location of the receiving node and then transmitting the data using directional antennas. This method not only defines a silent region for other nodes to avoid but it also enables communicating nodes to choose the best possible transmitting and receiving links to communicate through [24].

### 2.6.5.1. POWER CONTROL

Power control MAC protocols may serve a dual purpose of energy conservation and improved spatial reuse. The power control can work by

turning the radio off at appropriate times and putting the node into a sleep mode when it's not intending to transmit or receive data. Since the receiver will be disabled during such sleep modes, various (synchronous, asynchronous and out-of-band) wake-up methods have been devised to make devices wake up and perform tasks. Synchronous schemes organizes a schedule for communicating nodes to wake up at the same time while asynchronous schemes have nodes wake up according to their own schedule [27]. The out-of-band scheme proposed in this thesis enables a low-power radio to idly listen on a separate, wake-up channel and wakes the tranciever up when the out-of-band signal is received [28]. Transmission power control can also be used to increase the efficiency of space-time utilization because reducing the transmit power lowers interference to nearby receivers and thus enables more nodes to communicate simultaneously [29]. The most basic power control scheme is based on the RTS-CTS handshake procedure whereby the handshake is performed at highest power either in a single channel or using a control channel and used to determine the minimum power required to transmit the data and acknowledgment packets. Other power control MAC protocols employ power-aware routing optimisation in multihop networks to determine a route which consumes low energy [30]. The transmit power can also be varied based on the packet size as lowering the transmit power may cause more errors and thus more retransmissions that would end up consuming more energy rather than saving energy. Based on the same principle other schemes vary the transmit power based on the channel conditions [30].

## 2.7 Queuing Theory Analysis

Traditionally, queueing theory based models are extensively used in predicting the QoS of access networks with little emphasis given on vacation queues. In [31], an M/M/c queue was analysed with queue length independent vacations of the servers and their impact on average system delay and utilisation were studied. In [32], the authors studied two types of random vacations: (1) Queue length independent vacations to model wireless channel impairments, and (2) queue length dependent vacations to model sleep cycles. Both the arrival and the service discipline of packets were assumed to be memory-less Poisson type as a simplistic case. Hence, the respective scenarios were modelled as M/M/c and M/M/1/K queues with random vacations. Since both of these scenarios can be represented using simplistic Markov Chains, a Matrix Geometric Method (MGM) was adopted to solve these Markov Chains. In [33], the authors introduced random sleep cycles at the CHs to save energy in a vehicle-to-vehicle (V2V) communication scenario. To maximise energy savings and keep packet blocking probability within acceptable bounds, the packet blocking probability was maintained at 0.05 at each hour of the day. A higher average packet delay was observed which was acceptable for video streaming applications, but not for audio conferencing applications [33]. The arrival of the packets at the CHs was considered Poisson distributed. Since packet size distribution was considered random as a simplistic case, the service duration followed a negative exponential distribution. Hence, each CH was modelled as an M/M/1/K queue with random queue length dependent sleep cycles. However, this type of sleep cycle degrades the system performance at low load conditions since the server (BS, AP or RSU) switches to sleep mode

frequently due to its high inactivity period [33], [32], resulting in an unacceptable average packet delay [33] for audio-conferencing applications [34]. Thus, there is a need to introduce reactive sleep cycles, which can smartly terminate the sleep mode before its due completion time to maintain QoS.

## 2.8 Energy Efficiency in Vehicular Networks

The power consumption of a transceiver can be divided into two parts (i.e. power consumed in the electronic circuitry and power consumed by the output amplifier). In the case of signal reception, the total power consumption is due to the receiver's electronic circuitry only. Power savings can be achieved during the transmission activity by optimising the transmit power levels at the source nodes. For example, an RF output power optimisation strategy was utilised in [35] to achieve energy savings and the results showed that a significant amount of power can be saved with multihop communication as compared to direct communication from a source to the BS. In [36], the authors have enhanced the IEEE 802.11 Power Save Mechanism (PSM) to achieve energy savings in vehicular networks however without any sleep mechanism. Further, the only QoS parameter considered in their work, with respect to energy savings, was end-to-end delay. Thus, the other key QoS parameter for real time communications, the packet blocking probability, was not considered. Other studies showed that by considering a sleep strategy at a node during its inactivity, a certain amount of energy can be saved [37], [38]. Sleep strategies in the recent past have been introduced as a solution to reduce the network power consumption as they do not need a complete overhaul of

network devices and protocols. In [39] and [40], the authors proposed sleep strategies for the line-cards in the routers depending upon the backbone traffic. The heuristic in [39] achieved 79% reduction in energy consumption, which was achieved at the typical low link utilisation (30%) in the Internet Service Providers (ISPs) backbone. Such major reduction may not be feasible in wireless and mobile network (e.g. cellular or vehicular) as they are not intrinsically overprovisioned and the link quality which depends upon the varying wireless channel, makes it susceptible to degraded QoS. Nevertheless, several research groups around the world are considering various sleep strategies to make cellular network energy efficient [9], [41], [42]. Approaches where the transmitting circuitry is switched off thus setting the transceiver into low energy state are collectively grouped under sleep [28].

### 2.8.1 ENERGY EFFICIENT MAC PROTOCOLS

Although specialised MAC and routing protocols for cooperative networks have been given some attention in research, it has only been done with the intended purpose of throughput maximisation without taking power efficiency into consideration. Any new MAC and routing protocols developed for cooperative networks will need to ensure gains in QoS do not lead to a significant rise in energy consumption. The algorithms should also avoid too much complexity as this can lead to high energy expenditure in the form of processing power.

Chapter 4 illustrates how the high energy consumption of the 802.11p protocol in a motorway vehicular network scenario stems from the carrier sense multiple access with collision avoidance (CSMA/CA) requirement for

vehicles to continually listen to the medium. Since high vehicular mobility puts a barrier to implementing the typical beacon based synchronized sleep cycles used in 802.11 MAC schemes to save energy in the nodes, [36] proposed an asymmetric and asynchronous wake up for the dedicated short range communication (DSRC-AA) MAC protocol which utilises cluster routing schemes to define different synchronization for cluster heads and cluster members to enable energy saving sleep patterns.

### 2.8.1.1. COGNITIVE RADIO

Cognitive radio enables intelligent utilization of the allocated radio spectrum by sensing the spectrum and accessing unused frequency bands to compensate for underutilization. Although a 50% saving in power by an operator has been shown [43], the complexity of the proposed algorithms makes it an expensive and unappealing solution to vendors. Other challenges in cognitive radio that may hinder its role in enhancing energy efficiency is the increased requirement for spectrum sensing. Constant sensing and processing of sensed data may outweigh any energy efficiency gains from improved spectrum utilization [44].

### 2.8.2 ENERGY EFFICIENT ROUTING

Improving the energy efficiency of packet routing in traditional wireless networks has received a lot of attention with various perspectives in research. The majority of this effort has risen from the severe energy constraint of wireless sensor nodes driving extensive research in the design and numerous proposals for efficient energy-aware routing and MAC protocols specifically for ad hoc setups [45]. A number of approaches to energy efficiency have also been recently developed for cellular networks

including the use of small cells for nomadic users [9], large base station antenna arrays for dense users in city based base stations [46] among other techniques. These approaches hold much promise but cannot be translated directly to the sparse/variable density, highly mobile motorway vehicular networks. A network wide energy minimisation approach attempts to deliver a packet from the source to the destination using the lowest amount of energy possible. Energy efficient routing schemes can reduce the power needed by all three functions of the transceiver (reception, transmission and processing) by minimizing the amount of data that is replicated in the network when routing the packet to its destination. Other energy optimisation approaches focus on minimising only one or a combination of the functions of the transceiver.

The highest energy consumption of the transceiver arises from the amplifier during transmission. If the transmission power is considered to be constant, the reception and processing energy take precedence in optimisation. On the other hand if a variable transmission range is considered, the transmit power plays an important role. With the ultimate aim of getting packets as far as possible towards the destination using the minimum energy, a clear and common issue is the trade-off between transmission range and the number of hops required for the packet to reach its destination.

### 2.8.2.1. INFRASTRUCTURE

From an infrastructural point of view, energy efficient routing can reduce the energy consumption of both vehicles and road side units by catering for smaller propagation distances for both entities. The authors in [47] study the

feasibility of reducing the propagation distance for a single RSU serving a unidirectional vehicular flow by use of scheduling that takes account of vehicle velocities to satisfy vehicular requests while they are at the nearest point. An energy efficient extension of propagation distances to bypass multiple relays is proposed in [48] to achieve energy savings in intelligent road signs that disseminate data to vehicles. They focus on the use of multiple input and multiple output (MIMO) whereby multiple nodes can cooperate to transmit the same data to a single/multiple node/s thereby taking advantage of diversity gain in MIMO space time coding. Smart routing schemes are used to implement a network wide RSU schedule in [49]. The routing schemes enable road side units to be switched on and off within a given time period while maintaining connectivity in a city scenario. They minimise the number of RSUs and optimise the time sequence of switching RSU power status based on vehicular locations.

### 2.8.2.2. VEHICLES

Energy efficient routing between nodes reduces either, the number of replicated packets in the network, or propagation distances thereby lowering transmission, reception, and operational energies of the transceiver. The authors in [50, 51] studied the energy efficiency of QoS optimised link state routing (OLSR) protocol using differential evolution. Using 802.11p definitions along with real data to model urban vehicular mobility models, they analysed the performance of DE-OLSR in comparison with the original OLSR. The authors in [52] use a differential evolution algorithm and a Monte Carlo method to search for energy efficient Ad hoc on demand Vector (AODV) configurations for VANETS. In [35], the delay incurred in delay

tolerant networks is exploited to reduce the energy used in vehicles by minimizing the propagation distance between vehicles and base stations. They propose a store carry and forward (SCF) relaying within a fully covered cellular architecture where vehicles store packets and physically advance the packet as they move towards the BS. They form an optimisation problem to determine the optimal between relaying through vehicles, transmitting to the base station directly or having the vehicle carry the packet closer to the BS. The geographic adaptive fidelity (GAF) model studied in [53] is a clustering scheme that reduces the number of vehicles participating in relaying by dividing the motorway stretch into grids where one or more optimal set of relay nodes are chosen in each grid to form a network backbone enabling other grid members to sleep when not transmitting their own data. Other clustering schemes such as double cluster head (DCH) and single cluster head routing schemes investigated in [33] showed energy savings can be achieved with acceptable QoS. They further show the energy efficiency gains when considering various market penetration ratios.

### 2.8.3 ENERGY SAVING IN ROAD SIDE UNITS

Since centralised access schemes present one option of providing network connectivity to vehicles on the motorway, the energy efficiency concerns to tackle when deploying them are important.

#### 2.8.3.1. COMPONENT LEVEL

Energy saving in RSUs can be divided into three general categories. The first approach lies at the component level using energy efficient hardware designs for the base station. The amplifier which consumes up to 40% of the base station energy only performs at an efficiency range of 5-20% [54].

Promising research on pre-distorted Doherty-architectures and Aluminium Gallium nitride (GaN) based amplifiers can push these levels to 50% while additional gains from using switch-mode power amplifiers rather than the standard analogue PAs can achieve lower current draw and lead to an overall component efficiency of 70% [54].

### 2.8.3.2. POWER SAVING SCHEMES

The second category of base station energy efficiency schemes use power saving protocols to enable low power sleep modes. Research showing a network wide 40% BS utilization for 90% of the traffic at peak times renders BS switching off schemes all the more important. While some [46, 55] have assumed a central controller to coordinate sleep cycles focusing on enhancing activation delay and reducing the ping-pong delay when resources are activated/deactivated several times, others [56] are pushing for decentralised BS sleep control due to the flat system architecture of LTE whereby radio resource control functionality is integrated in the BS. Various algorithms have been developed to determine which base stations are switched off and when they are switched off and energy savings between 8% and 46% [55, 56] have been achieved in suburban areas with up to 75% energy savings in urban areas [56]. In [41], the authors proposed dynamic switching for a BS in low traffic conditions. However, fast switching may not be feasible to accommodate transient traffic behaviour because of the number of operations a large BS has to perform [46]. This makes the architecture inapplicable for vehicular networks. In another study [42], the authors studied periodic sleep strategy for cellular networks, which led to 46% reduction in operating energy expenditure. However, the architecture

proposed was of the multi-layered type and deployed a cell breathing technique. Again, the cell breathing solution with its incurred overhead cannot accommodate fast user movement and variation in traffic demand, making it inapplicable for vehicular networks, especially in a motorway environment. Hence a macro-micro cellular structure may be considered, where a macro-cell served by a BS offloads data to its micro-cells served by the APs/RSUs, where these APs/RSUs operate sleep cycles to save energy during their inactivity periods.

### 2.8.3.3. NETWORK PLANNING

With the incumbent network the most energy efficient way of providing higher data rates is to provide smaller micro, pico and femto-cells that will effectively decrease the propagation distance from the base station to vehicles in urban roads providing power efficient broadband coverage. Prevalence of WiFi enabled devices has also rendered WiFi offloading attractive for mobile devices and thus for vehicular applications within a city scenario. OFCOM and Plextek discovered a 7x operational energy advantage in providing broadband through femto cells instead of expanding a macro cell network to meet a similar performance requirement [57]. The use of heterogeneous systems including UMTS, HSDPA, LTE, WIMAX and Wi-Fi further exacerbates the problem of efficient resource management. Parallel operation of these technologies may cause mutual interference. Furthermore an excessive deployment of smaller sized cells within larger ones may cause inefficient system utilization as the larger cell will be operating under low load conditions. Extensive research is therefore required in finding the optimum deployment strategies for the different sized

## 2.9 Renewable Energy

communication networks from QoS and energy perspectives. Figure 2.4 illustrates research trend in greening communication networks.

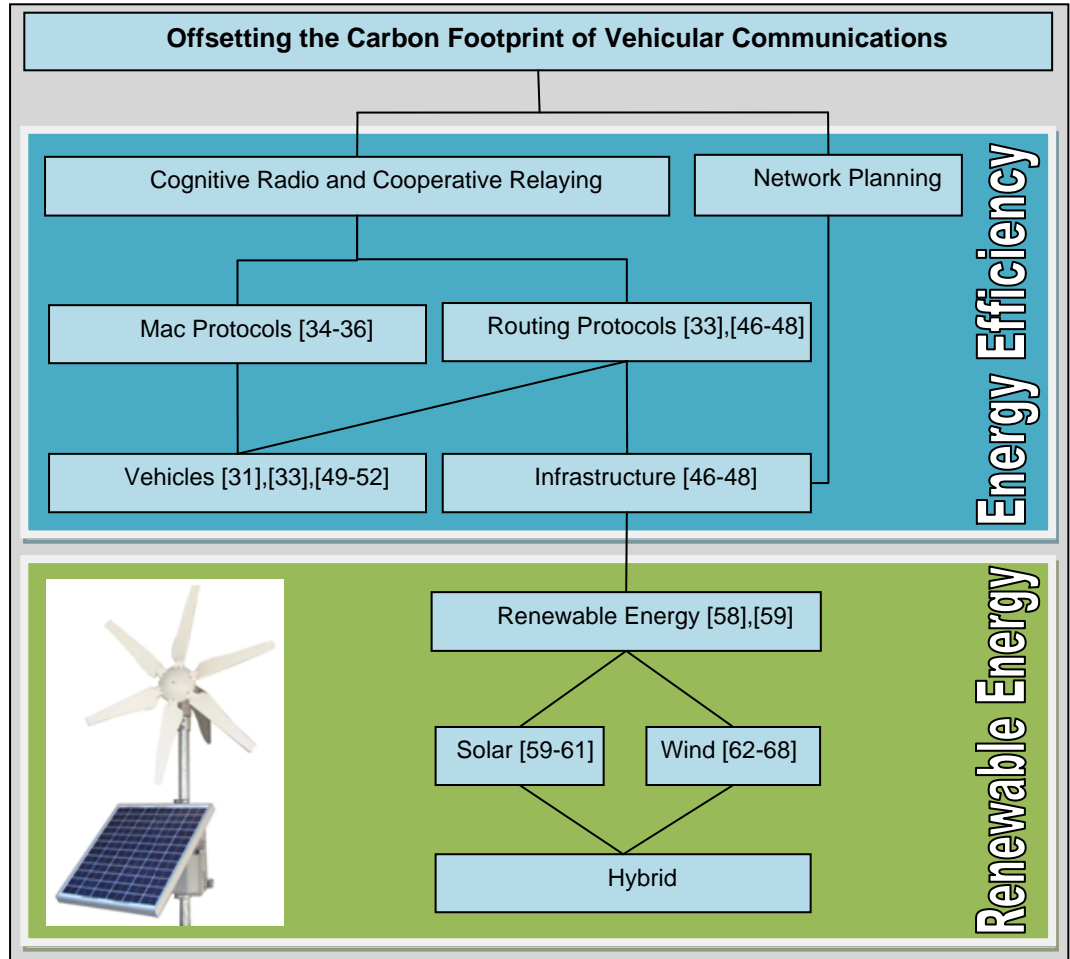


Figure 2.4: Main facets of greening vehicular networks.

## 2.9 Renewable Energy

Vehicular communication has always had more difficulty in meeting the QoS requirements compared to traditional wireless networks due to the dynamic environment in which it operates. The global push to reduce the carbon footprint has only amplified the challenges that must be addressed by VCNs. The dispersed nature of outdoor wireless systems presents both high economic and environmental costs in systems that provide full coverage. This is especially due to the fact that as we achieve mobility in the

wireless communication domain, ubiquitous deployments of wireless communication networks still retain the unyielding requirement of connecting to a power grid in rural areas. One such scenario is that of motorway communication, where continuous power supply to infrastructural devices is required to provide acceptable QoS. Traditionally base station optimisation strategies focusing on efficient deployments [9, 58] through the use of energy aware components and load adaptive hardware and software modules have been studied to address the environmental concern associated with the growing telecommunication industry. However a more economically attractive option that gives these devices complete independence is the use of renewable sources of energy such as wind or solar power [59]. A road side unit (RSU) with a wireless backhaul, or in a mesh network, coupled with a renewable source of energy significantly increases the speed and flexibility of deploying infrastructural telecommunication devices in such a scenario.

One approach to greening communication networks is to reduce their power consumption through energy efficient standardised technologies and protocols. A further reduction in the carbon foot print of the network (at the same power consumption level) can be achieved if renewable energy is used to replace the non-renewable energy sources. According to [60], renewable energy will power 4.5% of the world's mobile stations and more than 8% in developing countries by 2014. The sun is an excellent renewable energy source as it delivers up to  $1.2 \times 10^{14}$  kWh of energy (in just one hour) to the earth surface, which is equivalent to the total amount of energy consumed by human beings in one year [60]. In 2008, China Mobile had a number of BSs powered by renewable energy of which 76% were solar

## 2.9 Renewable Energy

powered BSs, and the remaining 24% were hybrid (solar + wind) powered [60]. NTT DoCoMo has also started considering hybrid wind and solar powered base stations, and has achieved 8.5 kWh from the sun and 6.0 kWh from the wind [60].

Various mesh networks have been deployed in America and developing nations which use solar power [61]. However, some of these networks' usage is limited to the day periods when solar power is available. On the other hand a motorway scenario relying on only renewable energy will require constant power even through the night as our real vehicular measurements show. Furthermore the solar irradiation values [62] that dictate the amount of solar energy that can be harnessed at those geographical locations are typically much higher than those of the UK, therefore a deployment of standalone solar powered RSU will require larger photovoltaic arrays and larger battery storage to provide enough energy for the expected load.

The viability of wind energy in such small scales has been tried and tested in several scenarios. Also known as small standalone wind energy conversion systems (SSWECS), these systems have been used to enhance the lives of rural residents in developing countries [63]. This work looking at the viability of wind power has developed methodologies to simulate the generating capacity and evaluate the adequacy of SSWECS. The evaluation however takes account of residential load and does not consider the stringent requirements seen in telecommunication networks to meet the QoS parameters.

The intermittent nature of wind power as wind speed rises and falls has pushed some, for example [64], to focus on energy storage systems coupled

## **2.10 Green Network Reliability**

---

with wind power generation, however most of these papers concentrate on wind farms that generate huge amounts of energy in the hundreds of mega Watts (MW) range to support large scale applications. These papers have also cited the necessity of appending storage systems to the generated wind energy, dealing with large amounts of energy without concern for flexibility. Hence, these studies fail to provide methods with which battery size can be scaled down to enhance the flexibility of deploying a dispersed system.

There is a significant variation in the achievable renewable energy depending on geographic locations and times periods. This introduces multiple variables in the design of communication systems and networks powered by renewable energy. Therefore when designing such standalone architectures, one needs to ensure that these renewable energy powered systems provide acceptable Quality of Service. With the decreasing cost of deploying small off-grid solar, wind and hybrid generators in the last few years, these renewable energy sources in conjunction with batteries will be an increasingly attractive option for standalone 5G BSs/RSUs in a vehicular environment especially in rural and country side motorway deployments.

## **2.10 Green Network Reliability**

The stochastic nature of power generation makes the analysis of reliability all the more important before deploying a standalone system. The reliability of power systems along with measurable indices have been looked at for various energy sources. The variable nature of wind power has also pushed for indices more specific to wind power generation [65]. All the reliability analysis available however has focused on extremely large loads with minor

variation divergent from vehicular network energy consumption profiles seen on the motorway.

To the best of our knowledge the analysis of the reliability of wind renewable energy has not been performed in conjunction with energy saving and QoS in any vehicular system. In Chapter 6 the use of sleep cycles is introduced in cluster heads to enhance energy saving while maintaining the QoS parameters. In Chapter 7 sleep cycles have been implemented in RSUs to lower the energy requirements so that the available supply coming from the wind power is sufficient at lower and variable wind speeds. In Chapter 8 the study of the reliability of RSUs supported by wind power will be performed through detailed reliability analysis with the use of probabilistic indices to define the performance of a standalone wind powered RSU on the M4 motorway.

The availability of vehicular communication systems becomes critical in the face of envisaged safety applications that have to be supported. When considering an off grid RSU powered by SSWECS, this reliability will be mainly dependent on wind availability. The reliability of power systems has received a lot of attention in research especially for critical systems [66] but more importantly for determining wind power generation system adequacy [67] when faced with the variable and stochastic nature of wind.

Achieving highly reliable communication systems becomes very difficult due to the intermittent nature of wind speeds as later discovered in this thesis. Hybrid mix of renewable and non-renewable energies therefore produce a better alternative for the critical telecommunications used in vehicular safety application. The impact of such distributed energy sources on the reliability of critical telecommunication facilities has been documented

in [66]. A probabilistic risk assessment associated with the possible power configurations available along with the optimal configuration was produced using non-renewable energy sources. By analysing the time to failure of the various power supplies they selected the most reliable energy sources and arranged them to be used in the most reliable order in case of failure thereby maximizing the reliability of critical telecommunications.

It has been noted that the modelling of wind generation cannot be approached in the same manner as conventional power systems [67]. Various metrics more applicable to the evaluation of wind power systems have been defined in [65], [67] and [68]. The authors in [67] choose the effective load carrying capability (ELCC) to denote the capacity value of wind power generation systems. They define a preferred method of calculation for a system with non-renewable power sources integrated with wind power renewables and analyse various approximate methodologies that have been employed in the calculation of capacity values.

Reliability analysis for wind energy embedded in power generation systems for an Indian scenario is also presented in [69]. They however define a reliability index as a loss of load expectation, or the probability that the power generating units of a system are unable to meet the demand.

Reliability and economic evaluation of small autonomous power systems (SAPSs) containing only renewable energy sources have been presented in [68]. Acknowledging the fact that power systems reliability indices are based on deterministic criteria, they perform a reliability cost and worth analysis on SAPSs deriving some basic probabilistic indices that define the performance of such systems. The probabilistic indices they consider include the LOLE but they go further by analysing the loss of energy expectation (LOEE) or the

expected energy that will not be supplied when the load exceeds the available generation.

Meantime to failure (MTTF) and mean time before failures (MTBF) discussed in [70] are two other reliability measures of software and hardware components that can be applied to gauge wind energy performance [69]. Such metrics along with mean time to repair (MTTR) have thus been used in [71] to predict network availability in terms of a forced outage rate (FOR).

## 2.11 Simulating Vehicular Communication Networks

The testing of communication protocols for VCNs becomes a problematic issue when one considers the complexity of VCNs that arise from the dynamic environment in which they operate along with the large-scale and extensive field test requirements. The cost and impracticality of such large scale field experiments has made simulations useful in validating VCN protocols. Using these simulators facilitates the implementation of scenarios several times enabling the modification of design parameters to get the desired results [72].

The two main features of VCN simulators are a detailed network simulator and a realistic simulation of vehicular mobility. The detailed network simulator as with MANETs must contain all the communication protocol layers necessary to evaluate the performance of the system. The complex features of node mobility such as speed, constraints on node movement patterns and user behaviour pose a challenge for simulating the mobility aspect [73]. As discussed earlier the vehicular environment and movement has a major impact on VCN MAC protocols, therefore a realistic mobility model implementation is as important as the network protocol model in

attaining reliable results. Various mobility models that have been researched for this purpose are reviewed in [74].

### 2.11.1 MOBILITY MODELING

Mobility models are a representation of how mobile nodes move. They describe the change in locations and speeds of mobile users in a dynamic environment so that the resulting effects can be implemented in the network simulators. As discussed earlier the high speed and mobility patterns associated with vehicles yields complexities in various communication layers which place restrictions on vehicular communications. On the other hand the mobility patterns also provide a setting for astute solutions that can lead to more efficient communication networks. For these reasons the study of mobility models is essential in developing the right VCN.

In recent years, substantial consideration has been given to vehicular mobility modelling. Vehicular mobile network research has witnessed progression from simple and unrealistic mobility patterns to complex precise and realistic models. Although both macro and micro mobility simulations have been developed and implemented by researchers, many still assume fully operational road networks devoid of various types of road incidents that may affect traffic flow and thus the whole mobility and network performance. Such challenges must be examined and mitigated in order to ensure the necessary QoS is provided to end users. This effort requires a rigorous investigation of the network simulator used to design these VCNs [74].

#### 2.11.1.1. CLASSIFICATION OF MOBILITY MODELS

Attention to details in mobility models is essential and dictates the accuracy of the models and thus the reliability of the simulation results. Such detailed mobility descriptions can be grouped into two main classes Macro-mobility and Micro-mobility. Macro-mobility describes all the macroscopic aspects that influence vehicular traffic such as motion constraints due to road topology, traffic lights, traffic flows, traffic density and initial vehicle distributions. Micro-mobility on the other hand describes individual driver behaviours when interacting with other drivers and road infrastructure such as accelerating, decelerating and overtaking [74, 75]. A functional way to classify mobility models is by having two functions. One for motion constraints as defined by the road topology and another, a traffic generator, that generates different types of cars and deals with their interactions according to the environment [74].

### 2.11.1.2. TECHNIQUES OF MOBILITY MODELING

Mobility models have come a long way since inception as they become more precise and realistic. Research evolution through four stages of mobility modelling has been presented in [76]. Early approaches began with a random node movement technique which was implemented within the network simulator. This was imprecise for vehicular movements. The next stage saw real-world mobility traces fed into the simulator. These traces were as precise as mobility models can get but lacked flexibility. Road traffic micro-simulation provided the flexibility that was lacking in real traces but introduced a level of artificiality. Finally Bidirectional coupled simulators allowed simulators to factor in the effects of traffic on the nodes [76].

#### ***Random Node Movement***

The first mobility model for ad-hoc networks was based on an unconstrained random movement of nodes. The ease of implementation of the scheme kept it around for a long time with minor adaptations such as the introduction of the Manhattan Grid which placed constraints on pedestrian mobility modelling. Other adaptations came later to consider inertia and vehicular constraints to road topology [76].

### ***Artificial Mobility Traces***

A move to artificial mobility traces was done in order to allow the manipulation of mobility parameters which was restricted in real-world mobility traces. A level of artificiality was introduced to the simulation; however a higher degree of realism can be achieved by increasing the complexity of the node mobility simulator. This merged the field of transportation and traffic sciences with communications allowing common mobility models to be applied to network simulators.

### ***Bidirectionally Coupled Simulators***

The data traffic in the networks such as accident information, hazard warnings, and road congestion information affected driver's behaviour and thus node mobility, and called for the development of bidirectionally coupled simulators. With these schemes, the network simulator and the traffic simulator exist as two interdependent processes running concurrently sharing mobility information. In such a way the network simulator sends parameter changes to the road traffic simulator which influence vehicle routing decisions. The road traffic simulator then recalculates vehicle movement and updates the network simulator.

### ***Real-World Mobility Traces***

Real world mobility traces were a significant step forward as they modelled mobility based on pre-recorded vehicle traces. The recordings were based on vehicle GPS readings taken periodically and stored. The processed readings are then fed to the simulator as trace files to simulate node positions with their corresponding vehicle locations at each time step. This scheme however lacked scalability due to the process required to obtain the data. It also lacks flexibility because the trace files are pre-recorded and thus place a bound on the mobility parameters that can be changed.

### **2.11.2 MOTORWAY VEHICULAR MOBILITY MODEL AND SIMULATION**

A vehicular network simulator is based on a communication layer and a vehicular mobility model. To integrate both of them in a seamless fashion is considered to be a very time consuming task [77]. Though the design of a detailed vehicular network protocol is straightforward, the challenging features of node mobility such as speed, constraints on node movement patterns and user behaviour still pose a challenge for simulating the mobility aspect [73].

To model vehicular mobility is quite challenging as one has to consider a number of parameters such as road network, number of vehicles, vehicles' average speeds, types of vehicles etc., and characteristics such as free flowing and congestion causing acceleration/deceleration, lane changing etc., and scenarios such as road works, accidents, incidents, road conditions. Such scenarios/incidents/occurrences will significantly alter the mobility pattern of vehicles that were previously moving at very high speeds.

These realistic sudden changes can present a mobility model that misrepresents the original vehicular mobility model used in simulations. The result would be the design of a communication system that does not cater for unexpected incidents. The vehicular environment and movement therefore have a major impact on these protocols; therefore a realistic mobility model implementation is as relevant as the network protocol model in attaining reliable results.

### **2.11.2.1. VEHICULAR TRAFFIC TRACES**

To fully grasp the mobility characteristics of motorway users, a comprehensive Statistical analysis has also been carried out on vehicular traffic flow profiles recorded by inductive loop ID 2255 on the M4 motorway, UK on Friday April 19, 2002 from 00:00 to 23:59 hours. Further analysis was carried out on the data based on other inductive loops at other times and dates and similar trends were observed. These trends provide important mobility characteristics that can be used to derive our accurate vehicular traffic model. The data recorded consists of traffic flow rate, type of vehicle, average speed and lane numbers. The data has been used to produce the probability density function (PDF) of the inter-arrival times for the vehicles as seen in Figure 2.5. The PDF reveals vehicular inter-arrival times of 1-4 seconds based on all three lanes of the motorway.

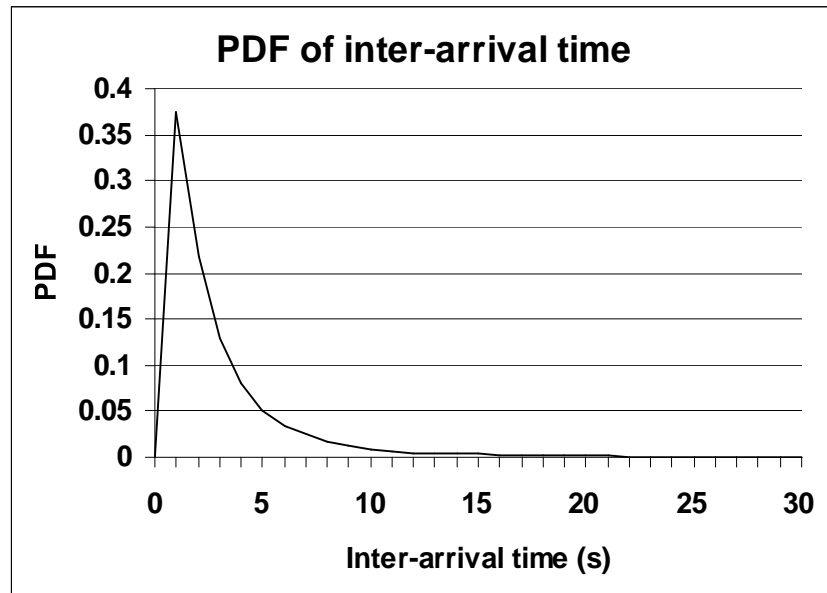


Figure 2.5: PDF of inter-arrival time

Another important parameter is the traffic intensity per lane. Figure 2.6 shows the number of vehicles in different motorway lanes. Interestingly, in the very early hours of the morning, lane 1 has the highest number of vehicles. The reason for this is a large number of heavy good vehicles (HGVs) travelling at that time as compared to the other vehicles and also HGVs normally travel in lane 1 unless and until they have to overtake any other vehicle or an obstacle. However, after 6:00am lane 2 and lane 3 exhibit a rising number of vehicles arriving at the motorway due to business traffic before 09:00am and subsequently in the afternoon still lane 2 and lane 3 have a much higher number of vehicles as compared to lane 1.

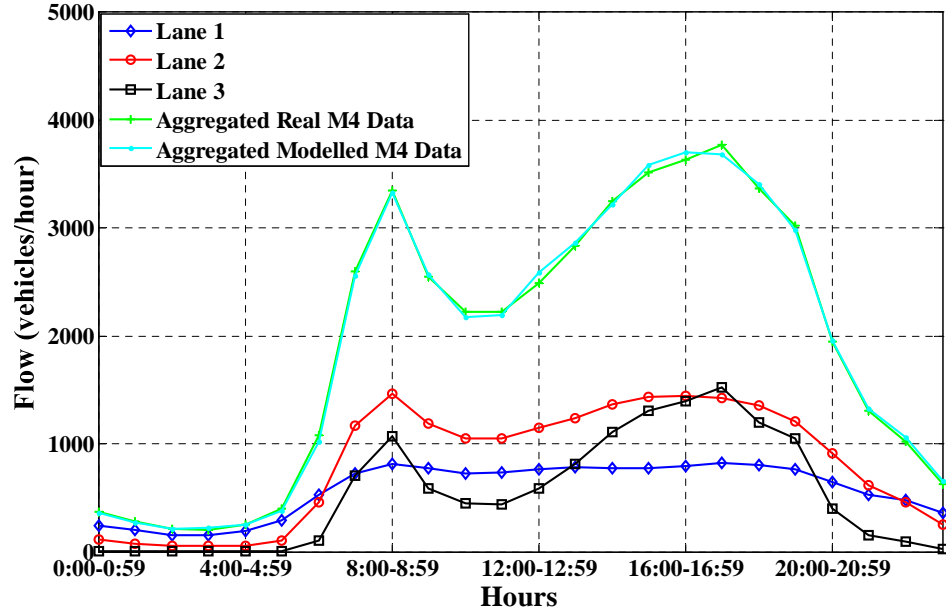


Figure 2.6: Vehicular flow per hour

Figure 2.6 also shows the per-lane and aggregated flow at the inductive loop for each hour. It also reveals that the busiest hours for that inductive loop were between 15:00 and 18:00 hours. Figure 2.6 demonstrates that both the real traffic flow data and modelled data are in good agreement. Consequently, this figure shows that the arrival of vehicles at a base station on the M4 follows a Poisson distribution, and illustrates the accuracy of the approach.

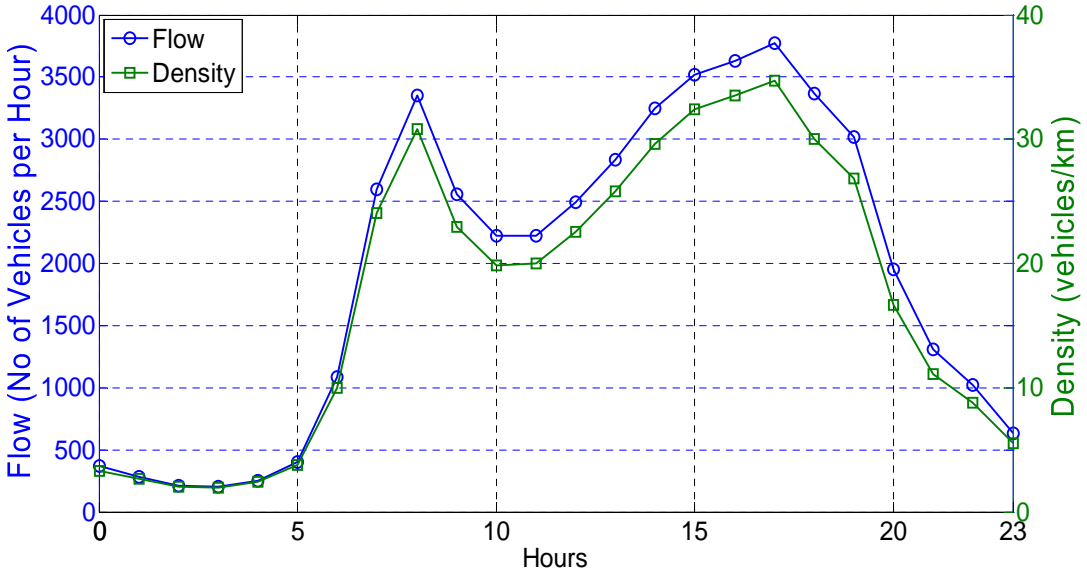


Figure 2.7: Hourly Vehicular Flow and Density

Vehicular traffic is traditionally modelled using vehicle traffic flow theory [78-81] in the transportation research literature. The three main parameters are flow  $q$  (vehicles/hour), speed  $v$  (km/h) and density  $d$  (vehicles/km). The average values of these quantities can be approximately related by the basic traffic stream model as [79, 80]:  $s = q/d_v$ . With fewer vehicles on the motorway, the density  $d_v$  approaches zero but vehicles are assumed to reach their free flow speed  $s$ . As soon as more vehicles enter the motorway, both the traffic flow  $q$  and the density increase until the flow reaches its maximum value. As additional vehicles continue to enter the motorway, the traffic density increases but the flow decreases. When the traffic density reaches the saturation point called jam density limit, the traffic flow becomes zero as all the vehicles stop and are tightly packed on the motorway causing traffic jam. Figure 2.7 shows the average density per km on hourly basis, using the speed equation, demonstrating the increase in the density with an increased flow.

Figure 2.8 illustrates the probability density function (PDF) of vehicles' average speed which demonstrates that the average speed for different types of vehicles, different lanes and different hours of the day is about 30 m/s. Furthermore, the PDF further indicates that in some cases the average speed is as high as 40 m/s, however, in some it is as low as 15 m/s.

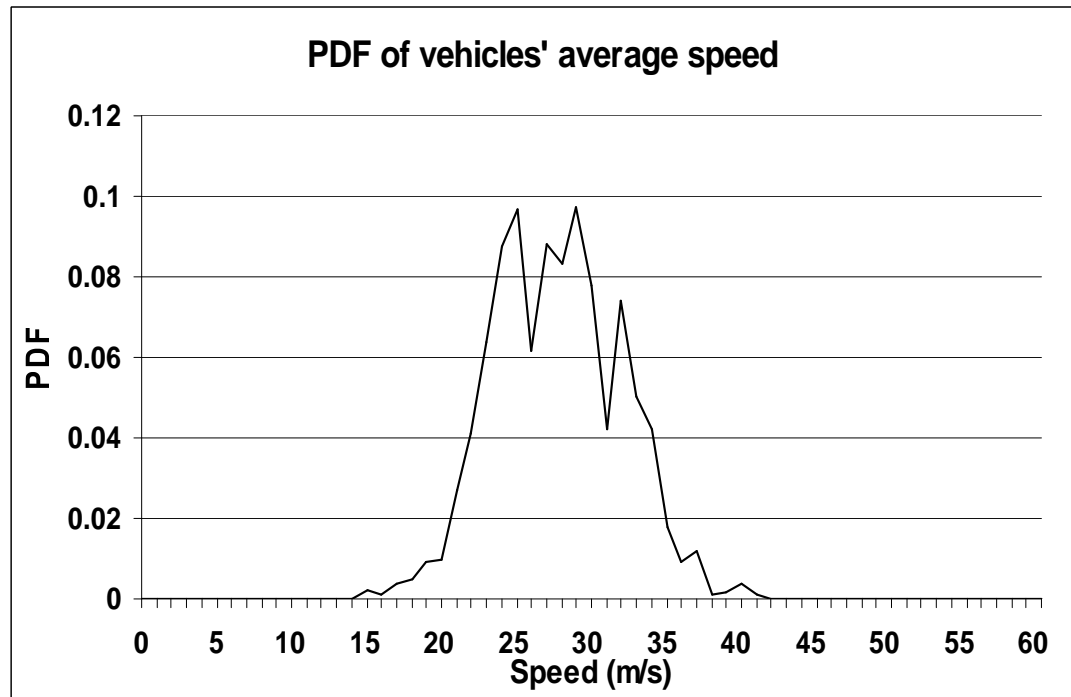


Figure 2.8: PDF of vehicles' average speed in m/s

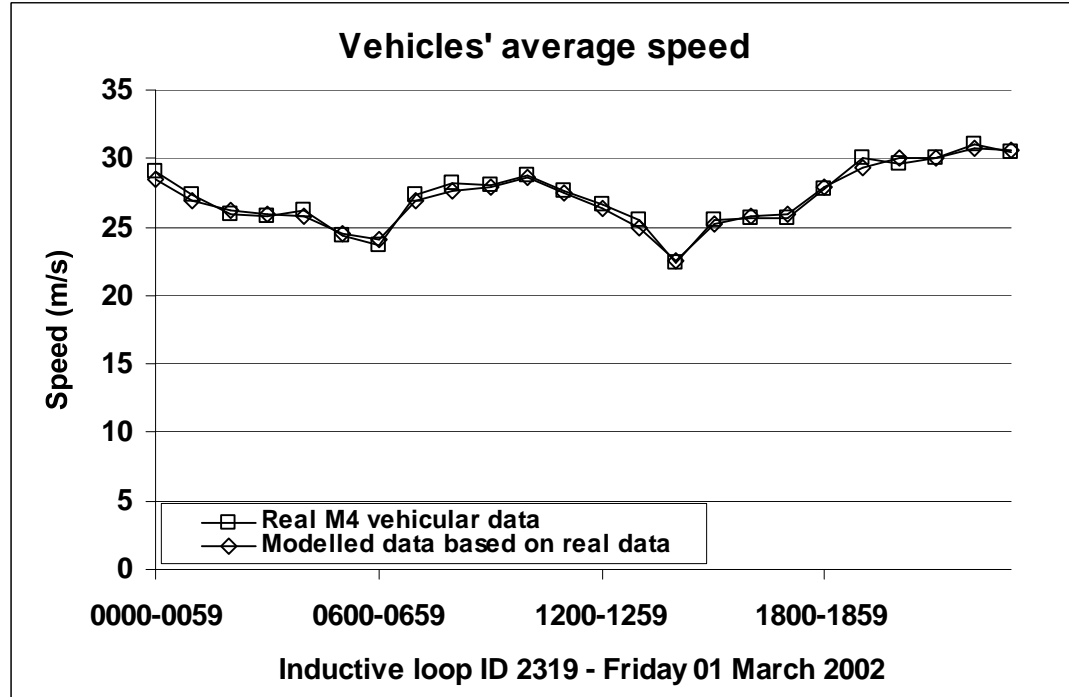


Figure 2.9: Vehicles' average speed in m/s

Figure 2.9 shows the distribution of vehicles' average speed in m/s for each hour of the day. A notable point is the rise in the vehicles' average speed after 7:00am which corresponds to drivers attempting to reach their offices generally before 9:00am. Furthermore, during rush hours in the afternoon, we can see a dip which is due to the increased number of vehicles at that time causing congestion thus reducing the average speed. Using a normal distribution (sum of many random vehicle speeds approaches normal distribution), we have modelled the average speed of the vehicles where the distribution parameters are extracted from measurements on a 1 minute interval and used these in the simulator. Both real vehicular and modelled data are in good agreement as shown in Figure 2.9.

### 2.11.2.2. VEHICULAR TRAFFIC SIMULATION

Vehicular networks, growing fast day by day, are placing immense pressure on the base stations to accommodate a large number of mobile sources for communications. This reason has motivated us to design a motorway simulator (vehicular and communication) which can adapt to the dynamic behaviour of the vehicles and their communication patterns in a motorway scenario.

Many variables have been defined to control the flow of the simulator procedure, as well as to execute the required tasks for managing vehicular communication with the base stations. The *sysTime* variable generates and controls any event during the simulation run time. It represents the number of seconds the simulation has been running and is responsible for the vehicles movement. A variable *vehCounts* keeps count of the vehicles initialised during that hour. The variable *hour* which ranges from 0-23 is entered by a user in an interactive fashion to make the simulator run at a specific hour and analyse specific characteristics of traffic flow parameters. The user can also decide to change settings to run the simulator for all 24 hours obtaining result printouts as the hours progress.

The *motorwayStructInitialisation()* method sets the length of the motorway and divides it into sections denoted by the variable *numberOfBoxes* where each Box represents an index of an array and is 5 meters in length. The vehicles keep a record of their original speed and lane, and can accelerate, decelerate and change lanes to overtake any slow moving vehicle or obstacle. Being an event-driven simulator, each vehicle on each iteration checks the distance to the vehicle ahead. If the vehicle is in its original lane

## **2.12 Summary**

---

and there is enough space ahead to cater for the speed of the vehicle, the vehicle remains in the same lane and maintains its speed. If there is not enough space for the vehicle to maintain the original speed, the next lane is checked and if enough space is found without compromising the speed of the vehicle, the vehicle changes lane but maintains the same speed.

In another scenario, if there is not enough space in the vehicles lane and the next lane or the previous lane does not have enough space, we assume that the vehicle can find out the lane which has maximum space and changes lane accordingly and reduces its speed if necessary. If the vehicle changes its lane or reduces speed during the course of the simulation, it keeps looking for space to go to its original lane and at its original speed [82]. Based on the analysis shown in Figure 2.8, the maximum speed of the vehicle is set to 40 m/s.

## **2.12 Summary**

This chapter has provided an overview of vehicular networks, their applications, and the motivation for research into the field. The literature on the aspects of vehicular networks that will be the focus of our research such as mobility, routing, medium access, physical layer, and energy efficiency have been reviewed, providing background information and illustrating the main problems and what aspects need further investigation. A brief description was given of the vehicular mobility simulator developed.

---

## 3 Energy Efficient Routing

### 3.1 Introduction

Paying particular attention to some special characteristics of vehicular networks, the network topology of the motorway can make use of multi-hop routing approaches to cover large areas with sparse base station deployments [35, 83]. The highest energy consumption of the transceiver is mainly due to the power amplifier while transmitting. If the transmission power is considered to be constant, the reception and processing energy take precedence in optimisation. On the other hand if a variable transmission range is considered the transmit power plays an important role. With the ultimate aim of getting packets as far as possible towards the destination consuming minimum energy, finding the optimal trade-off between transmission range and the number of hops required for the packet to reach its destination is essential.

This chapter examines a range of routing schemes to determine the network wide energy effects of routing a packet using vehicle to vehicle (V2V) communication through a 5 km motorway stretch to a base station. The impact of relaying the packet through a higher number of short ranged transmissions or fewer hops with long ranged transmissions at different experimentally measured vehicular densities is evaluated. A simulation is performed considering shortest hop, and a most forward hop scheme followed by linear programming optimisation which determine the optimum

### **3.2 Proposed Scenario**

---

number of hops and optimum hop lengths required at each hour of the day (different vehicular densities) to achieve the most efficient route to the base station. In order to determine whether the average hourly hop lengths for the various schemes are viable to achieve full connectivity on the 5 km motorway stretch, these distances have been applied to the cumulative distribution function of inter-vehicular spacing ( $CDF_{IVS}$ ) to obtain the probability of connectivity at each hour.

### **3.2 Proposed Scenario**

The motorway strip consists of 6 lanes with vehicles in 3 lanes going towards the base station while vehicles in the other lanes travel away from the base station. The vehicles' radios have a 1 km maximum transmission range and routing takes place with vehicles travelling in both directions. A simulation of the furthest vehicle from the base station requiring one packet to be routed to the base station is performed using the java based motorway simulator [84]. In the shortest hop scheme the packet is transmitted to the nearest vehicle in the direction of the base station until it reaches the base station. With the multi-hop scheme the packet is transmitted to the furthest vehicle within the radio coverage until it reaches the base station. To find the optimum trade-off we introduce a linear programming formulation to minimise energy consumption by considering all transmission and reception energy costs.

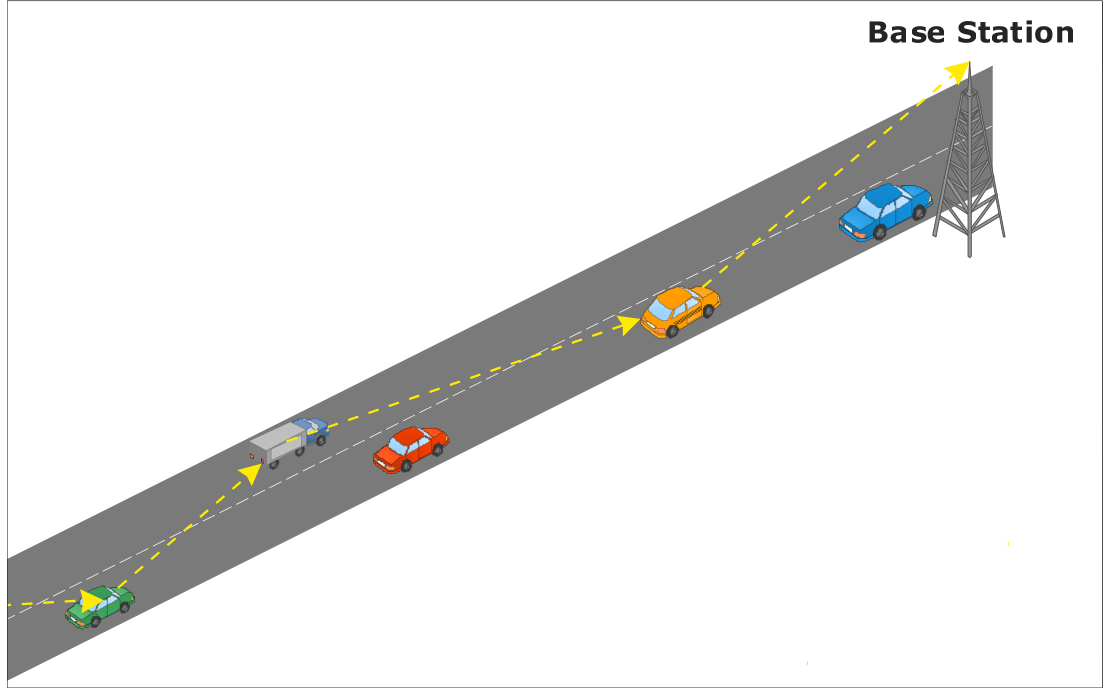


**Figure 3.1: Multihop routing scenario**

### 3.3 Energy Model

The energy consumed for a packet transmission is the sum of energies consumed in transmitting and receiving when routing a single packet to the base station sink. The energy consumption in the transmission state ( $e_t$ ) is given by [85],

$$e_t = e_e + e_a d^v = \frac{P_{tc}}{d_r} \quad (3.1)$$

where  $e_e$  is the electronic energy and  $e_a d^v$  is the distance dependent amplifier energy.  $P_{tc}$  is the total power consumed by the transmitter circuitry, and  $d_r$  is the data rate. The  $P_{tc}$  is a distance dependent value that reaches a maximum transmit power of 10 W which includes circuitry power and amplifier power consumption making  $1.67 \times 10^{-6} \text{ J/bit}$  the highest energy that can be consumed per bit.

$$e_{t\_bit} = \frac{10 \text{ W}}{6 \text{ Mbps}} = 1.67 \times 10^{-6} \text{ J/bit} \quad (3.2)$$

Based on direct measurements of input voltage and current draw of IEEE 802.11 network cards the power utilised by a receiver ( $P_{rc}$ ) is up to 75% of  $P_{tc}$ [85]. Hence the energy consumed for the reception of a bit ( $e_{r\_bit}$ ) is

$$e_{r\_bit} = \frac{P_{rc}}{d_r} = \frac{7.5 \text{ W}}{6 \text{ Mbps}} = 1.25 \times 10^{-6} \text{ J/bit} \quad (3.3)$$

## 3.4 Simulation of Shortest and Most Forward Hop Schemes

The shortest hop and most forward hop routing schemes were simulated on the motorway vehicular simulator with vehicles moving over a 24 hr period. The status of vehicular motion and data communication is updated every one second. In each second a packet is generated from the furthest vehicle from the base station and routed using the shortest hop. In addition we also examined using the most forward hop with the resulting number of hops and energy consumption of the routing being saved for each scheme, and averaged over 3600 seconds.

In the shortest hop scheme a packet is simply routed to the nearest vehicle in front of the vehicle currently holding the packet. The energy cost of each hop is calculated using the propagation and energy models developed earlier. In the most forward scheme, a vehicle holding a packet checks the distance of leading vehicles. Starting from the nearest vehicle, the transmitting vehicle progressively checks further vehicles until it is no longer able to scan beyond the limiting 1km radio range. The furthest vehicle within the range is thus chosen to be the next hop and the packet is transmitted

with costs being measured as done in the shortest hop scheme. At the end of the hour the average hop length and energy cost are calculated.

### 3.5 Linear Programming Optimisation Model

The java based motorway simulator has been used to obtain link details including the cost and distance for every link using 10 snapshots evenly spread within each hour. The AMPL/CPLEX Mixed Integer Linear Programming (MILP) solver was used to solve the LP model. The optimisation of this routing scenario is performed using network flows where the transmission and reception energies are minimised along the path. In the Linear Programming (LP) model, a network topology of  $G = (N, L)$  with  $N$  vehicles as nodes and  $L$  possible wireless links between vehicles is considered. Furthermore, the links are formed only in the direction of the base station, therefore vehicles closer to the base station cannot transmit to vehicles further away from the base station. The arcs and their costs are based on the locations of the vehicles along with the propagation and energy models. A unit of flow (packet) is inserted at the furthest vehicle from the base station and received at the base station. The LP model that minimises the energy to route the packet to the base station is as follows:

**Objective:** minimise

$$\sum_{(i,j) \in L} c_{ij} x_{ij} \quad (3.4)$$

**Subject to:**

$$\sum_{t_x, j} x_{t_x j} = 1 \quad \forall j \in N \quad (3.5)$$

$$\sum_{(i,k) \in L} x_{ik} = \sum_{(k,j) \in L} x_{kj} \quad \forall i, j, k \in N \quad (3.6)$$

where the variables, parameters and indices are defined in Table 3.1 . The cost of a link,  $c_{ij}$ , is the energy used by that link in transmitting and receiving a packet. The variables are the selected nodes in the routing path, and variables with a value of 1 comprise a minimum-cost path from the furthest vehicle to the base station. Constraint (3.5) ensures that exactly one packet is available at the entrance to the transmitting node. Constraint (3.6) ensures network balance where all nodes except the furthest vehicle have one packet received and one packet transmitted.

<b>System Configuration:</b>		
Channel bit rate		6Mb/s
Motorway stretch		5 km
No. of packets		1
Packet size		53 Bytes
Medium access control (MAC) protocol		802.11p
<b>Propagation:</b>		
Transmit power		20 dBm
Spectrum		5.9 GHz
<i>Antenna:</i>		<i>Base station</i>
Height	10 m	1.5 m
Gain	17.5 dB	17.5 dB
<b>Path loss:</b>		<i>V2R</i>
Breakpoint distance	1200 m	177 m
Path loss exponent 1	3.4	2
Path loss exponent 2	N/A	3.4
Path loss		0.34 dB
Receiver threshold		-86 dB
<b>Energy:</b>		
$e_{t\_bit}$		$1.67 \times 10^{-6}$ J/bit
$e_{r\_bit}$		$1.25 \times 10^{-6}$ J/bit
<b>Sets:</b>		
$N$	Vehicles	
$L$	Links	
<b>Parameters:</b>		
$t_x$	Tx Vehicle at location 0	

$c_{ij}$	Cost of each link $(i,j) \in L$ between node $i$ and $j$ ;
<b>Variables:</b>	
$x_{ij}$	Equals 1 if link $(i,j)$ is being used, 0 otherwise

Table 3.1: System Parameters [86], [87], [88], [89]

### 3.6 Performance Evaluation

The number of hops taken and the average hop distance for every hour in our scenario can be seen in Figure 3.2. The shortest distance hop scheme tends to cover the shortest distance per hop while using the most hops. The hop length can be seen to steadily rise to reach a 384 m peak at 2 am then fall again reaching the lowest average hop distance of 24 m at the peak hours of 3 pm and 4 pm. The increase in distance at early hours of the morning is due to the low vehicular flow and density. As seen in Figure 3.5, the CDF curve for low vehicular flow has a higher probability for higher inter-vehicular spacing, and with such high inter-vehicular spacing the shortest hops increase in distance at low vehicular flow. A reciprocal effect is seen in the number of hops with a minimum at the early hours and a maximum at the peak hours. The number of hops however is solely dependent on the vehicular density in the 5 km stretch as a packet traverses all intermediate nodes before reaching its destination. Ideally the most forward hop scheme should have used a full 1 km range in 5 hops to reach the base station. Due to the difficulty in locating nodes at the ideal 1 km separation for the maximum radio range, routing to the base station using the most forward hop required 6 hops throughout most of the day. Although the first five hops can approach 1000 m the final hop to the base station is typically small and brings the average hop length down to 833 m. The optimum path showed

### 3.6 Performance Evaluation

---

the same trends as that of the most forward hop scheme indicating the optimality of the most forward scheme.

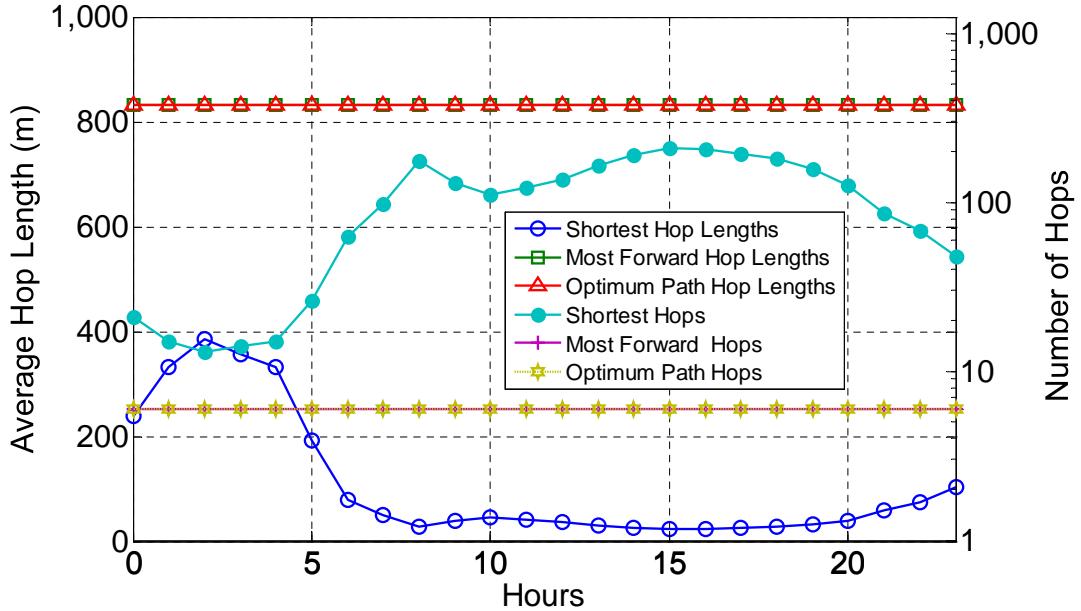


Figure 3.2: Average hops and hop lengths per hour

The resulting energy use for a packet to reach the base station is shown in Figure 3.3. The shortest hop scheme has the highest energy consumption out of the three schemes. The high consumption is due to an increase in the number of hops which incurs reception energy costs (note transmission energy costs are low here since the hop distance is short) as the vehicular density rises. The energy curve for shortest hop scheme therefore follows the vehicular density with minimum energy expenditure of 7.8E-3 J at the early hours and a peak of 0.11 J at the hour with the highest density. The most forward hop routing scheme used less than 4.5% of the shortest hop scheme power usage when both are compared at their peak. Peak energy use is observed in the highest density hours when the transmission range as seen in Figure 3.2 is maximised. The optimum path (LP) energy consumption was able to maintain 4% energy consumption most of the day.

### 3.6 Performance Evaluation

---

In essence, the optimum distance is the most forward distance which can thus be used in a motorway scenario to achieve the energy savings found in Figure 3.3. When considering the dynamic nature of vehicular communications however, selecting these optimum transmission distances may not maintain connectivity in the motorway scenario. There is thus a need to analyse the effect of vehicular mobility on the suggested transmission distances in the three schemes. This is later examined in Figure 3.6 after giving some attention first to the impact of transceiver design on energy efficiency in these energy efficient vehicular routing schemes.

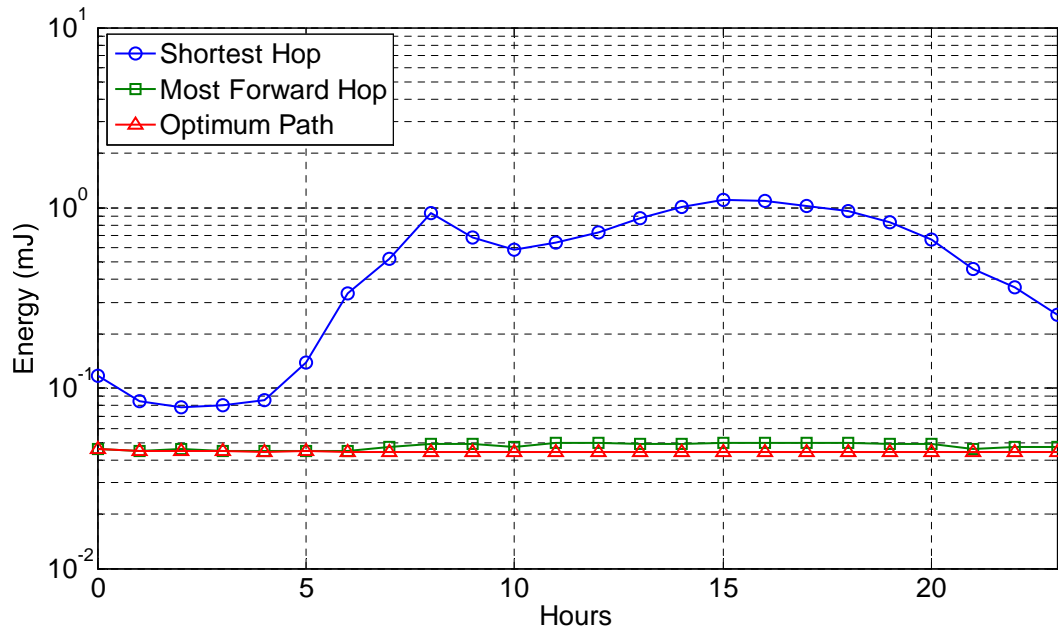


**Figure 3.3: Energy consumption**

To reduce the energy consumption of shortest hop schemes we propose energy efficient transceiver designs that aim to lower the energy consumed in the reception of a packet ( $e_r$ ). Figure 3.4 illustrates the effects of increasing the efficiency of a transceiver to attain lower energy consumption when receiving packets. The graph shows the resulting energy consumption at 1500 hr when the receive energy is decreased by a certain percentage.

### 3.7 Route Connectivity

---

The shortest hop scheme exhibits the highest gradient showing how the energy consumption of the scheme is mainly due to reception energy especially at 1500 hrs, therefore every 10% reduction in receive energy resulted in nearly 10% reduction in total energy consumption for the scheme. The most forward hop scheme and the optimum path once again showed the same trend since the most forward hop scheme has been determined to be near optimum. As the reception energy is reduced the reduction in overall energy was minimal in the most forward hop scheme because the main energy component at such a low hop count is the transmission energy.

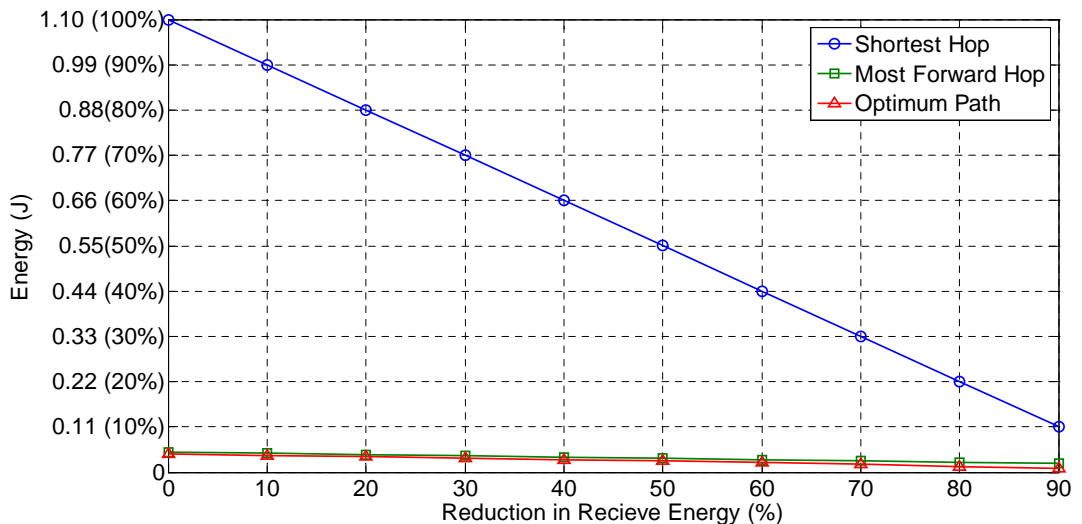


Figure 3.4: Energy consumption with lower reception energy.

### 3.7 Route Connectivity

Inter-vehicle spacing (IVS) plays an important role in the process of analysing and designing routing schemes for vehicular ad-hoc networks (VANETs). The analysis provided in this section helps determine the dynamic propagation range according to the hours of the day. We have mainly divided the traffic flow into three categories which are low, moderate and high. If the vehicles are estimated to be less than 2000 per hour (off-

### 3.7 Route Connectivity

---

peak i.e. early and late hours of a day), they are considered to reside in low traffic flow. Moderate traffic flow ranges from 2000 to 5000 vehicles per hour (off-peak approaching peak) whereas over 5000 vehicles per hour (peak traffic) represent high vehicular traffic flow. All these different flows are used accordingly to calculate the cumulative distribution function (*CDF*) for *IVS* as follows:  $CDF_{IVS} = 1 - e^{-\lambda_{IVS}s_m}$  where  $s_m$  refers to the spacing in meters and  $\lambda_{IVS} = q/(3600 \times v_{mps})$  where  $q$  refers to vehicular flow (vehicles per hour) and  $v_{mps}$  refers to the velocity in meters per second. The  $CDF_{IVS}$  depicts the true picture of vehicular connectivity in a UK motorway scenario. Figure 3.5 shows that approximately 92% and 97% of vehicles are within a range of 100 and 150 meters respectively for high vehicular traffic flow. For IVS of 100 and 150 meters, approximately 70% and 84% are within each other's range in the case of moderate traffic flow. With the same IVS of 100 and 150 meters for low vehicular traffic flow, only 18% and 26% of vehicular nodes are in each other's range which is a highly sparse network due to early and late hours of the day.

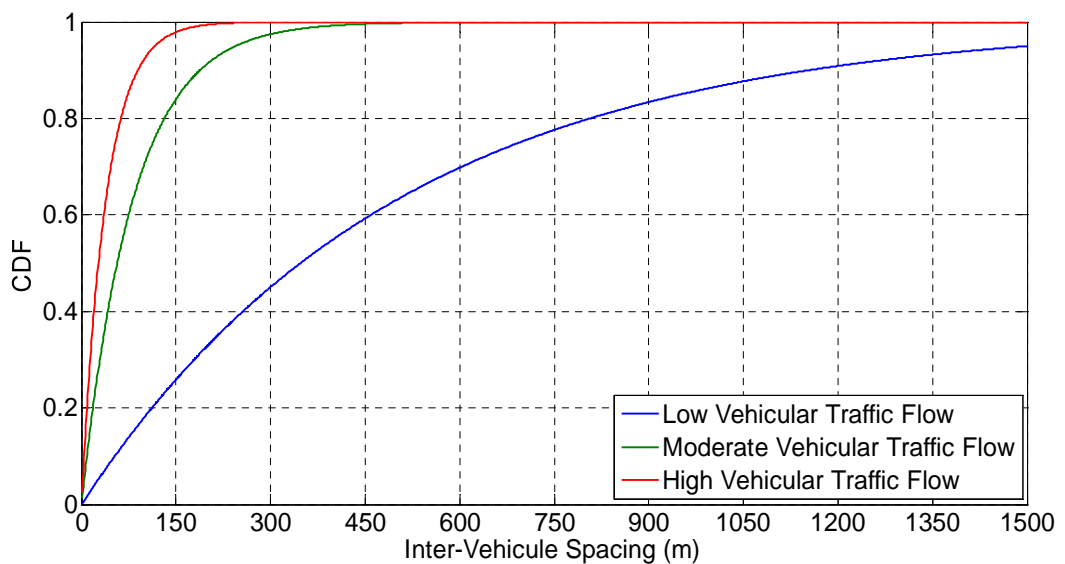


Figure 3.5: CDF of inter-vehicle spacing

To study the effect of vehicular mobility on the motorway routing schemes considered, the inter-vehicular spacing CDF is used to calculate the probability of the packet successfully finding a connected route to the base station. The probability of connectivity illustrated in Figure 3.6 takes account of the average hop distances for each scheme and the traffic level at each hour. Figure 3.6 illustrates that the selection of most forward routing and optimum path routing (LP) is viable between 7 am and 9 pm during moderate and high traffic as the probability of connectivity is above 99%. At low traffic times, ie late night and early morning hours, the probability of connectivity for most forward hop and optimum path routing (LP) falls to 80%. The fall in connectivity even when using maximum transmission range suggests that vehicular spacing may exceed the radio's range up to 20% of the time on average at low traffic. The shortest hop scheme has a probability of connectivity that lies between 20% and 40%. Though the trend may seem irregular, it first follows the distance curve for shortest hop scheme in Figure 3.2 steadily rising between 12 am and 3 am until it reaches the maximum hop distance at 3 am where it then steadily falls until 6 am. The curve then exhibits a sudden increase in probability of connectivity as vehicular traffic transitions to a moderate level. At moderate and high traffic levels the probability of connectivity for shortest hop scheme is then maintained between 20% and 25% through the hours of 8 am and 7 pm before steadily rising to 37% at 9 pm as hop distances increase at moderate level traffic. Finally a drop is seen in the final hours of the night as the curve transitions to low vehicular traffic category.

### 3.8 Summary

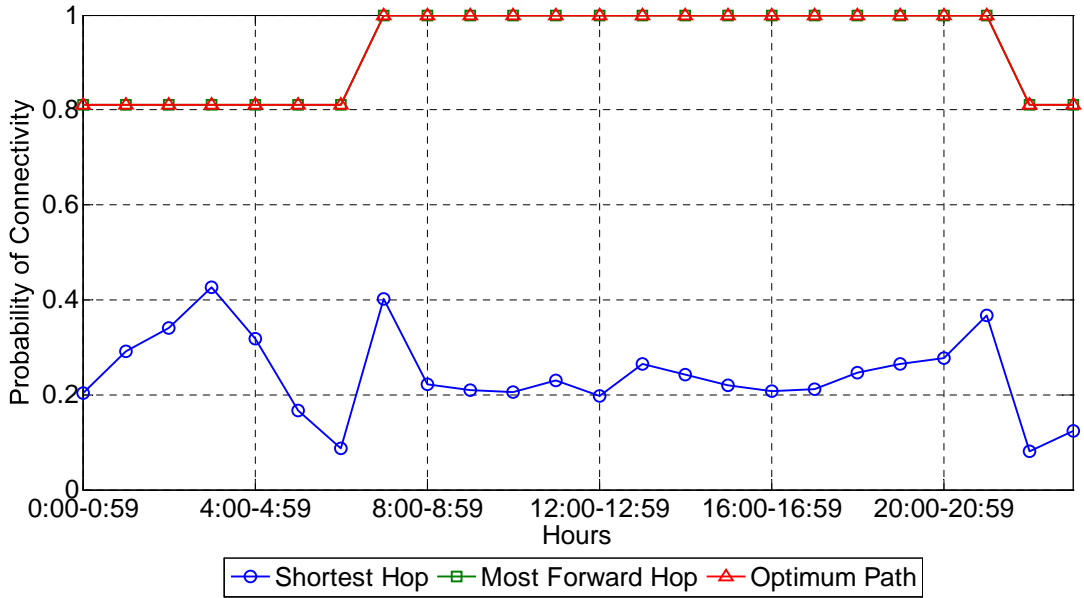


Figure 3.6: Probability of connectivity

To maintain connectivity at all hours of the day we propose (solar powered) road side units or relays to be placed at regular intervals to supplement the maximum vehicular transmission range. These road side units can ensure that all vehicles are connected even when the vehicular density is low. The road side units can relay vehicular data traffic through a mesh network of participating vehicles to the base station. Such a relay network warrants further study and is covered in Chapter 6.

### 3.8 Summary

In this chapter, the mobility profile of vehicles on the motorway has been analysed and used it to determine the energy consumption of a number of routing schemes with the aim of deriving the optimum number of hops and hop lengths required for a packet to traverse a 5 km motorway stretch (typical maximum base station coverage). A Linear Programming (LP) optimisation was used to derive an optimum routing scheme which was compared to other routing schemes. The shortest hop routing scheme

### 3.8 Summary

results have shown that minimizing the transmission range maximises the number of hops and thus the network wide reception energy becomes large. Transmitting with maximum range has been shown to be an optimum heuristic that achieves results comparable to those obtained from the optimum linear programming routing approach. The average hop lengths required in each scheme were then used with the CDF<sub>IWS</sub> to examine how the use of such transmission ranges affects the network connectivity given the dynamic nature of the motorway environment. The shortest hop distances are not an appropriate choice as the probability of connectivity is too low to achieve viable communication while the optimum (LP) and most forward hop scheme can be utilised at moderate to high traffic (over 99% connectivity) and have acceptable connectivity at low traffic (80%). To enhance the use of the derived optimum routing further, intermittent fixed relay nodes can be used to maintain connectivity during hours with low vehicular traffic. Chapters 6 and 7 will examine the viability of these relay nodes and will examine their use when they operate with energy efficient sleep cycle strategies and with time varying renewable energy.

---

## **4 Energy Performance of 802.11 and MPRMA**

### **4.1 Introduction**

With the advent of delay sensitive communication, enhancing the quality of service (QoS) in communication networks has become a primary goal in research. As environmental awareness became a global concern, research in energy efficiency has also intensified. As the network sizes and users increase, the need for energy efficient networks is becoming acute leading to research aimed at enhancing the energy efficiency of communication networks. Therefore there is a need to design and develop systems which can reduce the energy consumption while maintaining the QoS. To evaluate the performance of the network realistically, it is essential to take the physical channel characteristics (often neglected) of the wireless medium (see Appendix A.2) into consideration especially in dynamic environments such as vehicular networks. The on-going development of new communication protocols and a need to understand incumbent ones with respect to energy consumption requires more attention to be directed towards profiling the energy usage of such protocols.

This chapter studies the QoS and energy performance of the carrier sense multiple access with collision avoidance (CSMA/CA) based 802.11p scheme, and a modified version of packet reservation multiple access (M-

PRMA) scheme for a vehicle-to-roadside (V2R) networks in a motorway environment. The original simulator has been coupled this time with the aforementioned protocols and the implementation details are described in this chapter. To analyse the energy consumption of the protocols, an energy model has been developed while taking account of a realistic physical layer model, included in Appendix A.2<sup>1</sup>.

### 4.2 The Studied Scenario

The proposed setup is based on a motorway scenario with 3 unidirectional lanes and a base station covering up to 1.6 km (diameter), responsible for sharing the medium between the vehicular nodes, installed along the motorway as shown in Figure 4.1. The 1.6 km coverage area with the base station located at the center enables all vehicles with the 802.11p specified range of 800m to be able to transmit directly to the base station [90]. Real vehicular traffic profiles have been applied to the motorway simulator to incorporate vehicular mobility in simulating the communication protocols. Furthermore the simulation results for 802.11p have been compared with analytical results from [91] and are in good agreement.

---

<sup>1</sup> Note that this piece of work is done in collaboration with another PhD student, Mr Wanod Kumar of School of Electronic and Electrical Engineering, University of Leeds, United Kingdom.

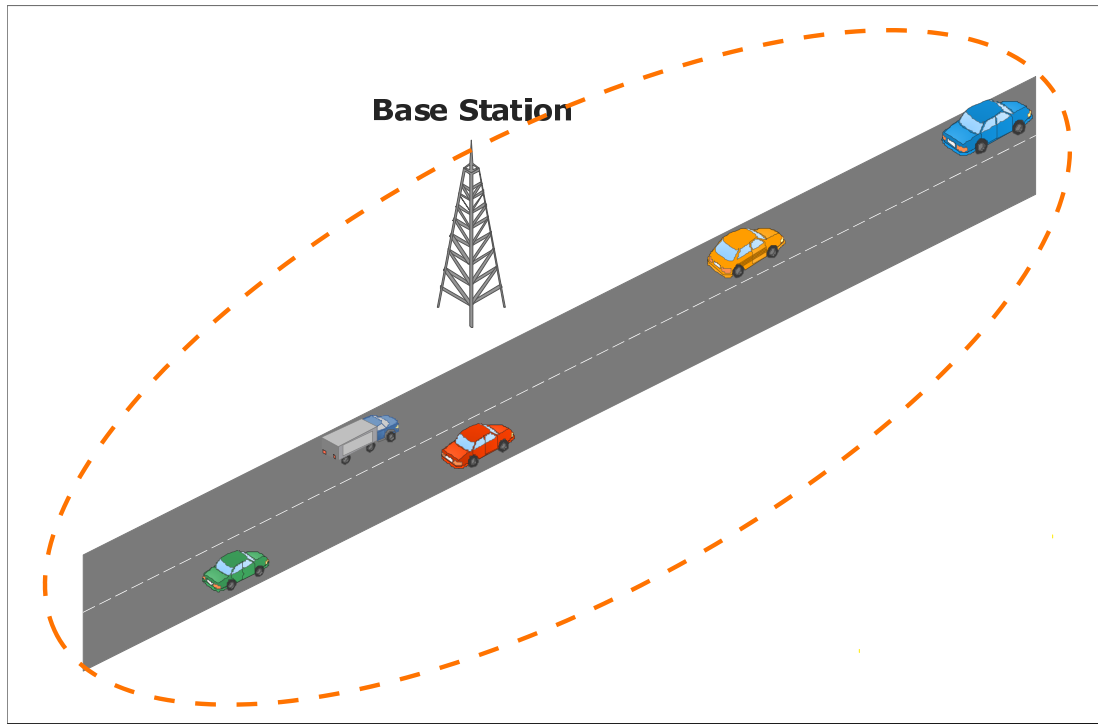


Figure 4.1: MPRMA/802.11p Proposed Scenario.

### 4.3 802.11p Simulator Design

To simulate the IEEE 802.11p protocol, an event driven execution of the protocol was programmed with microsecond time increments. A packet generation method is first used to initiate Poisson generated random packet arrivals with an inter-arrival time (IAT) of 6ms. As the packets arrive for each individual vehicle, they are placed into the respective vehicles medium access control (MAC) buffer in a first in first out queue with arrival times marked in order to analyse any delay incurred. The simulator then initiates a contention period using the *startContention()* method for all vehicles with packets in the MAC buffer. The method sets an AIFS countdown timer for vehicles with fresh packets that have not started their AIFS countdown while the *AIFSCounter()* decrements the AIFS countdown for vehicles that are already in the AIFS period. Furthermore, the *AIFSCounter()* flags a collision and starts a backoff algorithm for vehicles that finish their AIFS period when

multiple vehicles' AIFS counters reach zero simultaneously otherwise a contention winner is selected and a transmission is initiated followed by the start of a backoff algorithm for contention losers. A *backoffCounter()* method decrements the backoff counter for each vehicle whenever the channel is idle and initiates the AIFS counter when the backoff duration reaches 0 for any vehicle. The *timeout()* method ensures packets exceeding a threshold of 20ms delay are removed from the MAC buffer. The *transmission()* method is used to implement the transmission period of the packet by counting down a transmission timer with a duration that is based on the packet size and data rate. The method also implements a countdown period for a SIFS required before an acknowledgment is received. Once the SIFS period is over the method then sets an acknowledgement period and a flag to signal that the vehicle is receiving an acknowledgment. The *acknowledgement()* method is finally used to decrement a timer which indicates the reception of an acknowledgement packet followed by the release of the medium, removal of the packet from the buffer to show that it has been transmitted and the removal of the vehicle from the set of contending vehicles. The pseudocode (algorithm) for the related methods used to implement the 802.11p can be seen in Figure 4.2. The communication parameters for 802.11p protocol are given in Table 4.1.

<b><i>startContention( )</i></b>
<b>for all</b> $v \in V$ <ul style="list-style-type: none"> <li><b>If</b> <math>v_{buffer} \neq empty</math> and <math>v \notin V_{contend}</math>;</li> <li>  set <math>v_{counter} = AIFS</math>;</li> <li>  set <math>v \in V_{contend}</math>;</li> </ul> <b>end for</b>

<b>AIFSCounter()</b>
<pre> <b>for all</b> <math>v \in V_{contend}</math>;     <b>if</b> <math>v_{counter} = AIFS</math> and <math>AIFS_v &gt; 0</math> <b>then</b>         <math>AIFS_v --;</math>     <b>end if</b>     <b>if</b> <math>AIFS_v = 0</math> <b>then</b>         <b>if</b> <math>V_{AIFS_v=0} \leq 1</math> <b>then</b> //no collision             set <math>v = V_{Transmit}</math>;             set channel = busy;             set <math>v_{counter} = Tx</math>;             <b>for all</b> <math>v \in V_{contend}</math> and <math>v \notin V_{Transmit}</math> <b>do</b>                 set <math>v \in V_{backoff}</math>;                 set <math>v_{counter} = backoff</math>;             <b>end for</b>         <b>else</b>             <b>for all</b> <math>v \in V_{contend}</math> <b>do</b>                 set <math>v \in V_{backoff}</math>;                 set <math>v_{counter} = backoff</math>;             <b>end for</b>         <b>end if</b>     <b>end if</b> <b>end for</b> </pre>

<b>backOffCounter()</b>
<pre> <b>if</b> channel <math>\neq</math> busy <b>then</b>     <b>for all</b> <math>v \in V_{backoff}</math> <b>do</b>         <math>backoff_v --;</math>         <b>if</b> <math>backoff_v = 0</math> <b>then</b>             set <math>v_{counter} = AIFS</math>;         <b>end if</b>     <b>end for</b> <b>end if</b> </pre>

<b>timeOut()</b>
<pre> <b>for all</b> <math>v \in V</math> <b>do</b>     <b>if</b> <math>v_{buffer} \neq empty</math> <b>then</b>         get next <math>packet_{timestamp}</math>;         <b>if</b> <math>packet_{timestamp} \geq 20ms</math> <b>then</b>             dropPacket();             set <math>v \notin V_{contend}</math>         <b>end if</b>     <b>end if</b> <b>end for</b> </pre>

<b><i>transmission( )</i></b>
<pre> <b>for all</b> <math>v \in V_{Transmit}</math> <b>do</b>     <b>if</b> <math>Tx_v &gt; 0</math> <b>then</b>         <math>Tx_v --;</math>     <b>else if</b> <math>Tx_v = 0</math> <b>then</b>         set <math>SIFS_{counter}</math>;         set <math>channel \neq busy</math>;         set <math>Tx_v = -1</math>;     <b>else if</b> <math>Tx_v = -1</math> <b>then</b>         <b>if</b> <math>SIFS_{counter} &gt; 0</math> <b>then</b>             <math>SIFS_{counter} --;</math>             <b>if</b> <math>SIFS_{counter} = 0</math> <b>then</b>                 set <math>ACK_{counter}</math>;                 set <math>channel = busy</math>;             <b>end if</b>         <b>end if</b>     <b>end if</b> <b>end for</b> </pre>
<b><i>acknowledgement( )</i></b>
<pre> <b>if</b> <math>ACK_{counter} &gt; 0</math> <b>then</b>     <math>ACK_{counter} --;</math> <b>else if</b> <math>ACK_{counter} = 0</math> <b>then</b>     set <math>channel \neq busy</math>;     <b>for</b> <math>v \in V_{Transmit}</math> <b>do</b>         remove packet from <math>v_{buffer}</math>         set <math>v \notin V_{Transmit}</math>;         set <math>v \notin V_{contend}</math>;     <b>end for</b> <b>end if</b> </pre>

Figure 4.2: 802.11p pseudo code

## 4.4 MPRMA

The M-PRMA protocol [82] enables the dispersed nodes to transmit packetised information to the BS under time division duplex (TDD) mode where both uplink and downlink frames are on one duplex channel to facilitate bi-directional communication. Once a mobile node gets the reservation, it transmits the ON packets on the reserved slot in the uplink frame and as soon as an OFF period commences it relinquishes the slot to improve the efficiency of the MAC protocol. Orthogonal codes are used to

handle any collisions that may happen when two or more nodes try to reserve a slot at the same time. The characteristics of such a code can be used to distinguish mobile nodes by means of a correlative detector at the BS. Further details of the M-PRMA protocol can be found in [82], where its performance in terms of QoS was evaluated in a motorway vehicular environment. However, here and in contrast to [82], the energy efficiency of both M-PRMA and 802.11p are studied. The system parameters for the M-PRMA protocol [82] are presented in Table 4.1.

Variable	Notation	802.11p	M-PRMA
Channel bit rate	$d_r$	6 Mbps	6 Mbps
ON/OFF data peak bit rate	$R_s$	64 kbps	64 kbps
Data traffic ON mean duration	$T_{ON}$	1 s	1 s
Data traffic OFF mean Duration	$T_{OFF}$	1.35 s	1.35 s
IAT of packets	$T_f$	6 ms	6 ms
Maximum time delay	$D_{max}$	20 ms	20 ms
Payload	$P_L$	48 bytes	48 bytes
Packet header	$P_H$	49 bytes	5 bytes
Slot time	$t_s$	9 s	-
Arbitration Inter-frame space	$AIFS$	34 s	-
Short Inter-frame space	$SIFS$	16 s	-
Minimum contention window	$CW_{min}$	3	-
Maximum contention window	$CW_{max}$	1023	-
R slot duration	$R$	-	280 bits
Downlink timing signal	$T_d$	-	4 bits
No of slots per frame	$N_s$	-	47

**Table 4.1: System communication parameters**

## 4.5 Modelling Energy Consumption

The total energy consumption in a wireless communication network can be computed as a sum of energies consumed in transmitting, receiving and

## 4.5 Modelling Energy Consumption

---

listening states respectively [85, 92]. The energy consumption in transmission of a bit ( $e_{t\_bit}$ ) is given by,

$$e_{t\_bit} = \frac{P_{tc}}{d_r} = \frac{10 \text{ W}}{6 \text{ Mbps}} = 1.67 \times 10^{-6} \text{ J/bit} \quad (4.1)$$

where  $P_{tc}$  is the total power consumed by the circuitry while transmitting [86] and  $d_r$  is the data rate. The power utilised by the circuit while receiving ( $P_{rc}$ ) is up to 75% of  $P_{tc}$  [85]. Hence the energy consumed for the reception of a bit ( $e_{r\_bit}$ ) is

$$e_{r\_bit} = \frac{P_{rc}}{d_r} = \frac{7.5 \text{ W}}{6 \text{ Mbps}} = 1.25 \times 10^{-6} \text{ J/bit} \quad (4.2)$$

The total energy consumed for the transmission of packets ( $N$ ) from vehicles to a BS in one hour is

$$E_{t\_Vehs} = \sum_{i=1}^N e_t \times PktSize_i \quad (4.3)$$

where  $PktSize_i$  is the size of the  $i^{th}$  packet including the header in bits. Similarly  $E_{r\_Vehs}$  and  $E_{l\_Vehs}$  are the total energies consumed by all vehicles (to support centralised communication) in the receiving and the listening states (depending on the protocol being utilised), and are given by:

$$E_{r\_Vehs} = \sum_{i=1}^N e_r \times PktSize_i \quad (4.4)$$

and

$$E_{l\_Vehs} = P_{lc} \times (3600 - T_{t\_N} - T_{r\_N}) \times M \quad (4.5)$$

where

$$T_{t\_N} = T_{r\_N} = \frac{PktSize}{d_r} \times NoOfPkts \quad (4.6)$$

where  $P_{lc}$  is the power consumed in the listening state at the receiver which is the same as  $P_{rc}$ ;  $T_{t\_N}$  and  $T_{r\_N}$  correspond to the time taken for the transmission and the reception of the total number of packets ( $NoOfPkts$ ) in 3600 seconds duration (i.e. 1 hour). The notation  $M$  in this scenario represents vehicular density under a 1600m BS coverage.

For a base station, the total transmission and reception energies,  $E_{t\_BS}$  and  $E_{r\_BS}$ , are the same as  $E_{t\_Vehs}$  and  $E_{r\_Vehs}$  respectively.  $E_{l\_BS}$  is the total energy consumed in the listening state by a base station and is given by:

$$E_{l\_BS} = P_{lc} \times (3600 - T_{t\_BS} - T_{r\_BS}) \quad (4.7)$$

where  $T_{t\_BS}$  and  $T_{r\_BS}$  are the total transmit and receive times for a base station in an hour and are equivalent to  $T_{t\_N}$  and  $T_{r\_N}$  respectively. In this work we have considered centralised communication enabled with one BS to support bi-directional real time communication while maintaining the QoS in the 1.6 km coverage.

## 4.6 Performance Evaluation

The results outline the performance of the 802.11p, and the M-PRMA schemes with respect to QoS parameters including packet loss ratio (PLR) average access delay, goodput ( $\eta$ ) and energy consumption. The M-PRMA scheme outperforms the 802.11p protocol in all performance metrics and the results provide a useful insight. The PLR which is a ratio of packets lost to the total number of packets, has been determined while taking into account

#### 4.6 Performance Evaluation

---

the channel characteristics and delay threshold requirements. Although packet loss may occur due to channel impairments, our network configuration maintains transmission distances within an 800 m range thereby limiting these losses. The majority of the packet loss seen in Figure 4.3 is therefore attributed to packets exceeding a maximum threshold delay of 20 ms for audio related applications. The PLR and average access delay as seen in Figure 4.3 and Figure 4.4 reached unacceptable levels in the 802.11p scheme. The rush hour periods of 07:00 to 09:00 and 14:00 to 19:00 caused the PLR for the 802.11p scheme to rise to 0.13 which was in excess of a 0.01 ratio required to support real-time audio related communication. The MPRMA scheme on the other hand maintained a PLR below 0.01 throughout the day.

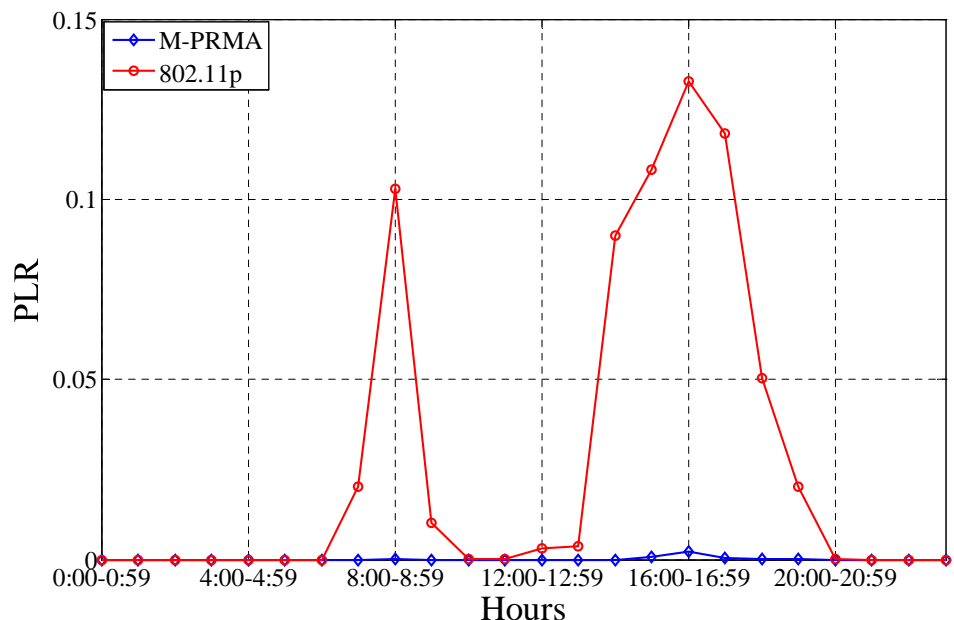


**Figure 4.3: Packet loss ratio**

The increase in PLR is due to the increase in vehicular traffic because the continuous generation of packets every 6 ms by all vehicles causes an increase in access delay as all vehicles contend for the medium. In this

#### 4.6 Performance Evaluation

---

scenario access delays of up to 400 ms caused packets to queue in each vehicles' MAC buffers. While some packets in the front of the buffer get served, trailing packets that exceed the threshold of 20 ms are eventually dropped. The M-PRMA scheme also slightly affected by the rush hour traffic, experienced a 3 ms increase in PLR at the highest vehicular traffic hour of 16:00-17:00 hrs.

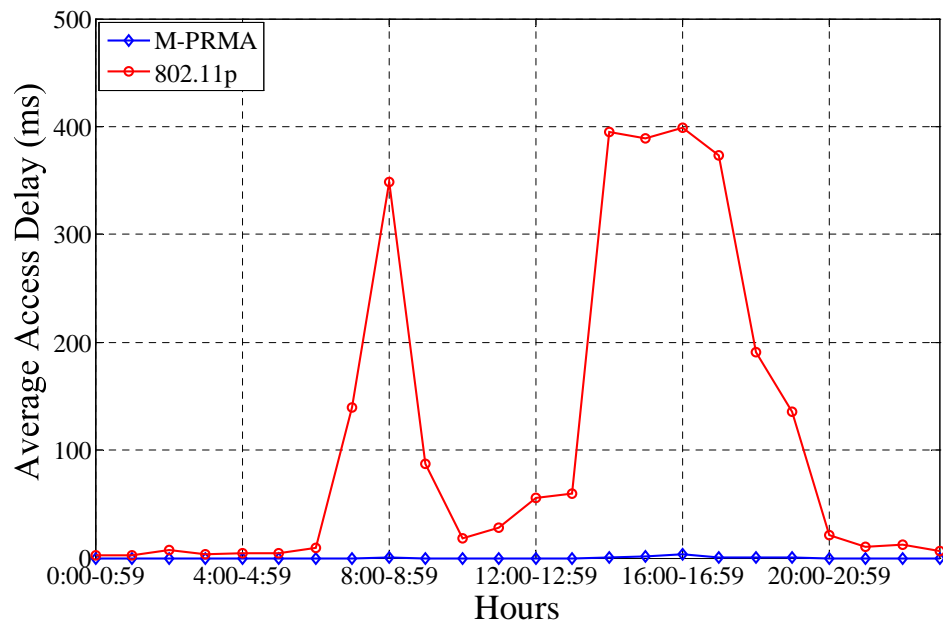


**Figure 4.4: Average access delay**

The goodput of the system (seen in Figure 4.5), which represents the ratio of useful information (payload ( $P_L$ )) to that of the total bits (payload + packet header ( $P_H$ )) when sending a packet, is important in illustrating the reason for an increase in PLR seen when higher traffic loads are generated by the vehicles. The M-PRMA scheme with a maximum goodput of 0.6 is approximately 2x higher in terms of goodput than the 802.11p scheme which only has a maximum goodput of 0.31. The goodput discrepancy between the two schemes is because 90% of the bits transmitted in the M-PRMA scheme contain useful information while the 802.11p scheme utilises only 49% of the

## 4.6 Performance Evaluation

---

bits in a useful transmission. Although both schemes have headers, the M-PRMA's  $P_L/(P_L+P_H)$  ratio is sufficient to maintain QoS. In contrast the 802.11p scheme has a larger header along with preambles and also suffers from SIFS, AIFS, and back-off waiting periods required to enable contention based communication. These drawbacks accumulate to place a limitation on the maximum goodput achievable with the 802.11p scheme. Subsequently a plateau is seen at high traffic hours between 14:00 and 17:00 hrs where the 802.11p scheme reaches a saturation point. Additional packets generated by vehicles exceed a 20 ms delay threshold and are thus dropped.

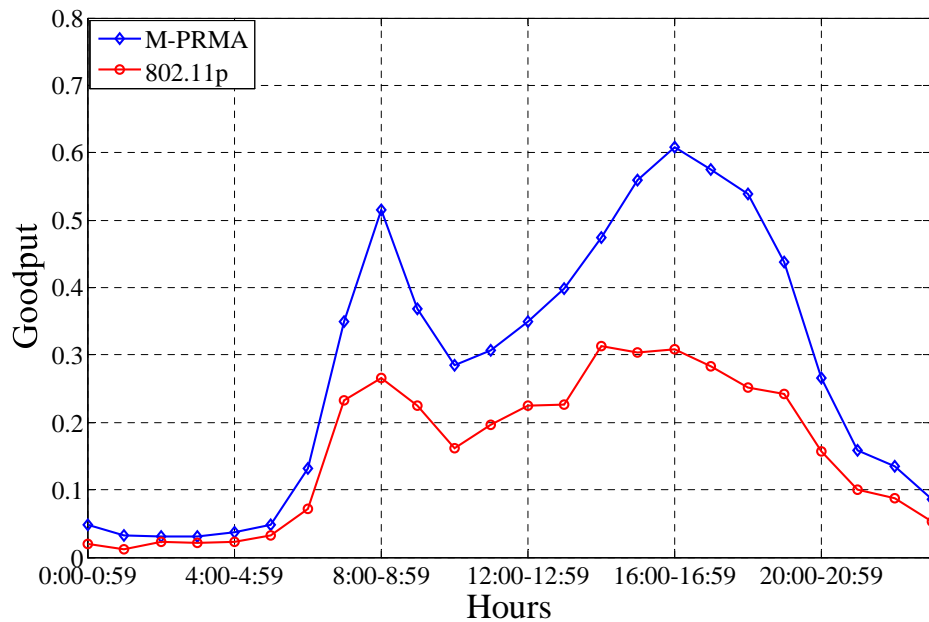


**Figure 4.5: Goodput**

The sum of the transmit and receive energies for both schemes, as depicted in Figure 4.6, reflects the vehicular flow as the energy expenditure is based on the amount of data that is transmitted and received in the system. The lower energy during early and late hours of the day corresponds to a lower number of packets (generated, transmitted and received) in the system due to the lower number of vehicular nodes during

## 4.6 Performance Evaluation

---

those hours. Another important insight can be observed during busy hours when the system under 802.11p reached the saturation point, as shown in Figure 4.5, the curve follows a similar trend as that of the goodput (Figure 4.5: ) because the packets that queued in the MAC buffer and were subsequently dropped (Figure 4.3) due to high access delays, resulted in lower energy levels since no transmission or reception took place in such cases.

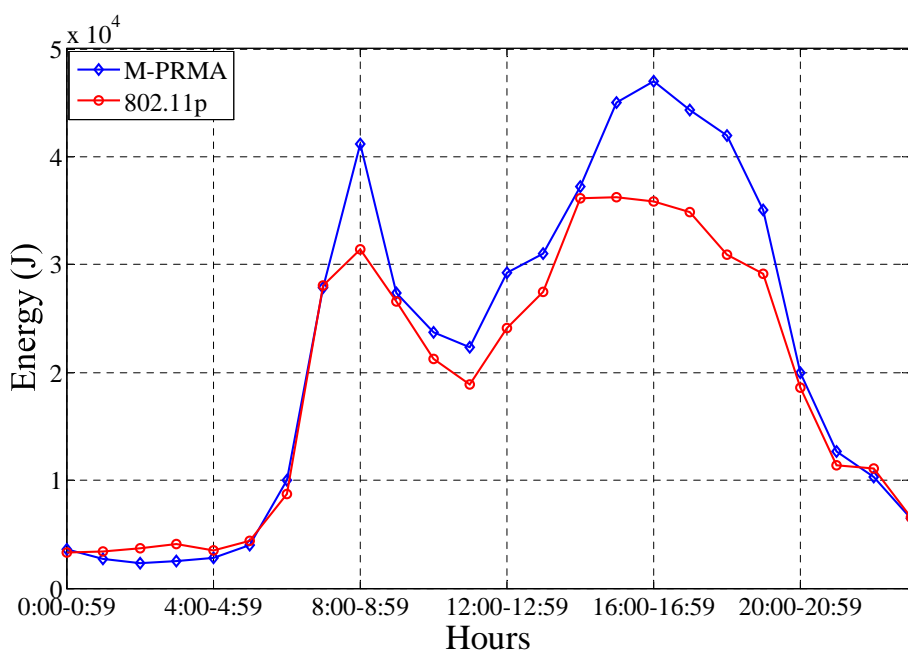


**Figure 4.6: Total transmitting and receiving energy for data packets**

The listening energy results significantly distinguish the energy usage of the two protocols as seen in Figure 4.7. The maximum listening energy for 802.11p reaches up to 1 MJ while the M-PRMA only reaches up to 13 kJ at 17:00. The 802.11p curve reflects the traffic flow since more vehicles on the motorway result in more communication nodes, under the coverage of a base station, consuming energy in the listening state. The significant increase in the listening energy seen in the 802.11p curve in comparison to the M-PRMA curve is due to the contention based communication method of

the 802.11p protocol. The contention requires vigilant carrier sensing by nodes in order to avoid collisions, and the constant carrier sensing results in much higher listening energy consumption. The M-PRMA protocol is designed and synchronised in such a way that the vehicular nodes go into an idle state (i.e. consume very low power typically about 4% of  $P_{tc}$  [85]) when there is no transmission or reception where power is mainly consumed to maintain synchronisation. The listening energy expenditure in the M-PRMA corresponds to the energy consumed by the BS while operating in the listening state and vehicles in the idle state.

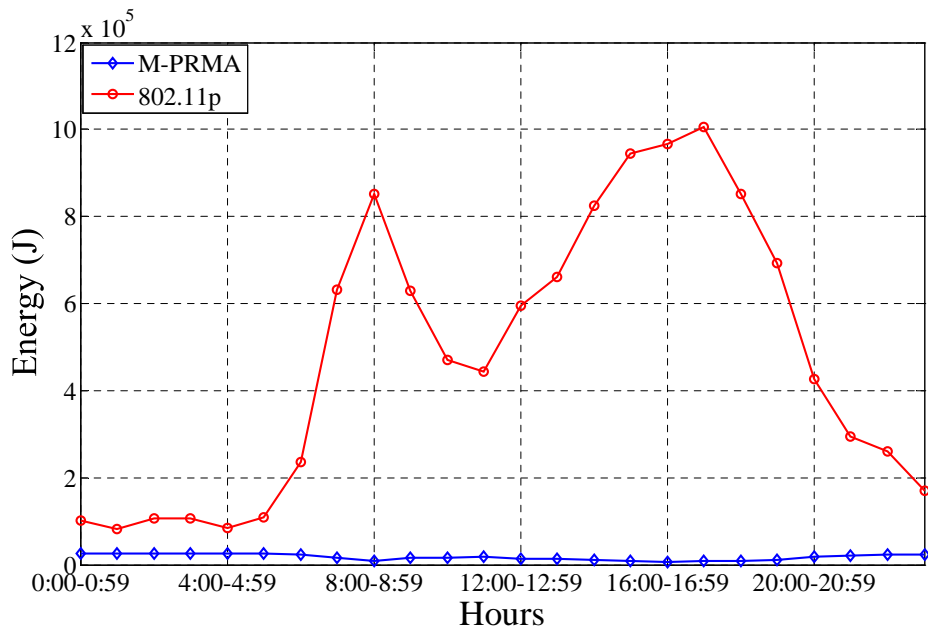


**Figure 4.7: Total listening energy**

Observing the large difference between the listening and the sum of transmit and receive energies for the 802.11p protocol as seen in Figure 4.7 and Figure 4.6 respectively, further analysis was required to ensure the accuracy of the results. The (listening energy)/(transmit plus receive energy) is compared to the (listening time)/(transmit plus receive time). As can be seen from Figure 4.8 both ratios are in good agreement. The slight

#### 4.6 Performance Evaluation

---

difference during busy hours can be attributed to the fact that the listening state consumes less power than that of transmission.

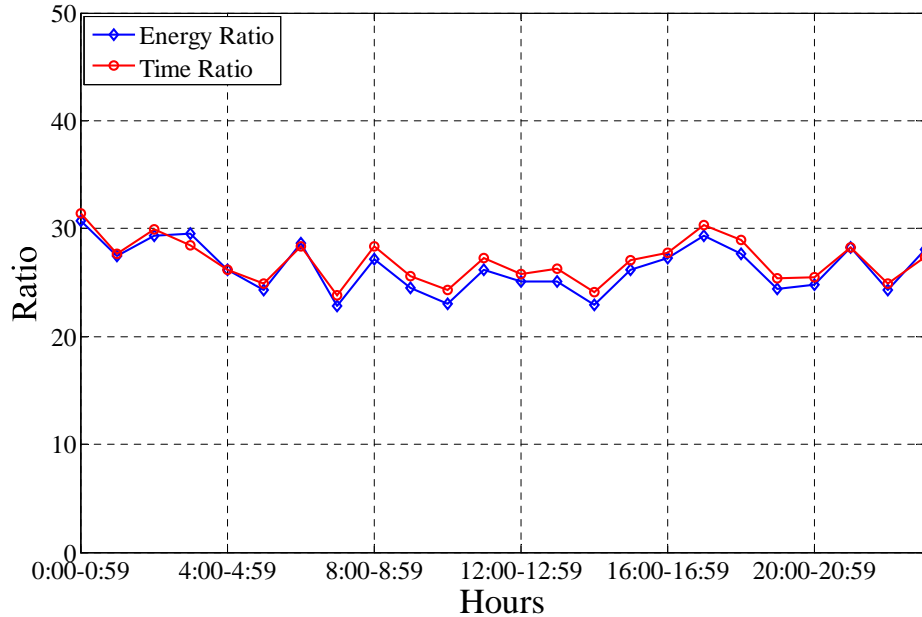


**Figure 4.8: Energy and time ratio**

The total network energy seen in Figure 4.9 is mainly a representation of the listening energy. This occurs because the magnitude of the listening energy overshadows the contribution of transmit and receive energies. The results further highlight the significance of the listening energy contribution to the total network energy consumption in this case. At 17:00, under 802.11p, the energy consumption reaches 1.04 MJ compared to only 52 kJ for the M-PRMA protocol. This reveals that for that hour, the M-PRMA utilised less than 19 times the energy consumed by the 802.11p protocol. Note that these results refer to the energy consumption of one day and each point corresponds to one hour. During the whole day, the energy consumption for 802.11p was more than 12 times than that of the M-PRMA protocol. This significant impact of energy consumption, shown in Figure 4.9, underlines the importance of selecting an appropriate MAC protocol especially for a

## 4.7 Summary

---

centralised vehicular network. Having consumed such a significant amount of energy during busy hours, the 802.11p protocol still fails to achieve the minimum acceptable level of PLR as shown in Figure 4.3. The 802.11p power consumption can be reduced through enhanced hardware design where partial receiver sleep can lead to a lower listening energy much smaller than the receiving energy.

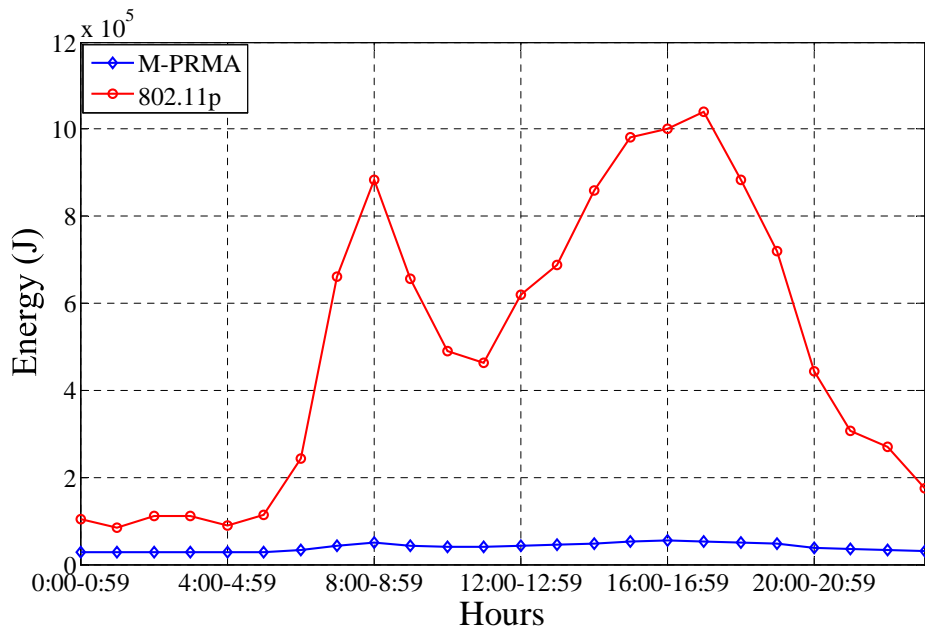


**Figure 4.9: Total network energy including energy used in collisions**

## 4.7 Summary

The performance of typical MAC protocols in terms of energy and QoS, has been evaluated in a motorway environment where the M-PRMA and 802.11p protocols have been employed to carry traffic generated by vehicular nodes. A detailed analysis of the physical propagation (Appendix A.2) and energy model has been presented. QoS metrics been evaluated including PLR, delay and goodput; and energy consumption was evaluated taking into account physical channel characteristics (outage requirement) in

#### 4.7 Summary

such a dynamic environment. During the whole day, the 802.11p consumed more than 12 times more energy than the M-PRMA protocol, and at some instances (hours) even more than 19 times. The results reveal that the bulk of the energy expenditure is from vehicles listening to the medium in the case of the 802.11p. The 802.11p energy consumption can be significantly reduced through an enhanced receiver design where partial receiver sleep can lead to a listening energy much smaller than the receiving energy. This suits the CSMA/CA scheme which spends most of its time in the listening state during busy periods.

---

## **5 Energy Efficiency in a Motorway Vehicular Network**

### **5.1 Introduction**

To mitigate the connectivity problems of a solely V2V communication system, low power road side units (RSUs) are proposed in Chapter 5. These RSUs enhance quality of service (QoS) and offer higher data rates for content such as multimedia applications. With growing demand of bandwidth hungry applications, the energy consumption of a vehicular network (V2V and V2R) increases manyfold. Thus there is a need to reduce the energy consumption and carbon footprint of such networks. Since an RSU in such networks consumes significant energy, suitable sleep cycle schemes may yield substantial energy savings. However, existing energy saving techniques such as proactive sleep strategies, achieve marginal energy savings especially in a motorway vehicular environments due to the stringent QoS requirements for multimedia services such as audio conferencing. To maximise energy savings at the RSUs in a motorway vehicle-to-roadside (V2R) network, a reactive sleep strategy namely adaptive sleep cycles with traffic shaping techniques is introduced in this chapter. An analytical model for the RSU with such sleep cycles is proposed. Real packet sizes measured and modelled in [93] have led to the use of a G/G/1/K vacation queueing model, where real vehicular traffic profiles used in [33] and this chapter have

changed arrival to a general distribution. Furthermore, two types of traffic shaping techniques (time-based and length-based traffic shaping) are introduced to minimise the adaptive sleep cycle overhead and thereby maximise transmission energy savings<sup>2</sup>.

### 5.2 Proposed Setup

The proposed motorway vehicular scenario uses micro/pico-cells served by RSUs (within a macro cell) that enable higher data rates [9], as shown in Figure 5.1. In the micro cell, the vehicles utilise a double cluster-head (DCH) scheme [33] to communicate with an RSU, which in turn connects to the main BS, to access external resources such as the Internet. The coverage of the RSU is assumed to be 1 km, which is in line with the WAVE standard [94]. The output data traffic of the cluster-heads in the DCH scheme becomes input to the RSU. As we are interested in determining QoS and the possible energy savings through sleep cycles, ideal medium access control (MAC) and wireless channel (no contention, and lossless) is assumed between the cluster-heads and the RSU. Thus, the output traffic of the cluster-heads of the DCH scheme becomes the arrival traffic at the RSU.

---

<sup>2</sup> Note that this piece of work is done in collaboration with another PhD student, Mr Wanod Kumar of School of Electronic and Electrical Engineering, University of Leeds, United Kingdom.

## 5.2 Proposed Setup

---

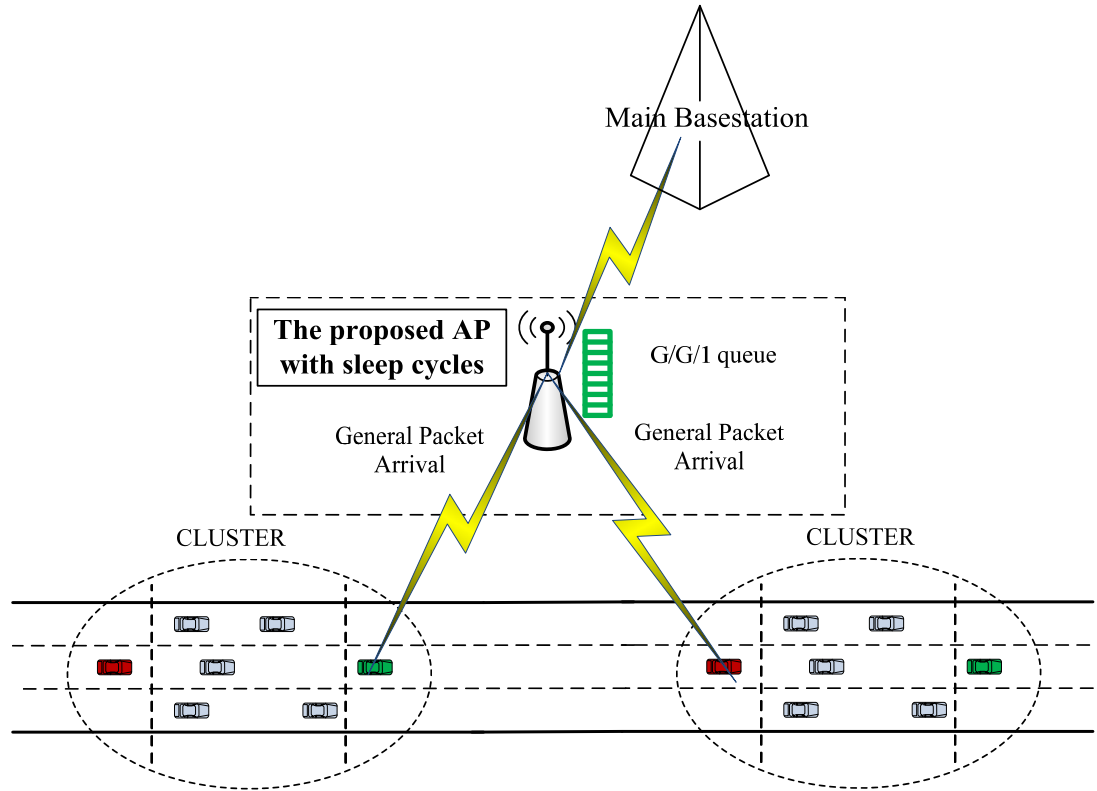


**Figure 5.1: Energy efficient RSU operation in a motor vehicular network.**

The RSU operates sleep cycles to save significant amount of energy during its inactivity period, which may degrade QoS. However, certain end-to-end QoS bounds on delay and packet blocking/loss need to be met for video and audio conferencing applications. Since the introduction of random sleep cycles at the CHs had already caused the average packet delay to exceed the threshold required for audio conferencing applications [33], the random sleep cycles operating at the CHs in [33] need to be modified in order to maintain QoS parameters within acceptable bounds so that energy savings at the RSU can be introduced. The proposed technique attempts to minimise delay. Furthermore, we can assume symmetric traffic for such applications and consider evaluating the performance of up-link (vehicles to the RSU) transmission without loss of generality. An uplink data rate ( $d_r$ ) of

54 Mbps [95] supports a packet service rate ( $\mu$ ) of  $(d_r)/(P_S \times 8)$  where the average packet size ( $P_S$ ) is 867.4 bytes [93].

Variable	Notation	DCH	RSU
Up-link channel data rate	$d_r$	6 Mbps per CH	54Mbps
No of vehicles	$M$	3 to 36	N/A
Video conferencing data generation rate	$d_i$	320 kbps	N/A
Average packet size	$P_S$	867.4 Bytes	867.4 Bytes
Packet arrival rate per CH	$\lambda$	$d_i/(P_S \times 8 \times 2)$	N/A
Packet service rate	$\mu$	$d_r/(P_S \times 8)$	$d_r/(P_S \times 8)$

Table 5.1: System Parameters.

### 5.3 Average Packet Delay Minimisation at the Cluster Heads

To minimise the average packet delay, the first step is to find the required buffer size of a CH in the DCH scheme which trades-off the average packet delay and the packet blocking probability. A small buffer results in a lower average packet delay, but higher packet blocking probability. On the other hand a large buffer can achieve very low packet blocking probability, but results in higher average packet delay. We, therefore, obtain the required buffer size of the CHs by rearranging Equation. (14) of [33] as

$$P_B = 1 - \frac{\frac{(1 - q_0 - r_0)\bar{X}}{(q_0 + r_0)\bar{S} + (1 - q_0 - r_0)\bar{X}}}{\frac{M\lambda}{2}\bar{X}} \quad (5.1)$$

Simplifying Equation (5.1) in terms of buffer size ( $K$ ), we obtain:

$$\sum_{k=K}^{\infty} f_k + \sum_{k=0}^{K-1} \beta_k = \frac{1 - \frac{M\lambda}{2}(1 - P_B)(\bar{X} - \bar{S})}{1 - \frac{M\lambda}{2}\bar{X}(1 - P_B)} \quad (5.2)$$

The variable under consideration,  $K$ , is the index of Equation. (5.2), which needs to be solved iteratively to obtain  $K_{opt}^{mvk}$ , which considers service time

distribution to be memory-less. The exact solution for the optimal buffer size,  $K_{opt}^{gen}$ , for any given packet size distribution [93] and channel data rate (Table 5.1) is not feasible to the best of our knowledge. Hence, we use a two moment approximation method [96, 97], according to which,  $K_{opt}^{gen}$  can be expressed as

$$K_{opt}^{gen} = K_{opt}^{mvk} + NINT[0.5(c_s^2 - 1)\sqrt{\rho_{max}} K_{opt}^{mvk}] \quad (5.3)$$

where  $\rho_{max}$  is the offered load corresponding to the maximum number of vehicles in an hour of the day,  $c_s^2$  is the squared coefficient of variation of the service time distribution, and *NINT* refers to the nearest integer function. Note that the value of  $K_{opt}^{gen}$  (i.e. 10) is smaller than that of  $K_{opt}^{mvk}$  (i.e. 14) as the variance of the packet size distribution is less than that for the case of Markovian service discipline. For all the notations used, please refer to [33].

Having determined the required buffer size, we modify the random sleep cycle strategy of [33] as follows: During a sleep cycle if a packet arrives, it waits for a maximum of 10 ms ( $D_{max}$ ) time, after which the CH ends the sleep mode and starts serving. Note that this condition applies only to the first arrived packet. None of the trailing packets wait for ( $D_{max}$ ), ensuring a delay bound on the served packets. Since the acceptable end-to-end delay for audio-related applications is 20 ms [34], we assumed a fair and equal distribution of ( $D_{max} = 10\text{ ms}$ ) each at CHs and at the RSU.

Applying the delay minimisation technique, we generated 30,000 samples of the modified sleep cycles through simulations for different vehicular densities, which are reasonably large to perform a statistical analysis. We observed that the pdf of these sleep cycles in each case is exponentially

### 5.3 Average Packet Delay Minimisation at the Cluster Heads

---

distributed with different mean sleep durations and respective scaling coefficients. The pdf of the modified sleep cycles is modelled as

$$f_s(t) = C_0 \frac{1}{\bar{S}} e^{-\frac{1}{\bar{S}}t} \quad (5.4)$$

where  $C_0$  is the co-efficient and  $\bar{S}$  is the mean sleep duration. These parameters, respectively, follow Morgan-Mercer-Flodin (MMF) and Vapour Pressure models [98] with varying vehicular density ( $M$ ) and are expressed as

$$C_0 = \frac{ab + cM^d}{b + M^d} \quad (5.5)$$

$$\bar{S} = e^{\left(a' + \frac{b'}{M} + c' \ln(M)\right)} \quad (5.6)$$

where  $a = 0.82968549$ ,  $b = 245548.34$ ,  $c = 1.1482568$ ,  $d = 4.3715514$ ,  $a' = 6.1065977$ ,  $b' = -9.7847988$  and  $c' = -1.5998211$ . Figure 5.2 shows the sleep pdf with minimised delay. The pdf of the modified sleep cycles has been incorporated in the analytical model of [33] to derive the delay minimisation results shown in Figure 5.3 and Figure 5.4.

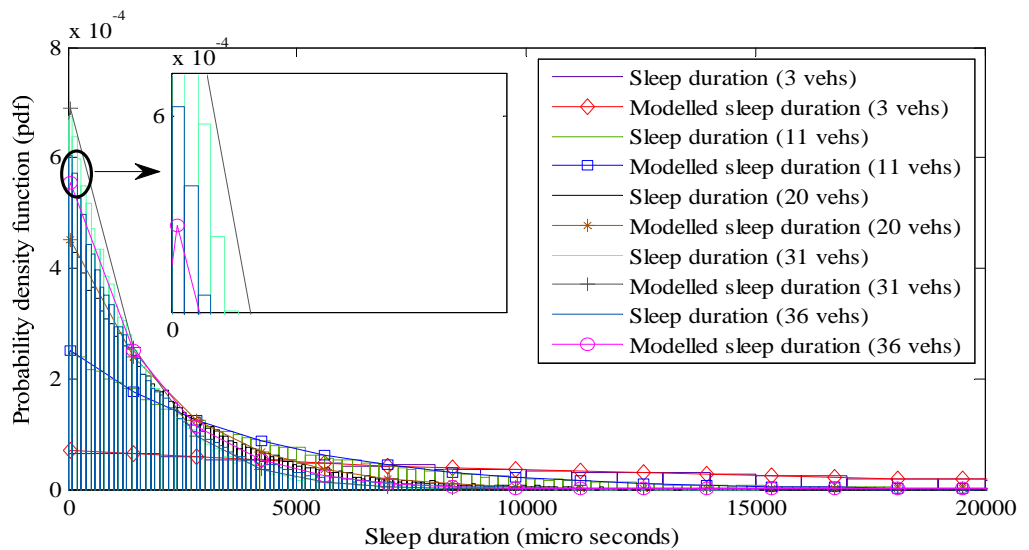


**Figure 5.2: Sleep pdf with delay minimisation.**

The performance at the CH in the DCH scheme, in terms of average packet delay  $W$  and packet blocking probability  $P_B$ , is evaluated with and without delay minimisation. The analytical results are verified using simulations. Without delay minimisation,  $W$ , shown in Figure 5.3, reduces with an increase in the number of vehicles because the CHs seldom sleep and thus serve all the packets (in the buffers) quickly. On the other hand  $W$  reaches 40 ms during off-peak hours, which becomes unacceptable for audio-conferencing applications. The modified sleep cycles of the CHs reduce  $W$  to a maximum of 7.8 ms, even during off-peak periods. Since the analytical model is based on the stochastic property of the events altogether, it becomes less accurate with fewer events. For example, in Figure 5.3, the modelled  $W$  has significant variation when the number of vehicles is low, generating lower traffic. On the other hand, simulation results are more accurate as they are able to account for all the events (according to their arrivals).

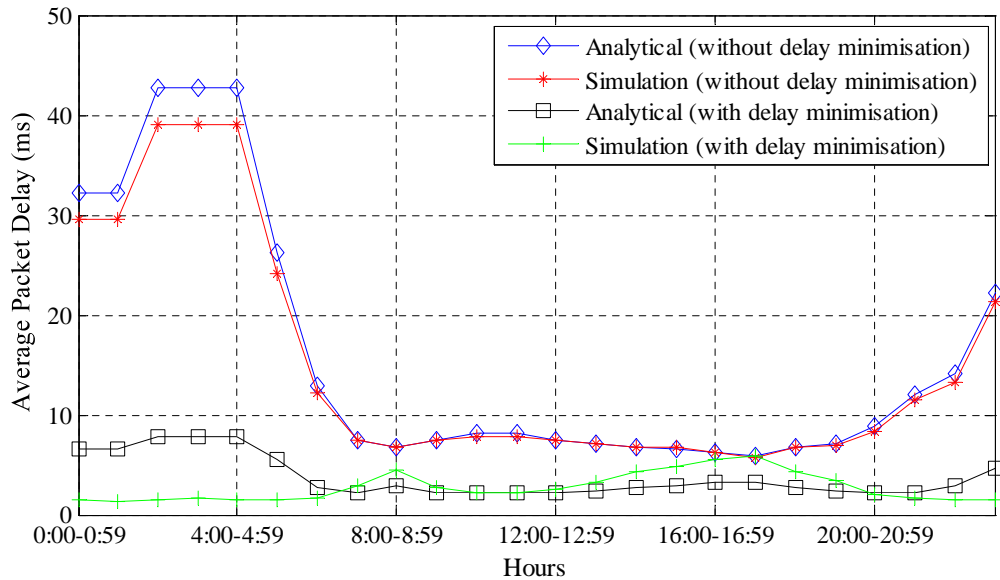
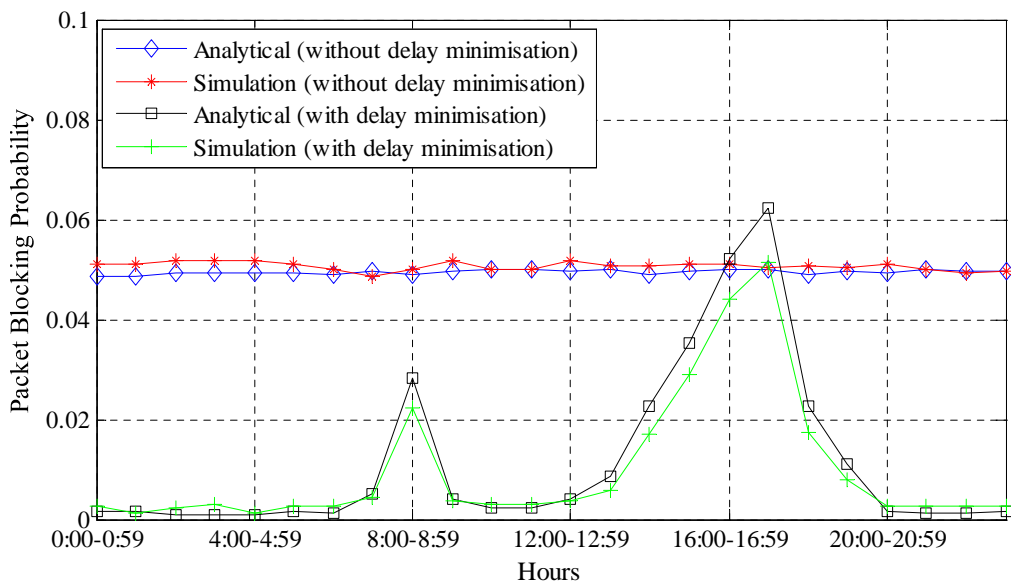


Figure 5.3: Average packet delay with and without delay minimisation.

## 5.4 Analysis of Packet Arrival Process at the RSU

---

Figure 5.4 shows the variation of  $P_B$  for both random and modified sleep cycles. Without delay minimisation,  $P_B$  was maintained at 0.05 to maximise energy savings  $E_S$  at the CHs [33], however at the expense of higher  $W$ . The introduction of delay minimisation through modified sleep cycles also improves  $P_B$  (less than 0.01 for the majority of the day). At 17:00 hour,  $P_B$  reaches the threshold (i.e. 0.05). Due to the variations between the actual and the modelled sleep duration data, shown in Figure 5.2, the analytical results slightly differ from those of the simulations.



**Figure 5.4: Packet blocking probability with and without delay minimisation.**

## 5.4 Analysis of Packet Arrival Process at the RSU

The served packets at the CHs no longer follow a memory-less Poisson process because of the generalised packet service discipline and delay minimisation (modified sleep cycles) at the CHs. This is despite the fact that packet arrivals from vehicles to the CHs has been chosen to be memory-less Poisson process in order to simplify the mathematical analysis. Thus the arrival traffic at the RSU becomes General distributed. Figure 5.5-Figure

## 5.4 Analysis of Packet Arrival Process at the RSU

---

5.7 shows the inter-arrival time (IAT) pdfs of packets arriving from both cluster-heads for varying number of vehicles. It is observed that the irregularities in the pdfs of the IAT, due to the generalised packet service discipline and the adaptive sleep cycle operations employed by each CH, tend to increase as the number of vehicles or CHs feeding the RSU increases.

We analyse the packet arrival process at the RSU for three representative load conditions corresponding to minimum, average and maximum number of vehicles, as shown in Figure 5.5, Figure 5.6 and Figure 5.7, respectively.

Figure 5.5 reveals that with minimum number of vehicles, the inter-arrival time of the packets at the RSU closely follows a negative exponential distribution. However, as the load increases with the number of vehicles, the irregularity in the distribution increases as shown in Figure 5.6. At high load, the inter-arrival time of the packets at the RSU becomes extremely irregularly distributed (Figure 5.7) and the resultant pdf largely deviates from being negative exponential. These provide important insight to develop an analytical model for the RSU with sleep cycles in the next section.

## 5.4 Analysis of Packet Arrival Process at the RSU

---

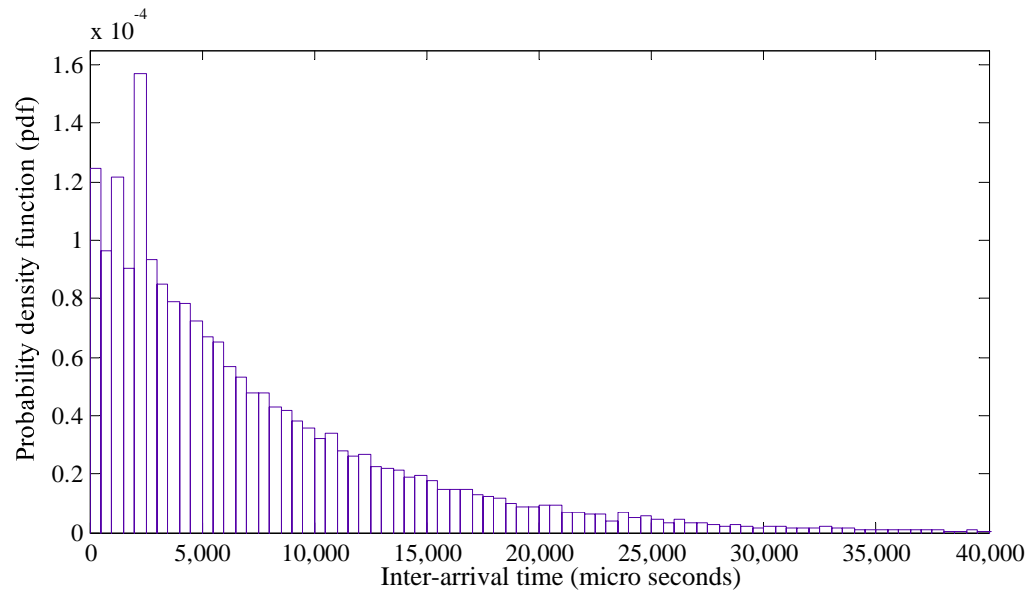


**Figure 5.5: Pdf of Inter-arrival time (IAT) of the packets at the RSU for min. no. of vehicles.**

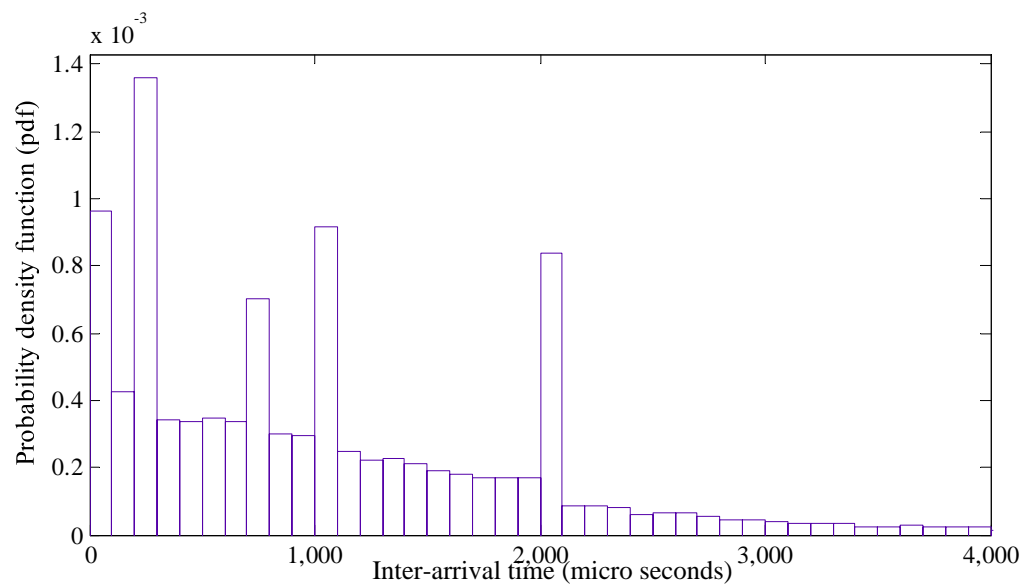


**Figure 5.6: Pdf of Inter-arrival time (IAT) of the packets at the RSU for avg. no. of vehicles**

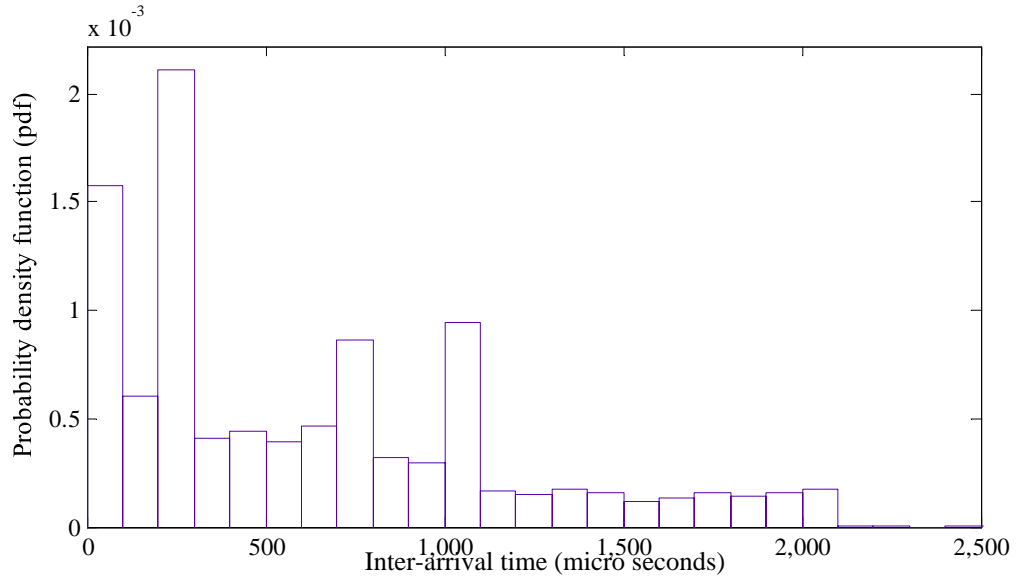


**Figure 5.7: Pdf of Inter-arrival time (IAT) of the packets at the RSU for max. no. of vehicles**

## 5.5 Analytical Model of an RSU with Sleep Cycles

The RSU in the proposed scenario saves energy by switching to sleep mode when it is idle. The sleep process can be described by two attributes:

(1) The time epoch - the RSU becomes inactive when there is no packet to be served; and (2) The time duration - through which the RSU remains inactive. The first attribute depends upon the stochastic property of the traffic (arrival and service of the packets) and the hardware, thus is not tuneable. However, the second attribute, the time duration, can be tuned. A multiple sleep model is considered where the RSU, on returning from sleep mode, switches to another sleep cycle if it still finds the buffer empty. It is evident that this leads to higher energy savings compared to a single sleep mode where the RSU remains awake even if there is no inbound traffic. In [33], random sleep cycles were used, where the CH remains in sleep mode for the entire time duration (randomly generated with a certain mean value) even if packets are waiting to be served. This type of sleep cycle degrades

the system performance when a large number of packets wait to be served. Since an RSU operates at higher data rates and processes large data compared to a CH, random sleep cycles are unsuitable for an RSU. Therefore, adaptive sleep cycles are considered for the RSU, where it wakes up if a packet arrives. Otherwise, it remains in sleep mode for the entire time duration as in case of random sleep cycles. Therefore, the adaptive sleep cycle duration is considered to be General distributed with mean  $\bar{S}$  and pdf  $f_s(t)$ . The service duration of the RSU is also considered General distributed with mean  $\bar{X} = \mu^{-1}$  and pdf  $b(t)$  for the real packet sizes obtained from [93]. The service duration and sleep duration are independent and identically distributed (IID) random variables which are also independent of each other. We assume that the RSU has a large buffer, which can hold a maximum of  $K'$  packets (including the packet being processed). The inter-arrival process at the RSU has been modelled as General distribution by characterising the distinctive outputs of the CHs and considering the RSU as a separate entity, which independently contributes to the end-to-end QoS parameters and overall energy savings in the entire system. Such an assumption is not farfetched as the RSU (without sleep cycles) behaves as G/G/1 queue for which only bounds on QoS parameters can be obtained analytically. Thus, the RSU, under the above conditions, can be modelled as a queue of type G/G/1/K/M with adaptive sleep cycle, as shown in Figure 5.8.

Further, solving a G/G/1/... queuing model with adaptive sleep cycle is not analytically possible to the best of our knowledge. In the literature, only approximate bounds on the QoS parameters, such as average packet delay, are obtained under different traffic conditions for G/G/1 queues [99]. The corresponding queuing model is shown in Figure 5.8. Without loss of

generality, it can be inferred that the arrival pdfs can be approximately bounded by exponential pdfs if the worst case scenario is used to predict the bounds on average packet delay. Considering the radio range of the RSU and the CHs (i.e. 1 km) in the studied scenario, only two CHs from adjacent clusters feed one RSU as shown in Figure 5.1. Thus in the worst case (i.e. with the maximum number of vehicles), IAT can be bounded by an exponential pdf with mean  $M\lambda'$  where each CH serves  $M/2$  vehicles on average and  $\lambda' = 1/(\text{Mean IAT})$ .

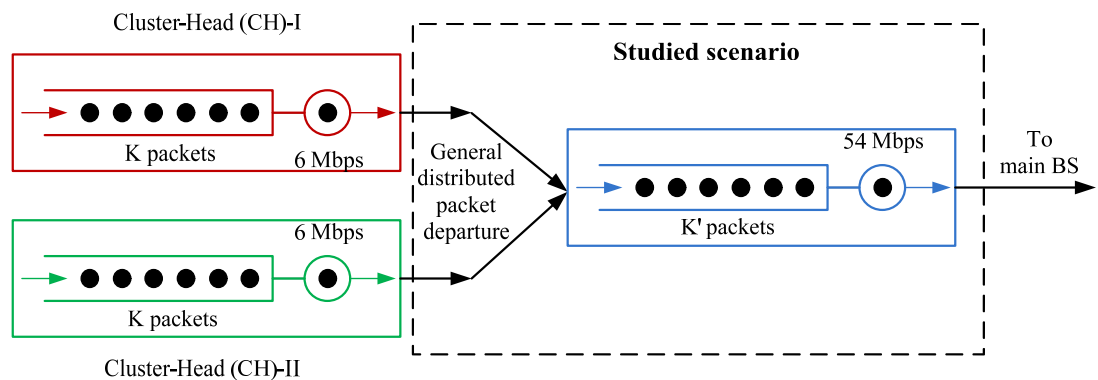


**Figure 5.8: Queuing model for the RSU.**

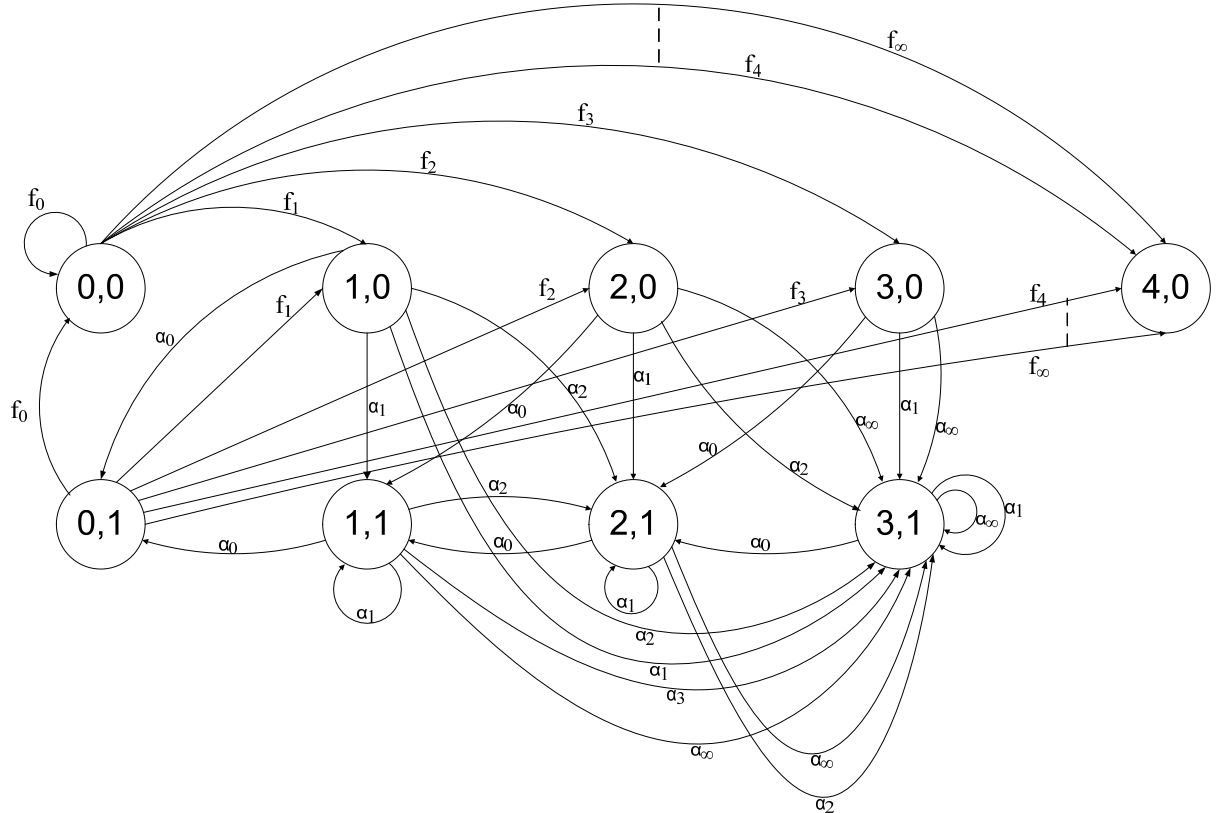


**Figure 5.9: Embedded state diagram of the RSU (for  $K' = 4$ ).**

The states of the RSU at the embedded transition points, shown in Figure 5.9, are represented by the number of packets in the RSU (waiting and in service) immediately after the selected time instant and the nature of the embedded point (i.e. whether it is a service completion or a sleep cycle completion). The system state at the  $i^{th}$  embedded point is represented by  $(n_i, \phi_i)$ , where

$n_i$  = number of packets in the RSU just after the  $i^{th}$  embedded point and

$$\phi_i = \begin{cases} 0 & \text{if the } i^{th} \text{ embedded point was a sleep cycle completion} \\ 1 & \text{if the } i^{th} \text{ embedded point was a service completion} \end{cases}$$

Considering the system in equilibrium, let  $q_k$ ,  $k = 0, 1, \dots, K'$  be the probability of the state  $(k, 0)$  and  $r_k$ ,  $k = 0, 1, \dots, (K' - 1)$  be the probability of the state  $(k, 1)$ . Note that  $r_k$  is only defined till  $k = (K' - 1)$  since the system, just after a service completion, cannot be in state  $(K', 1)$ . Let  $f_j$  ( $j =$

$0, 1, \dots, \infty$ ) be the probability of  $j$  packet arrivals in the system within a sleep cycle. The probability  $f_j$  can be obtained as a continuous summation of the products of the probability of  $j$  packet arrivals during a sleep cycle duration  $t$  and the probability that a sleep cycle is of time duration  $t$ , where  $t$  varies from 0 to  $\infty$ . The probability  $f_j$  can be expressed as

$$f_j = \int_0^{\infty} \frac{M\lambda' t}{j!} e^{-(M\lambda' t)} f_s(t) dt \quad j = 0, \dots, \infty \quad (5.7)$$

Let  $\alpha_j$  ( $j = 0, 1, \dots, \infty$ ) be similarly defined as the probability of  $j$  packet arrivals in a service time which can be expressed as

$$\alpha_j = \int_0^{\infty} \frac{(M\lambda' t)^j}{j!} e^{-(M\lambda' t)} b(t) dt \quad j = 0, \dots, \infty \quad (5.8)$$

Equation (5.8) denotes a continuous summation of the products of the probability of  $j$  packets arriving during a service duration  $t$  and the probability that a service duration is of time period  $t$ , where  $t$  varies from 0 to  $\infty$ . The embedded state diagram is shown in Figure 5.9 for four packets in the RSU (for simplicity) which helps generalise the transition equations as

$$q_k = (q_0 + r_0) f_k \quad k = 0, 1, \dots, (K' - 1) \quad (5.9)$$

$$q_{K'} = (q_0 + r_0) \sum_{j=K}^{\infty} f_j \quad k = K' \quad (5.10)$$

$$r_k = \sum_{j=K}^{k+1} (q_j + r_j) \alpha_{k-j+1} \quad k = 0, 1, \dots, (K' - 2) \quad (5.11)$$

$$r_{K'-1} = q_{K'} + \sum_{j=1}^{K'-1} (q_j + r_j) \sum_{k=K}^{\infty} \alpha_k \quad k = K' - 1 \quad (5.12)$$

where  $q_0$  and  $r_0$  represent the probabilities of the system being empty after a sleep cycle completion and a service completion, respectively. Equation (5.9) denotes the probability of  $k$  packet arrivals during a sleep cycle when the RSU was initially empty. Similarly, Equation (5.10) denotes the probability of  $K'$  packets in the RSU during a sleep cycle, which can only occur through  $K'$  or more than  $K'$  arrivals. It is to be noted that the RSU can simultaneously hold up to  $K'$  packets (in buffer and in service) only. Equation (5.11) denotes the probability of  $k$  packets in the system during a service period. This can only happen in  $k + 1$  mutually exclusive ways, each of which denotes  $k + 1 - j$  packet arrivals during a service period after the  $j^{th}$  embedded point. Equation (5.12) is obtained in a similar fashion. Summing up the probabilities of all possible states:

$$\sum_{j=0}^{K'} q_j + \sum_{j=0}^{K'-1} r_j = 1 \quad (5.13)$$

To solve Equations (5.9)-(5.13) recursively for  $q_k$ ,  $r_k$ , an intermediate variable  $\beta_k$  ( $k = 0, 1, \dots, K' - 1$ ) is defined as

$$\beta_k = \frac{q_k + r_k}{q_0 + r_0} \quad (5.14)$$

It is a ratio of the probability of the system having  $k$  packets to the probability of the system being empty. Using Equation (5.9) and (5.11), Equation (5.14) is recursively defined as

$$\beta_0 = 1 \quad \text{and}$$

$$\beta_1 = \frac{\beta_0 - f_0}{\alpha_0} \quad \text{and}$$

$$\beta_k = \frac{(q_0 + r_0)f_k + \sum_{j=K}^{k+1} (q_j + r_j)\alpha_{k-j+1}}{(q_0 + r_0)} \quad \text{and}$$

$$\beta_{k+1} = \frac{\beta_k - f_k - \sum_{j=K}^{k+1} \beta_j \alpha_{k-j+1}}{\alpha_0} \quad k = 2, \dots, K' - 1 \quad (5.15)$$

Substituting Equation (5.9), (5.10), (5.14) in Equation (5.13), the expression becomes

$$(q_0 + r_0) \sum_{k=K'}^{\infty} f_k + \sum_{k=0}^{K'-1} q_k + \sum_{j=0}^{K'-1} r_j = 1 \quad (5.16)$$

$$(q_0 + r_0) \left[ \sum_{k=K'}^{\infty} f_k + 1 + \sum_{k=1}^{K'-1} \beta_k \right] = 1 \quad (5.17)$$

Using  $\beta_0 = 1$ , the probability of the system being empty  $(q_0 + r_0)$  is expressed as

$$(q_0 + r_0) = \frac{1}{[\sum_{k=K'}^{\infty} f_k + \sum_{k=0}^{K'-1} \beta_k]} \quad (5.18)$$

Substituting the value of  $(q_0 + r_0)$  from Equation (5.18) in Equation (5.9) and (5.10),  $q_k$ ,  $k = 0, 1, \dots, K'$  is obtained. Further, using these values of  $q_k$  and values of  $\beta_k$  (derived earlier),  $r_k$   $k = 0, 1, \dots, (K' - 1)$  is obtained as

$$r_k = (q_0 + r_0) \beta_k - q_k \quad k = 0, 1, \dots, (K' - 1) \quad (5.19)$$

The probabilities,  $q_k$  and  $r_k$ , are now used to compute the QoS and energy parameters of the system. Let  $\rho_c$  be defined as the carried load, i.e. the probability that the RSU is busy at an arbitrary time. Analysing all the intervals between successive embedded points over a long time duration (say  $T$ ), where  $T \rightarrow \infty$ ,  $\rho_c$  can be expressed as

$$\begin{aligned}\rho_c &= \lim_{T \rightarrow \infty} \frac{\sum \text{service times in } T}{\sum \text{sleep cycle times in } T + \sum \text{service times in } T} \\ &= \frac{(1 - q_0 - r_0)\bar{X}}{(q_0 + r_0)\bar{S} + (1 - q_0 - r_0)\bar{X}}\end{aligned}\quad (5.20)$$

The offered load,  $\rho$ , is defined as

$$\rho = M\lambda'\bar{X} \quad (5.21)$$

Using Equation (5.20) and Equation (5.21), the packet blocking probability,  $P_B$ , is obtained as

$$P_B = \frac{\rho - \rho_c}{\rho} \quad (5.22)$$

In order to determine the other performance parameters like the average packet delay,  $W$  and the number of packets in the RSU,  $N$ , a quantity,  $D$ , is defined which denotes the mean time between successive embedded points, when the system is in equilibrium. The quantity  $D$  can be expressed as

$$D = (q_0 + r_0)\bar{S} + (1 - q_0 - r_0)\bar{X} \quad (5.23)$$

Using Equation (5.23),  $N$  and  $W$  are, respectively, obtained as

$$N = \frac{1}{M\lambda'D} \sum_{j=0}^{K'-1} jr_j + K' \left( \frac{\rho - \rho_c}{\rho} \right) \quad (5.24)$$

$$W = \frac{N}{M\lambda'(1 - P_B)} \quad (5.25)$$

Since a fraction,  $P_B$ , of the arrivals is blocked due to the buffer overflow at the RSU, the utilisation,  $U$ , of the system can be obtained as

$$U = M\lambda'\bar{X}(1 - P_B) = \rho_c \quad (5.26)$$

The transmission energy savings,  $E'_S$ , per hour through sleep cycles is expressed as

$$E'_S = (1 - U) \times P_{APt} \times 3600 \quad (5.27)$$

where  $P_{APt}$  denotes the transmitter power of the RSU [100], as given in Table 5.2. The energy model utilised in this chapter is based on [100] where the energy per bit (in the transmission state) can be determined, if required, as a ratio between the transmitter power and the data rate [100]. Energy savings are achieved at the RSU through sleep cycles, where the transmitter part of the RSU is switched OFF. The ratio of the fully operational power and low state power is given in Table 5.2. The total energy overhead of a RSU in an hour depends upon two parameters, viz. (i) wake-up overhead associated with each sleep cycle ( $E_{WO}$ ) and (ii) the number of times the RSU sleeps and wakes up, i.e. sleep count ( $N_S$ ). The wake-up overhead,  $E_{WO}$  (see Table 5.2), accounts for system initialisation, frequency management, synchronisation, routing table updates etc. Since  $N_S$  becomes a large quantity in an hour (see Table 5.3, where  $N_S$  is obtained through simulations) compared to the value of  $E_{WO}$ , it plays a dominant role in the transmission energy efficiency of an RSU. Analytically,  $N_S$  can be obtained as

$$N_S = \frac{(q_0 + r_0) \times 3600}{Avg.\ sleep\ duration} \quad (5.28)$$

Considering the wake-up overhead for the RSU, Equation (5.27) is modified as

$$E_S = (1 - U) \times P_{APt} \times 3600 - (E_{wo} \times N_S) \quad (5.29)$$

Variable	Notation	RSU
Max. operational power	$P_{MAX}$	30 W [95]
Min. operational power	$P_{MIN}$	$P_{MAX}/1.3548$ [28]
Transmit power	$P_t$	$P_{MAX} - P_{MIN}$
Energy for wake-up	$E_{wo}$	0.0175 J

Table 5.2: RSU energy parameters

## 5.6 Traffic Shaping at the RSU

Adaptive sleep cycles improve QoS compared to random sleep cycles as they follow traffic variation more accurately than the random sleep cycles. However, this is achieved at the expense of higher number of sleep cycles (i.e. sleep count), which is associated with wake-up overheads, and therefore, should be studied in detail. To achieve maximum energy savings, sleep count should be minimised and the sleep duration of each sleep cycle should be maximised. In this section, we propose two different traffic shaping techniques (viz. length-based traffic shaping and time-based traffic shaping) at the RSU, which enhance the un-interrupted sleep duration, reduce the number of sleep cycles and thereby reduce the wake-up overheads of the RSU. This improves the overall energy savings considerably compared to the unshaped traffic case. Evidently, the traffic shaping deteriorates the delay of some packets, thereby affecting the average packet delay. Thus, it is important to study the effects on QoS parameters with varying operation parameters. Thus, various operating scenario(s) that maximise(s) the overall energy savings and maintain(s) the end-to-end QoS are studied.

In the case of unshaped arrivals (Figure 5.5-5.7) at the RSU, the pdf of the adaptive sleep cycles is the pdf of the packet inter-arrival time. Thus, the corresponding bound function of the sleep pdf will be exponential distributed with mean  $\bar{S} = 1/(M\lambda')$  where  $M$  is the average number of vehicles during off-peak hours and maximum number of vehicles during rest of the day. This distribution is substituted in Equation (5.7) to compute QoS parameters for the case of unshaped arrivals.

In length-based traffic shaping, the RSU accumulates a certain number of packets in its buffer before it starts processing them at a stretch. During the accumulation process, the RSU switches to sleep mode and wakes up when the burst of the certain number of packets is ready to be processed. The pdf of the adaptive sleep cycle with length-based traffic shaping is shown in Figure 5.10. The burstiness in IAT pdf occurs due to the limited number of packet arrivals. Therefore, the sleep cycle pdf for length-based traffic shaping can be approximately modelled by Gamma distribution as

$$f(t; \phi, \varphi) = \frac{1}{\varphi^\phi \Gamma(\phi)} t^{\phi-1} e^{\frac{-t}{\varphi}} \quad (5.30)$$

where  $\phi$  follows the polynomial regression of degree 3 and can be expressed as

$$\phi = v_1 + v_2 M + v_3 M^2 + v_4 M^3 \quad (5.31)$$

and  $\varphi$  follows the logistic power model, expressed as

$$\varphi = \frac{u_1}{1 + \left(\frac{M}{u_2}\right)^{u_3}} \quad (5.32)$$

where  $v_1 = 4.036, v_2 = -0.0611803, v_3 = 0.00237949, v_4 = -0.0000295271, u_1 = 41567.7577, u_2 = 0.7594$  and  $u_3 = 1.1013285$ .

The distribution is substituted in Equation (5.7) to compute QoS parameters for the case of length based traffic shaping.

In time-based traffic shaping, the RSU accumulates the arrived packets for a certain time duration in its buffer before it starts processing them at a stretch. During the accumulation process, the RSU switches to sleep mode and wakes up after the specified duration to serve the burst. The pdf of the adaptive sleep cycle with time-based traffic shaping is shown in Figure 5.11.

## 5.6 Traffic Shaping at the RSU

---

The sleep cycle pdf is found to follow an exponential distribution with a shifted origin ( $\omega'$ ) which is initially equal to the burst length (10 ms in this case to keep the end-to-end delay less than or equal to 20 ms [34]). Thus, the corresponding sleep pdf is given as

$$f(t; \omega, \omega') = \frac{1}{\bar{S} - \omega} e^{-\left(\frac{t-\omega'}{\bar{S}-\omega}\right)} \quad (5.33)$$

where  $\omega$  is the burst length period ( $\omega \geq \omega'$ ). Eqns. (5.20) and (5.23) are respectively modified as

$$\rho_c = \frac{(1 - q_0 - r_0)\bar{X}}{(q_0 + r_0)(\bar{S} + \omega') + (1 - q_0 - r_0)\bar{X}} \quad (5.34)$$

and

$$D = (q_0 + r_0)(\bar{S} + \omega') + (1 - q_0 - r_0)\bar{X} \quad (5.35)$$

The parameter  $\omega'$  accounts for the burstiness of the IAT and its value can be iteratively obtained to achieve a bound on  $W$ . Sleep count for each case is shown in Table 5.3 of Section 6.6.

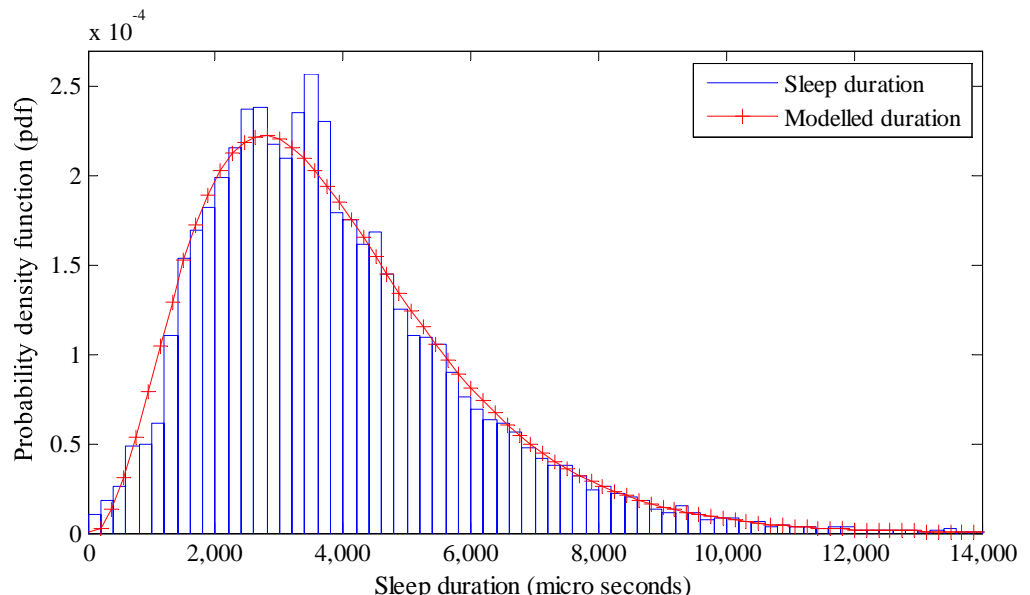


**Figure 5.10: Shaped sleep pdf with length-based traffic shaping.**

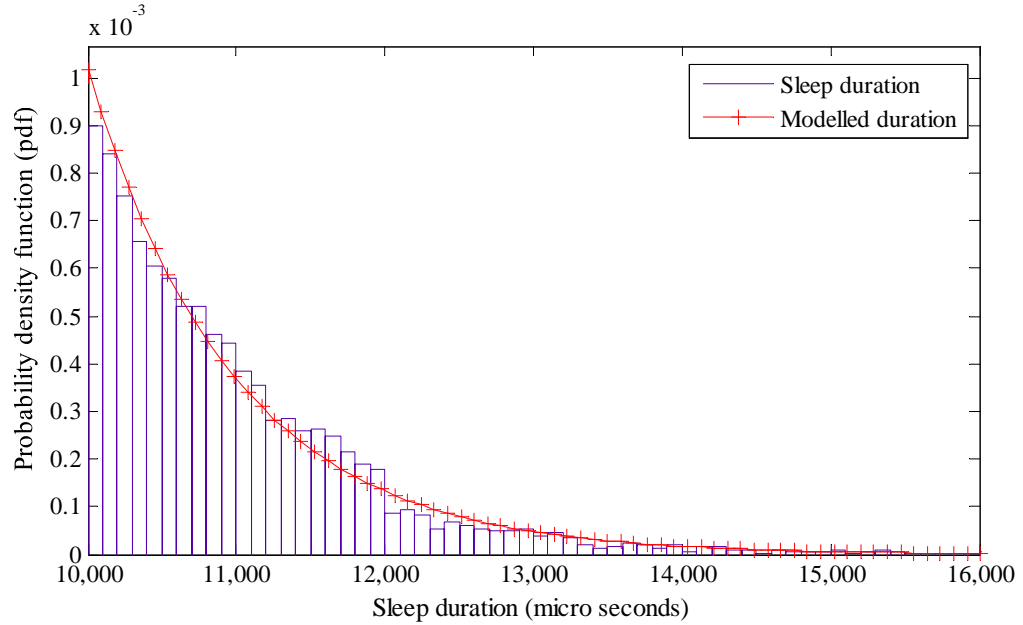


**Figure 5.11: Shaped sleep pdf with time-based traffic shaping.**

A packet leading the burst will always incur a delay  $d$  with a maximum value  $D_{max}$  in case of time-based traffic shaping and  $d'$  in case of length-based traffic shaping ( $d \neq d' \neq D_{max}$ ). With traffic shaping, the RSU will remain in sleep mode much longer significantly reducing the wake-up overhead of the RSU.

## 5.7 Simulation Setup

An event driven simulator is developed to implement adaptive sleep cycles at the RSU. The vacation in RSU, representing a sleep cycle to save energy, is queue-length dependent. The newly arrived packets are added to the buffer and the waiting time for each packet is registered. This waiting time is used to calculate the average packet delay. When the buffer becomes empty and the RSU is not in service, the RSU switches to sleep mode for a certain time duration, which is negative exponential distributed. A counter ‘sleepCount’ is defined to count the number of times the RSU

## 5.7 Simulation Setup

---

switches to sleep mode. This accounts for the energy overhead associated with sleep cycles. The RSU may become unavailable because of two reasons: It is either serving another packet or is in the sleep mode. In case of adaptive sleep cycles, without traffic shaping, the RSU prematurely wakes up from sleep and starts to serve the newly arrived packet immediately. In the case of length-based traffic shaping, the RSU remains in the sleep mode until the shaper accumulates a predetermined number of packets, here 4 packets in the buffer. If the shaper has accumulated another burst of 4 packets before the RSU finishes serving the previous burst, the RSU will also serve that burst before it could switch to sleep mode again. In the case of time-based traffic shaping, the RSU remains in sleep mode until the shaper accumulates packets for 10 ms duration. The accumulation starts from the arrival of the first packet of the burst. Once the burst is formed, the RSU wakes up and starts serving the burst.

Hours	Vehicular density	Unshaped	Length-based	Time-based
000-0059	4	648690	165280	234150
0100-0159	4	646550	168150	233590
0200-0259	3	488840	193820	209090
0300-0359	3	490910	124820	208430
0400-0459	3	491870	124900	209090
0500-0559	5	810480	208990	251270
0600-0659	11	1717610	455320	301260
0700-0759	25	3572170	1029250	333480
0800-0859	32	4326720	1288850	338960
0900-0959	24	3453030	990980	332320
1000-1059	21	3074290	868340	328430
1100-1159	21	3077150	867890	328280
1200-1259	24	3455080	988960	333150
1300-1359	27	3811100	1107120	335410
1400-1459	31	4226240	1254580	338220
1500-1559	33	4411460	1320200	339470
1600-1659	35	4561890	1375520	340260
1700-1759	36	4616140	1396770	340680
1800-1859	31	4235290	1256240	338450
1900-1959	28	3914600	1147610	336110

## 5.8 Performance Evaluation

---

2000-2059	18	2680390	743390	322910
2100-2159	12	1857350	496170	305900
2200-2259	10	1562960	414410	296560
2300-2359	6	964150	248460	264520

**Table 5.3: Sleep count in an hour with and without traffic shaping.**

## 5.8 Performance Evaluation

The performance of the RSU has been evaluated in terms of delay ( $W$ ) and energy savings ( $E_S$ ) with traffic shaping (length-based and time-based) and without traffic shaping. Note that the packets are not blocked in this scenario as an infinite buffer of the RSU shaper has been assumed which is realistic, considering the substantial number of operations an RSU has to perform. Figure 5.12 shows  $W$  at the RSU in all three cases with their respective analytical bounds. Without any traffic shaping, the RSU becomes immediately available (from the sleep) at the arrival of a packet. Therefore,  $W$  in this case is very low, (i.e. 0.13-0.15 ms) throughout the day. The introduction of length-based traffic shaping strategy degrades  $W$  significantly in low vehicular density. During off-peak hours,  $W$  reaches up to 12 ms compared to only 1.3 ms during peak hours as it takes a significantly longer time to fill the burst of 4 packets during off-peak hours. However, in the case of time-based traffic shaping, varying vehicular density (off-peak hours to peak hours) does not have such an impact on  $W$ , which is found to be between 6 ms and 7 ms. This is because in time-based traffic shaping, the first packet in each burst waits for a minimum of  $D_{max}$  regardless of the subsequent packet arrival time. Note that further analysis was carried out on time-based traffic shaping with a burst period of 15 ms and 18 ms. The average packet delay is found to be increasing without much gain in  $E_S$ . On

the other hand, decreasing the burst period to 5 or 8 ms reduces  $E_S$  significantly. Therefore, we have used 10 ms as the optimal burst period in this study. In each case, the simulation results are within the analytical bound.

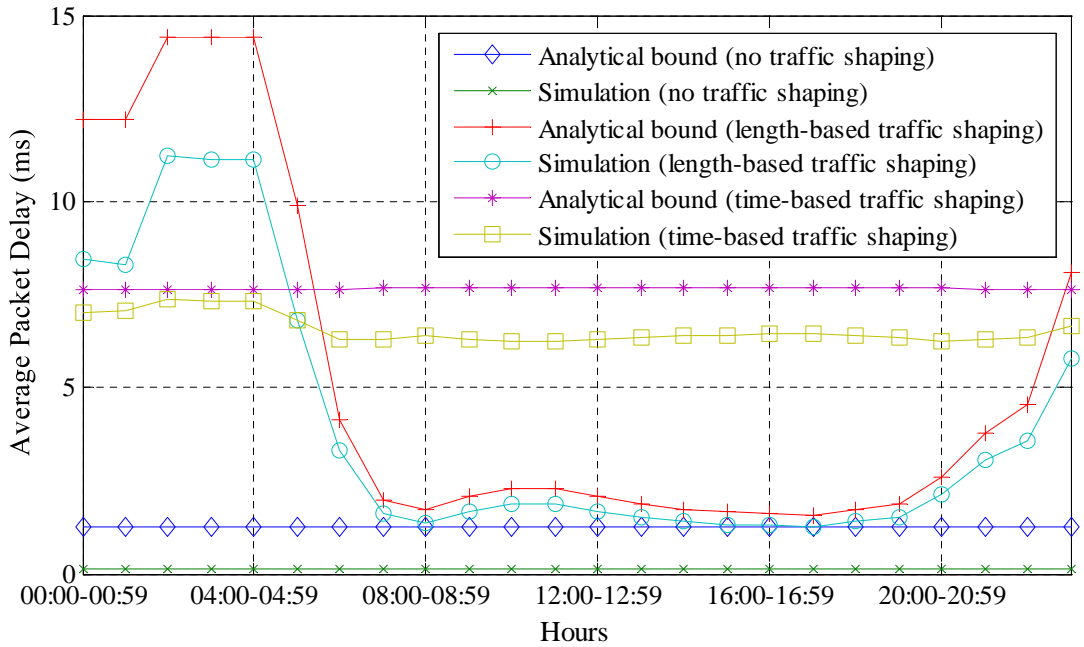


**Figure 5.12: Average packet delay with and without traffic shaping**

Figure 5.13 shows  $E_S$  at the RSU with traffic shaping (length-based and time-based) and without traffic shaping. The number of sleep cycles in all three cases is shown in Table 5.3. Each wake-up is assumed to incur an energy overhead ( $E_{wo}$ ) of 0.0175 J and contributes negatively to  $E_S$ . Even though, no traffic shaping case outperformed both types of traffic shaping in terms of  $W$ , it suffers more in terms of  $E_S$ . Since, in the case of no traffic shaping, the RSU needs to be immediately available (from sleep or after serving the previous packet) for each and every packet, the number of wake-ups (overhead) is almost equivalent to the total number of packets to be served by the RSU.

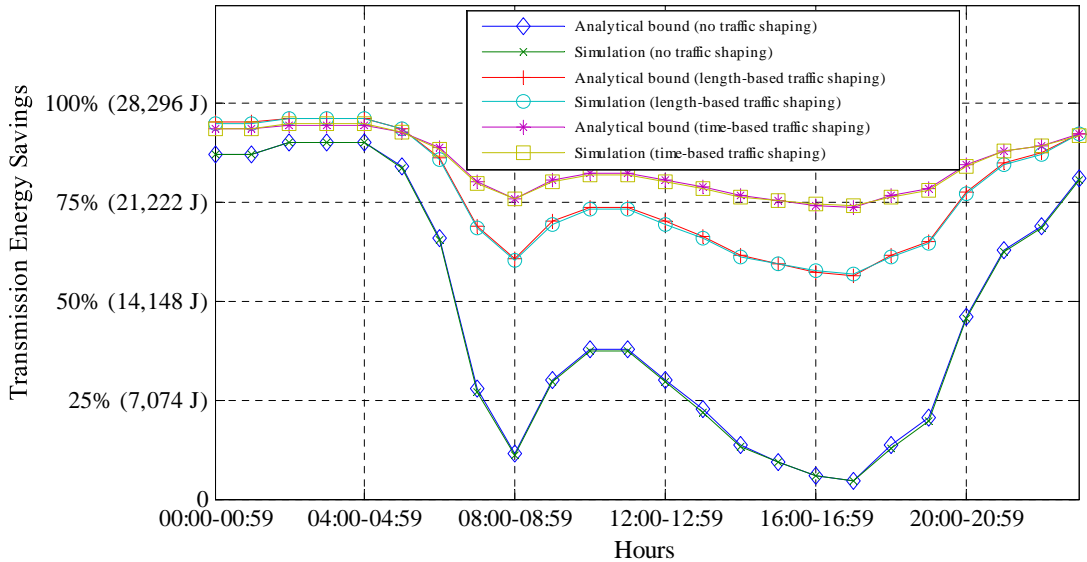


**Figure 5.13: Energy savings with and without traffic shaping.**

This overhead becomes significantly higher during peak hours due to the higher load. Figure 5.13 reveals that even though the RSU is able to save 90% (i.e. 25.5 kJ) transmission energy during off-peak hours, it only saves 4.7% (i.e. 1.3 kJ) during peak hours. In the case of length-based traffic shaping, the RSU, during peak hours, is able to save significantly more energy compared to that of no traffic shaping. However, the time-based traffic shaping outperforms both length-based traffic shaping and no traffic shaping as the number of wake-ups for the RSU is noticeably lower compared to the other cases especially during the peak hours (see Table II). At 17:00 hour,  $E_S$  of 74.1% (21 kJ) is achieved in the case of time-based traffic shaping compared to 57% (16.1 kJ) and 4.7% (1.3 kJ) for length-based and no traffic shaping, respectively. Similarly during the whole day,  $E_S$ , in total, for no traffic shaping, length-based and time-based traffic shaping is 317 kJ, 523 kJ and 573 kJ, respectively. The transmission energy consumption with sleep strategies (no traffic shaping: 356 kJ, length-based traffic shaping: 150 kJ, time-based traffic shaping: 100 kJ) are significantly

lower compared to the case where no sleep strategy was introduced at the RSU (i.e. 673 kJ). In each case, the simulation results are closely matched to the analytical bounds.

### 5.9 Summary

To introduce energy savings at the RSU while serving QoS aware multimedia traffic, the random sleep cycles in [32] were modified bringing the average packet delay down to a maximum of 7.8 ms while keeping the packet blocking probability less than or equal to 0.01 for the majority of the day. Adaptive sleep cycles and traffic shaping were introduced at the RSUs to achieve maximum transmission energy savings while maintaining the QoS for multimedia communication. The scenario is modelled using G/G/1/K vacation queueing. Maximum energy savings were achieved by reducing the number of sleep cycles (hence the wake-up overhead of adaptive sleep cycles) through length-based and time-based traffic shaping techniques borrowed from core networks where they are used in optical burst switching and in general for improving QoS. These techniques respectively achieved 77% and 84% energy savings on average compared to 46% in the case of sleep with no traffic shaping. In the case of time-based traffic shaping, the average packet delay smoothed out throughout the entire day at approximately 6.5 ms whereas the length-based traffic shaping incurred high variation in delay (12 ms during off-peak hours compared to only 1.3 ms during peak hours). However, this ensures that the end-to-end average packet delay of the entire system (vehicle to CH to RSU) is below 20 ms (a threshold for audio-related applications) with both traffic shaping techniques. This fulfills the stringent QoS requirement of audio-conferencing applications

## 5.9 Summary

---

(which covers all multimedia services) while saving significant amounts of energy. Considering the total length of motorways and major roads in Great Britain [3], 51,000 RSUs (with 1 km spacing [94]) will be required for futuristic vehicular infotainment. Since the transmission power for each RSU is 7.86 W (please refer to Table 5.2), the total transmission energy consumption in a month is approximately 289 MWh. On average, an energy saving of 84% through adaptive sleep cycles and time based traffic shaping could potentially save up to 242 MWh in a month while maintaining the required QoS for multimedia services. With each home, for example, typically consuming 150 W for lighting using compact fluorescent lamp (CFL), the energy expenditure of a home in a month will amount to 108 kWh. Hence, the energy savings achieved (i.e. 242 MWh) is equivalent to lighting 2,245 houses throughout a month.

---

## **6 Using Renewable Energy in a Motorway**

### **Vehicular V2R Network**

#### **6.1 Introduction**

The dispersed nature of outdoor wireless systems results in both high economic and environmental costs as ubiquitous deployments of such systems require connectivity to a power grid. One such scenario is motorway vehicular communication, where continuous power supply to infrastructural devices is required to provide acceptable QoS and connectivity. Traditionally, base station optimisation strategies focuses on efficient deployments [9, 58] through the use of energy aware components. Load adaptive hardware and software modules are essential to address the ever increasing environmental concern associated with the growing telecommunication industry. However a more economically attractive option that can further reduce the carbon foot print of energy aware communication systems is the use of renewable energy sources such as wind or solar power [59]. A road side unit (RSU) with a wireless backhaul or in a mesh network, powered with a renewable source of energy significantly increases the speed and flexibility of off-grid deployment.

In this chapter, the performance of the roadside units (RSUs) in a vehicular motorway vehicular V2R network is investigated. The objective is to study the feasibility of their standalone and off-grid operations using wind

## **6.2 Proposed Scenario**

---

energy. The RSUs use sleep cycles to reduce their energy consumption so that the available wind power meets the load demand of the RSU. To maintain QoS, the integration of small and large battery sizes with these renewable energy sources is studied. Therefore thorough analytical and simulation studies of such an RSU are carried out, which define its performance in terms of both QoS and energy consumption.

### **6.2 Proposed Scenario**

The proposed scenario considers a set of road side units (RSUs), typically spaced 1 km apart, along a 3 lane motorway stretch, with approximately 300 such RSUs in a single motorway [33]. Each RSU receives data from moving vehicles and relays to a base station that is beyond the transmitting range of the vehicles. This investigation examines the energy profile of these road side units if they are considered to be off grid entities and are dependent on renewable energy (generated on site) and use sleep cycles to conserve energy, which pushes the blocking probability and delay to their acceptable QoS thresholds. Considering a single RSU, the energy consumption of the RSU, which is primarily dependent on the vehicular traffic profile, is examined along with the wind energy generated, which is dependent on statistically derived average power in the wind. While this chapter simply considers the average power obtained from the wind speeds, further statistical analysis is performed in chapter 7 to determine the instantaneous power available at any moment.

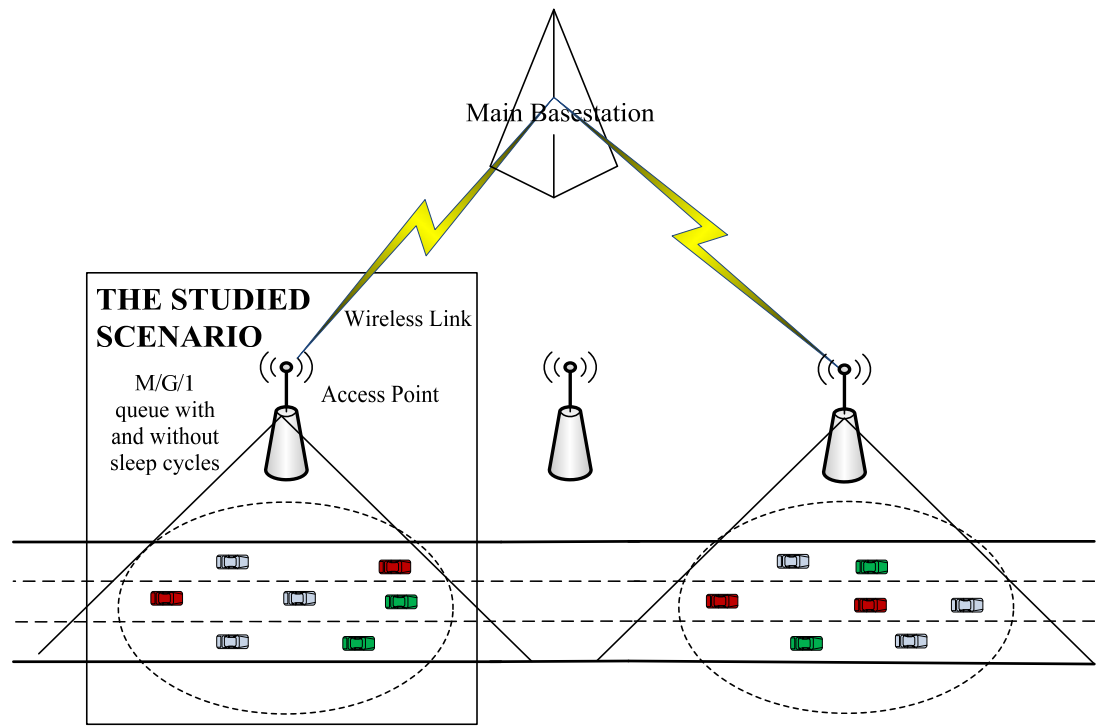


**Figure 6.1: RSU with sleep cycles and renewable energy in a motorway V2R scenario.**

### 6.3 Wind Energy Analysis

To analyse the adequacy of wind power in supporting the load demand, the first step is to determine how much energy can be harnessed from the wind. The wind power harnessed is given by [101]

$$P_w = \frac{1}{2} C_p \zeta A v^3 \quad (6.1)$$

where  $C_p$  is the coefficient of performance of the wind turbine, which accounts for the decrease in the actual power harnessed from the wind due to several factors such as rotor and blade design that lead to friction and equipment losses. The other parameters are  $\zeta$ , the air density in  $\text{kg/m}^3$ ,  $A$ , the cross-sectional area in  $\text{m}^2$  of the turbine,  $D$  the diameter of the blade and the wind speed,  $v$ , in  $\text{m/s}$ . The wind speed measured values for this analysis have been obtained from the UK air information resource (AIR) database

### 6.3 Wind Energy Analysis

---

provided by the Department for Environment Food and Rural Affairs [102]. The data is comprised of hourly wind speeds for the whole of 2011 measured at one of their monitoring sites in Reading Newton, UK. The readings have been selected for this specific site as it is in the same geographical position as that of the M4 vehicular profiles and thus the location of the proposed network deployment. For the purpose of the analysis, it is necessary to derive the average generated wind power for each hour. The nonlinear relationship between generated power and wind speed means average wind speeds cannot simply be used to determine the average power generated. Therefore rewriting the generated power in terms of average quantity [102]

$$P_{avg} = \left( \frac{1}{2} C_p \zeta A v^3 \right)_{avg} = \frac{1}{2} C_p \zeta A (v^3)_{avg} \quad (6.2)$$

In probabilistic terms the average value of  $v^3$  is

$$(v^3)_{avg} = \sum_i [v_i^3 P(v = v_i)] \quad (6.3)$$

By considering the wind speeds in each hour for the whole year, the average wind generated power in a 24 hour period is obtained as shown in Figure 6.2 for the study. The significant variation in the power generated calls for integrating energy storage devices to better guarantee the QoS required for communication. The system parameters are presented in Table 6.1.

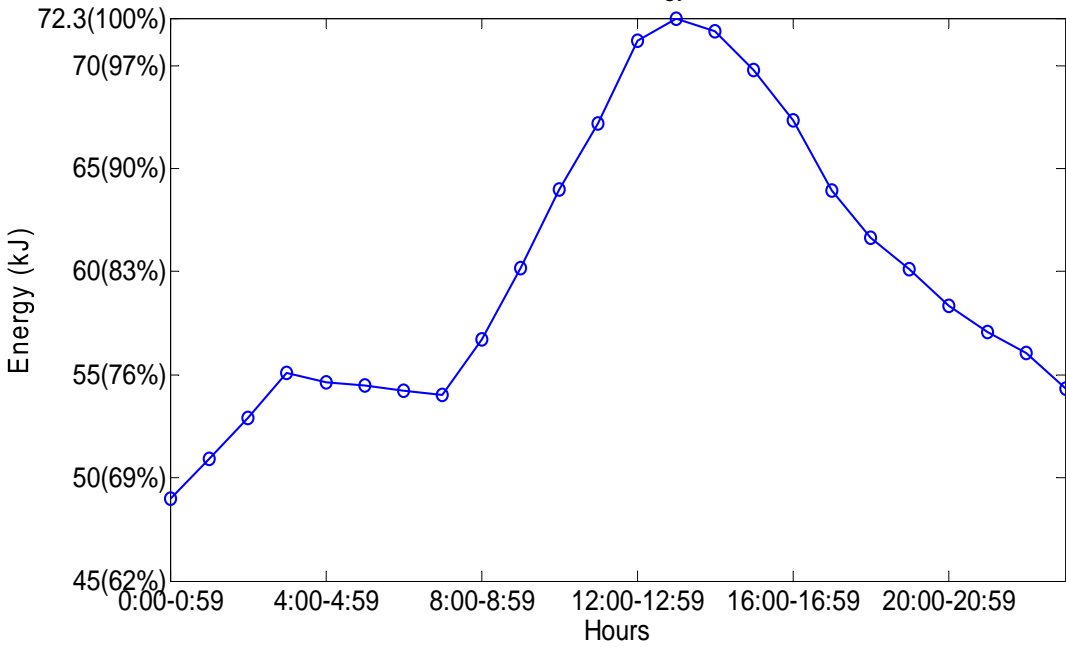


Figure 6.2: Average wind over a day at Reading, UK.

Parameters	Notation	Values
RSU data rate	$d_r$	15 Mbps [103]
Vehicle data generation rate	$d_t$	320 kbps [34]
Average packet size	$P_s$	867.4 bytes [93]
Packet arrival rate	$\lambda$	$d_t/(P_s \times 8)$
Packet departure rate	$\mu$	$d_r/(P_s \times 8)$
RSU (fully operational) power	$P$	20 W [104]
Energy per bit	$E_b$	$P_t/d_r$ (J/bit)
Propeller diameter length	$D$	0.5 m [105]
Swept area	$A$	0.2 m <sup>2</sup>
coefficient of performance	$C_p$	0.45 [105]
Air density at 15°C	$\varsigma$	1.225 kg/m <sup>3</sup> [102]

Table 6.1: Wind Energy System Parameters

## 6.4 System Model and QoS Metrics

The proposed model considers three different situations depending upon the energy available to operate a standalone RSU. In the first situation whenever the wind power is insufficient for operation, the RSU has access to an alternative source of energy (non-renewable electric power). In such a

condition, the carbon foot print of the RSU will be highest and the RSU transmits the aggregated data generated by all the in-range vehicles to the nearby base station. The performance of the RSU in this case can be modelled as a simple M/G/1/K queue, where M corresponds to the memoryless Poisson process of the packet stream from the vehicles within the range of the RSU, G represents the General distributed packet service discipline corresponding to real packet size measurement obtained from [93] (with average packet size of 867.4 bytes, dominated by acknowledgement packets and maximum Ethernet size packets), 1 represents the single server, i.e. the RSU, and K represents the maximum number of packets that can be held by the RSU in its buffer.

In the second situation the RSU switches to a sleep state or low energy state with duration S when its buffer becomes empty. The sleep duration S is assumed to be negative exponentially distributed with mean  $\bar{S}$  reflecting the arrival process. In the low state, the transmitter circuitry is switched off to save energy [28]. Thus, only the battery powered receiver and buffer circuitry of the RSU remains active. In this scenario the RSU transmitter does only have access to wind power. As soon as the transmitter of the RSU becomes active, the RSU starts processing the buffered packets (if any) along with the newly arriving packets.

In the third situation the RSU follows a sleep cycle, irrespective of the available wind energy, in such a way that the required QoS is met throughout the day. The RSU, as in the second situation, is considered to be a standalone entity but now has a rechargeable battery (or capacitor) for its transmitter circuitry. The energy saved through sleep cycles as well as any excess wind energy is stored in the battery for future use to meet any energy

deficit. Thus, the main objectives here are (i) to determine whether the available wind energy can meet the energy demand of the RSU maintaining the QoS and subsequently, (ii) the minimum battery size for successful operation, and (iii) maximum battery size -- for storing excess energy for future use.

The RSU in the second and third situations is modelled as an M/G/1/K queue with sleep cycles [33]. The first scenario is a special case of M/G/1/K queue with sleep cycles, where  $\bar{S} \rightarrow 0$ .

Let  $f_j$  ( $j = 0, 1, \dots, \infty$ ) be the probability of  $j$  packet arrivals in the system within a sleep cycle. The probability  $f_j$  can be obtained as a continuous summation of the products of the probability of  $j$  packet arrivals during a sleep cycle duration  $t$  and the probability that a sleep cycle is of time duration  $t$ , where  $t$  varies from 0 to  $\infty$ . The probability  $f_j$  [33] can be expressed as

$$f_j = \int_0^{\infty} \frac{(M\lambda t)^j}{j!} e^{-(M\lambda t)} \frac{1}{\bar{S}} e^{-\left(\frac{t}{\bar{S}}\right)} dt \quad (6.4)$$

where  $M$  is the number of vehicles in the RSUs range and  $\lambda$  is the packet arrival rate for vehicles. Let  $\alpha_j$  ( $j = 0, 1, \dots, \infty$ ) be similarly defined as the probability of  $j$  packet arrivals in a service time period which for realistic packet size distributions can be rewritten as

$$\alpha_j = \sum_{t=t_1}^{t_n} \left[ \frac{(M\lambda t)^j}{j!} e^{-(M\lambda t)} B(t) \right] \quad (6.5)$$

where  $B(t_1), B(t_2), \dots, B(t_n)$ , are the probabilities of service durations corresponding to different packet sizes obtained from [93]. Thus, the mean service duration can be expressed as

$$\bar{X} = \sum_{t=t_1}^{t_n} tB(t) \quad (6.6)$$

Thus, the offered load ( $\rho$ ), can be expressed as

$$\rho = M\lambda\bar{X} \quad (6.7)$$

Since, the expression for carried load  $\rho_c$  remains unchanged [33], the packet blocking probability  $P_B$  can therefore be computed. The utilisation of the RSU can therefore be obtained as

$$U = M\lambda\bar{X}(1 - P_B) = \rho_c \quad (6.8)$$

The energy savings,  $E_s$  per hour through sleep cycles can be obtained as

$$E_s = (1 - U)P_t \cdot 3600 \quad (6.9)$$

where  $P_t$  denotes the transmit power saved when the RSU switches to the low state [28]. This can be obtained using the fully operational power consumption of the RSU [104] and the ratio between the fully operational power and the low state power consumptions [28]. Finally, the average packet delay can be expressed as

$$W = \frac{k}{M\lambda(1 - P_B)} \quad (6.10)$$

where  $k$  denotes the average number of packets in the RSU (including waiting and transmitting packets) and is obtained from [33].

## 6.5 Simulation

The java based simulator is implemented using four classes comprised of a Vehicle class that maintains vehicular packet generation, the AccessPoint class which maintains the RSU buffer and sleep durations, a Distributions class that is used to generate the packet arrival, packet size and RSU sleep

duration distributions, and a main class to run the simulation. The simulation implements three main methods that generate packets from the vehicles (`getPackets()`), serve the packets at the RSU (`servePkt()`), and calculate performance parameters (`performanceEvaluation()`) over a 24 hr period. The `getPackets()` method checks if the negative exponentially distributed waiting duration for each vehicle has elapsed before adding it to the RSUs service queue if the buffer is not full. Packets successfully added are given a timestamp while packets arriving at a full queue are marked blocked by incrementing a packet blocking counter. The `servePkt()` method increments a sleep or service time duration variable depending on the RSU's state. If the RSU is not serving any packets and the buffer is not empty, this method also retrieves a packet from the buffer to be served by the RSU. In the event of an empty queue with no packets in service, a negative exponentially distributed sleep time is generated and the RSU is switched to sleep mode. Finally the `performanceEvaluation()` is called after a 3600 second period to calculate the QoS parameters based on variables incremented and packet timestamps used during the communication phase of that hour. The hour is then incremented and the simulator reset with a new hour dependent vehicular density to get the results for each hour of the day.

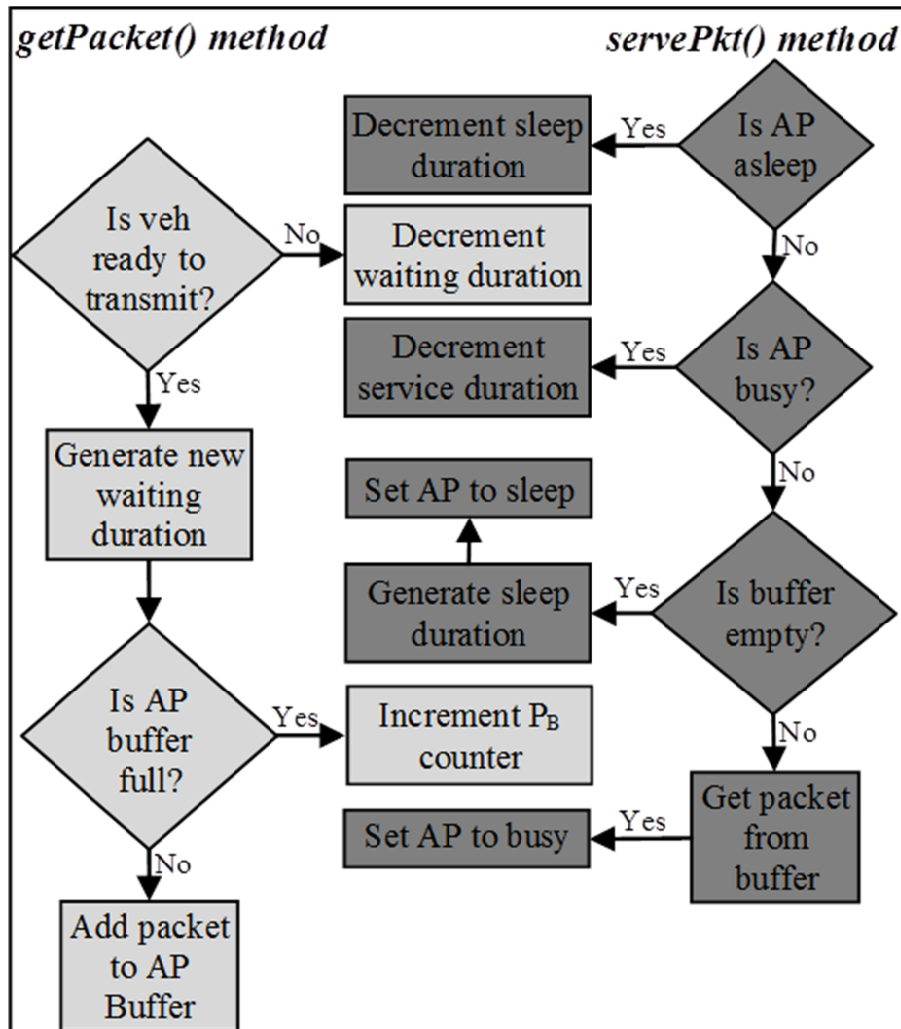


**Figure 6.3: Simulation flow chart.**

## 6.6 Performance Evaluation

The performance of the system has been evaluated in terms of energy usage, packet blocking probability and average packet delay. First, analytical results are shown for the transmission and operational energy requirements for the RSU connected to a power grid under normal circumstances to compare this reference case with the proposed strategies. The (original) energy required in this case is calculated by finding the total time required to transmit all the packets from all the vehicles in that hour. This time is then multiplied by the power required to transmit packets to determine the energy

used in transmitting the total data traffic [100]. This is then added to the minimum operational energy of an RSU. This is followed by a set of results assuming a large battery with no sleep cycle implementation. The next set of results shows the performance with sleep cycles implemented on an off grid RSU assuming no battery is available and no bounds are placed on the QoS parameters. The final analytical results present a sleep cycle implementation using a small battery and putting bounds on the QoS parameters. These bounded analytical QoS results are verified through simulations and are found to be in good agreement with the simulations.

The original energy consumption, in Figure 6.4, shows the system energy usage when assuming a grid connected RSU. The energy curve follows the vehicular density curve as an increase in vehicles also increases the intensity of packet arrivals. Accordingly, low energy usage is seen in the early hours with a minimum of 54 kJ at 4 am. The energy usage has two peaks during the rush hour periods with 66 kJ in the morning and 67.6 kJ in the evening.

The curve representing a system with no sleep cycles using renewable energy and a large battery exhibits the same energy consumption as that of the original system connected to the grid. This is because a large battery provides sufficient energy throughout the day for the RSU and thus it behaves like a grid connected system.

Next, sleep cycles are introduced without keeping bounds on the QoS parameters to study the impact of this policy on packet blocking probability and average packet delay. Applying the sleep cycles at the RSU without QoS bounds (and also without using batteries) achieves a lower energy curve with a minimum of 36.7 kJ consumed at 3 am. Since this sleep is only

applied at the time periods when the average wind energy (Figure 6.2) is deemed insufficient for the original energy consumption, sleep cycles are not used in the early morning hours of 3 am and 4 am. Hence, the system exhibits an increase in energy requirement at these hours matching that of the original and no sleep cases. Though the wind energy does not peak at these times, the vehicular traffic is low enough and can be supported by the available low wind energy. The same effect is seen at mid-day when wind energy peaks beyond the originally required energy between 10 am and 4 pm. During those periods, sleep cycles are not applied as well to save energy. Therefore the curve follows that of the original energy requirements (without sleep cycles). Although the original load energy falls towards the end of the day, the power in the wind concurrently falls at that time (Figure 6.2). Therefore, sleep cycles are applied to reduce energy consumption. Note that the rush hour periods of 8 am to 9 am in the morning and 5 pm-6 pm in the evening correspond to higher vehicular traffic but there is a fall in the wind power during those time periods (Figure 6.2). Hence, sleep cycles are applied to gain just enough energy at those times to serve all packets (waiting to be served in the buffer) eventually. However, this causes serious performance deterioration in terms of packet blocking probability and average packet delay as shown in Figure 6.5 and Figure 6.6, respectively.

To improve both packet blocking probability and average packet delay, and keep them under the bounds of 0.05 and 150 ms, respectively (for video-related applications) [33] while saving energy and meeting the demand, a small battery (see Section VB) is used. The mean duration of sleep cycles is set appropriately. This scenario primarily accounts a more realistic battery size that allows flexibility in network deployment. Secondly,

## 6.6 Performance Evaluation

---

by enabling the sleep to rely on QoS parameter bounds, energy savings can be maximised by maximising the sleep durations. Furthermore the battery allows surplus energy to be saved which can then be used at periods where the wind energy dips such as that seen at 9 am. With the dip in energy at high traffic hours the battery also allows QoS to be met while meeting the energy requirement with stored energy. Overall, the enhanced system is able to save a maximum energy of up to 32% at the lowest traffic hour and a minimum of 7.5% at the highest traffic hour with an average of 20% energy savings in the 24 hr period. Simulation results for this case (bounded QoS) are in good agreement with the analytical results, as shown in Figure 6.4.

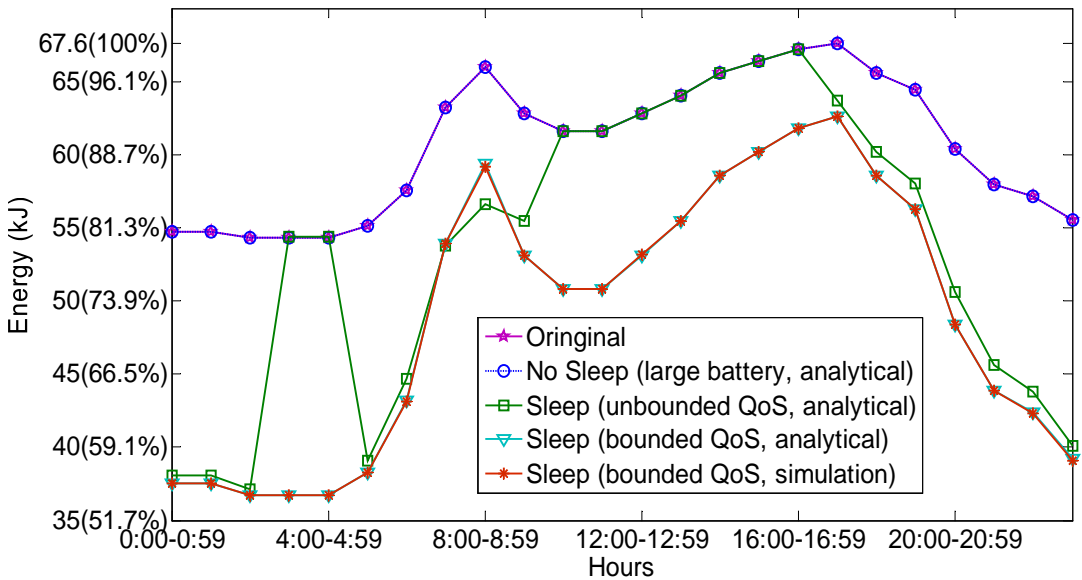


**Figure 6.4: Energy Required**

The packet blocking probability is shown in Figure 6.5. The case of without sleep using a large battery shows the system is very efficient and exhibits excellent QoS performance with negligible packet blocking throughout the day. The case of sleep with an unbounded QoS has a peak. It starts rising at 7 am and reaches an unacceptable level of 0.27 at 8 am and then declines to a very small value at 9 am to maximise energy savings

## 6.6 Performance Evaluation

---

without fulfilling the QoS. Therefore, the energy demands are met through sleep at the cost of poor QoS. The rest of the day then exhibits very low packet blocking probability since sleep is only used to meet energy requirements, without causing a rise in the packet blocking probability.

The case of sleep cycles with bounded QoS also exhibit a trend where the system keeps the packet blocking very low, near zero in the early hours of the day. This trend changes from 7 am but remains within a packet blocking probability bound below 0.05 between 8 am and 8 pm after which it drops to a  $P_B$  of 0.007 at 9 pm and then back to very low, near zero  $P_B$  for the rest of the night. These trends show that the introduction of sleep cycles is bound to increase the packet blocking probability at moderate and high traffic levels. The packet blocking probability, however, can be maintained within the 0.05 bound. A simulation of this bounded system has also been performed and is in good agreement with the analytical results.

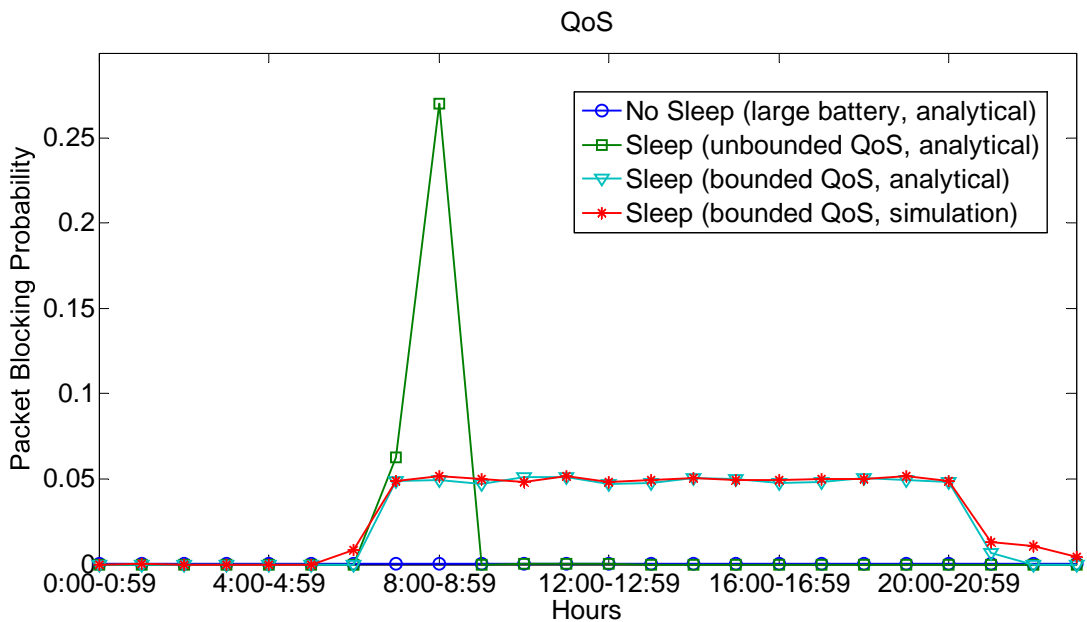
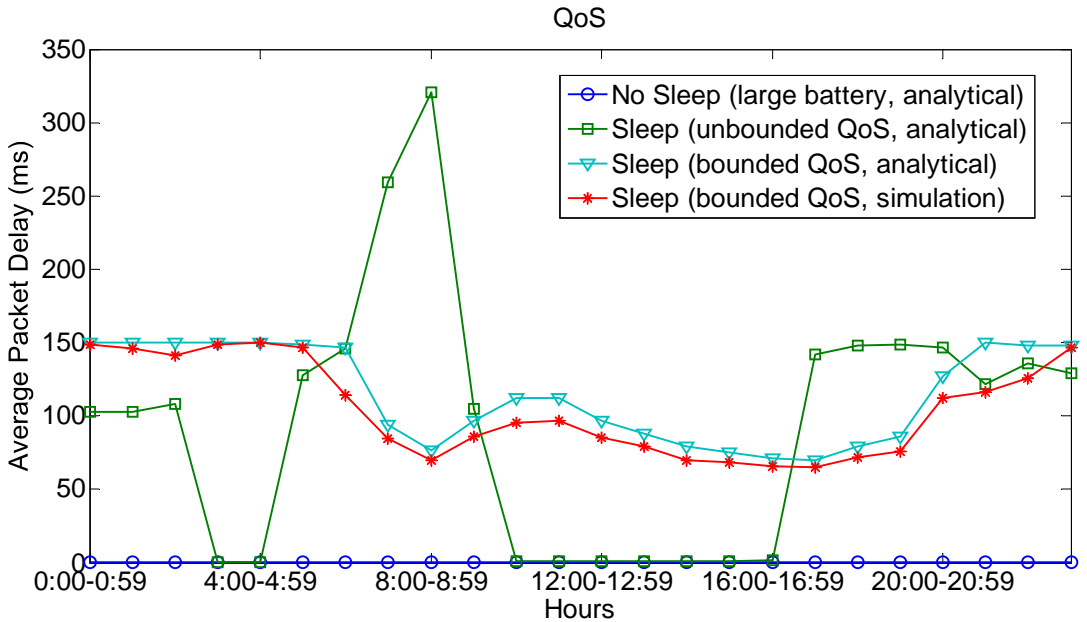


Figure 6.5: Packet blocking probability.

## 6.6 Performance Evaluation

---

The average packet delay is shown in Figure 6.6. As expected the system without sleep only incurred minimal delay of less than 67  $\mu$ s (approximately equivalent to the service duration) throughout the day. The system with sleep cycles and with unbounded QoS exhibits increased average packet delay at all points where extra energy was required to meet the original load demand. The average packet delay is however within an acceptable level of 150 ms throughout the day except for the morning rush hours of 8 am and 9 am where the energy demands had to be met at the cost of QoS. At this time, the average packet delay peaked to 259 ms at 8 am and 321 ms at 9 am.



**Figure 6.6: Average packet delay**

The system with sleep cycles and bounded QoS maintained delay at 150 ms until 7 am where the stricter bound on packet blocking caused the average packet delay to fall even lower during moderate and high vehicular traffic. Subsequently the fall in average packet delay can be seen to follow the vehicular traffic between 7 am and 10 pm. The delay obtained through

simulation with bounded QoS falls slightly lower than the analytical result because of the sensitivity of the delay when the packet blocking probability is bounded.

With the original energy consumption of the RSU, it is evident that there are certain durations of the day, when the traffic is high and the wind power is low. Thus, the wind energy is unable to support the operation of the RSU during those time periods. Sleep cycle techniques have been examined in these periods where the RSU by going into a low operational state lowers energy consumption. This greedy sleep cycle technique meets the power deficit during the required periods. However, it deteriorates the QoS beyond acceptable levels in some instances. Thus, a constrained sleep cycle is proposed which bounds the QoS within an acceptable level as well as meets the energy requirements. This leads to an overall surplus of wind energy at certain hours of the day because the total energy consumption reduces substantially through sleep cycles. However, it is observed that there can be a time period where the instantaneous energy demand is not met by the wind energy, though the number of such instances and their durations decreased considerably. Thus energy storage is needed in the form of capacitor or battery. The capacity of battery depends upon the intention behind its usage. If the battery is strictly used to meet only the instantaneous deficit, the battery size can become negligibly small and thus a capacitor might serve the purpose. But, if the aim is to store as much energy as possible for future support of a calm day (little wind energy available), then a small battery is needed.

## 6.7 Battery Capacity

Figure 6.7 shows the “supply minus demand” i.e. the excess energy that can be accumulated in a battery. From Figure 6.7, it is evident that if the battery only needs to meet the in-hour emergency demand then there is only one decline in the cumulative energy storage in the considered scenario. This decline corresponds to the 8 am morning hour when the traffic demand is high and the wind energy is low. The deficit is about 2.68 kJ. Thus, for a small battery we need to store only the energy corresponding to the dip. Expressing energy in terms of capacity of the battery in Ah and considering 50% depth of discharge (DOD) [106], the battery capacity should be 124.07 mAh for a 12V battery. In the case of a large battery, the aim is to store the surplus wind energy in each hour where the RSU uses sleep cycles. The maximum cumulative surplus for this case is 262 kJ. Thus, in a similar fashion, a 12V battery size is obtained as 12.13 Ah. Note that the capacity of a small family vehicle battery is typically 40 Ah [107].

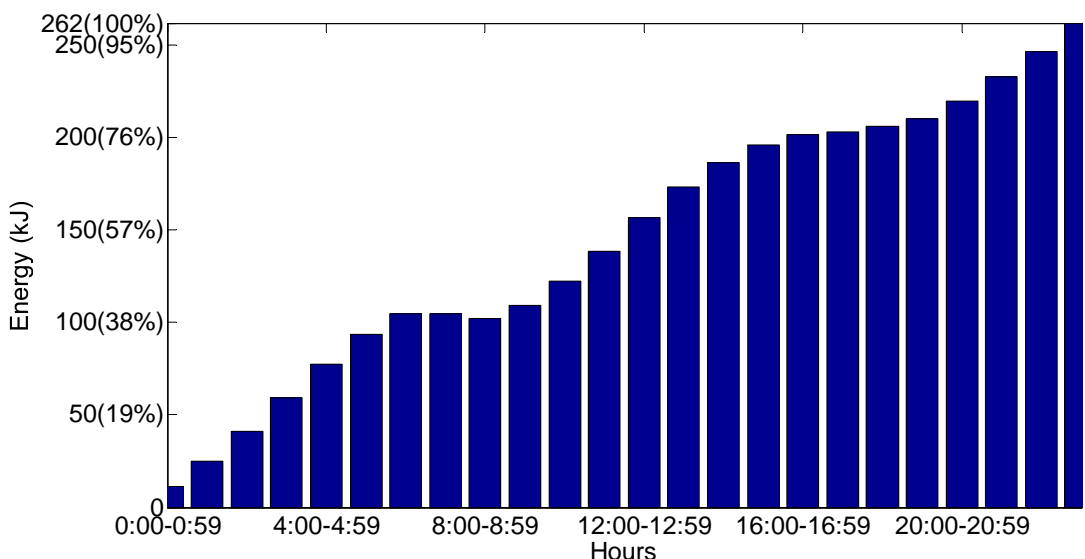


Figure 6.7: Cumulate energy storage.

### 6.8 Summary

With the aim of reducing the carbon footprint of a motorway V2R system, various deployment strategies of ubiquitous coverage along a motorway stretch have been proposed. A combined investigation of energy supply and load along with the effects on QoS of a RSU has been carried out and reported. Increased accuracy in representing the system is provided through the input parameters to the investigation which include statistical vehicular profiles and wind energy profiles for the same location at a stretch of the M4 motorway, UK. The resulting performance of the network was examined with bounds on QoS parameters along with proposed battery analysis which suggested that a very small battery size (capacitor) is needed to meet these bounds. The wind powered road side units reduce the carbon foot print of the proposed vehicular communication system, while the proposed sleep cycles with bounded QoS can save up to 32% of the current RSU's energy expenditure while meeting the QoS.

---

# **7 Reliability Analysis for Standalone Wind Powered RSUs**

## **7.1 Introduction**

Following on from the wind renewable energy system design in Chapter 7, this chapter delves deeper to provide reliability analysis for such a system. To analyse the system using various reliability indices, the first step is to derive the expected value of wind energy at any hour. Analysing the wind speed distribution, two different methods have been recommended to derive hourly wind energy values. The first method uses Weibull wind speeds and a specific power curve for a  $0.79 \text{ m}^2$  turbine. It achieved the same results as the second method which uses a perturbation theory derivation of the expected power values based also based on Weibull wind speeds. A suitable battery size is chosen by examining the RSU's outage with different battery capacities. Finally statistical indices are used to show the system's reliability with and without the use of the battery.

## **7.2 Wind Speed Profile**

The primary step in our analysis is obtaining the probability distribution of our wind speed samples. A number of treatments [108, 109] have modelled wind speed using different probability density functions. While the Rayleigh distribution is a commonly used function for fitting measured wind speed

## 7.2 Wind Speed Profile

---

probability distributions, the majority have used the Weibull distribution model for wind energy potential assessment. The Weibull probability density function is given by:

$$f(v) = \frac{b}{a} \left(\frac{v}{a}\right)^{b-1} e^{-\left(\frac{v}{a}\right)^b} \quad (7.1)$$

where  $v$  is the wind speed in m/s,  $a$  is the scale parameter in m/s,  $b$  is the unit-less shape parameter. The shape and scale parameters estimated using the maximum likelihood method [108] and the parameters for our sampled data can be seen in Table 7.1.

<b>b</b>	<b>a (m/s)</b>	<b>V<sub>m</sub>(m/s)</b>	<b>Power density (W/m<sup>2</sup>)</b>
2.22	6.09	5.39	166.8

**Table 7.1: Weibull parameters**

Comparing our sample with the Weibull generated samples, the distribution can be seen in Figure 7.1.

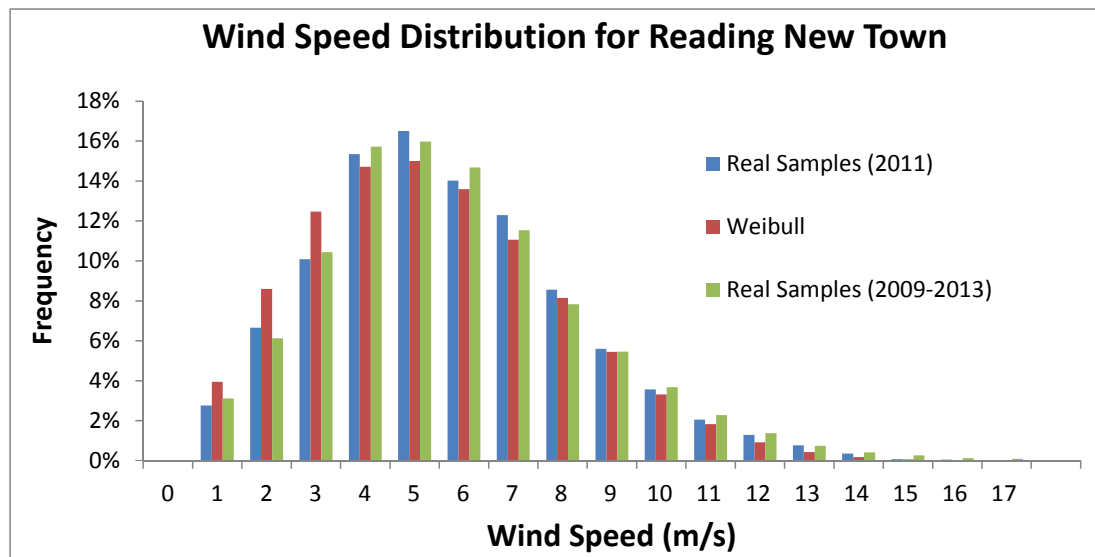


**Figure 7.1: Weibull wind speed distribution**

As seen in Figure 7.1 the analysis for a 5 year wind speed observation has been included and shows there is minimal deviation when the sample size is increased. This is further illustrated by coefficient of determination given by:

$$R^2 = 1 - \frac{\sum_{i=1}^N (y_i - x_i)^2}{\sum_{i=1}^N (y_i - \bar{y})^2} \quad (7.2)$$

where  $N$  is the number of bins,  $y_i$  is the frequency of areal wind sample,  $\bar{y}$  is the average of the  $y_i$  values, and  $x_i$  is the frequency distribution of the Weibull generated samples. An  $R^2$  of 97.2% and 97.6% is obtained for 1 year and 5 year samples respectively showing a good fit between the real data and our Weibull model.

### 7.3 Wind Power

Using the parameters in Table 7.1, we can thus generate Weibull random wind speeds to calculate the power generated from a wind turbine. One model uses the specifications for a 1m Wren Micro-turbine [110] along with the power curve to generate instantaneous power values for different wind speeds. To generate this model we first interpolate using the provided power curve. Using a curve fitting tool in Matlab, we obtained a 6th order polynomial curve given by:  $5.54\nu^6 + 0.005\nu^5 - 0.23\nu^4 + 3\nu^3 - 7.54\nu^2 + 5.42\nu + 8.65$  plotted in Figure 7.2 below.

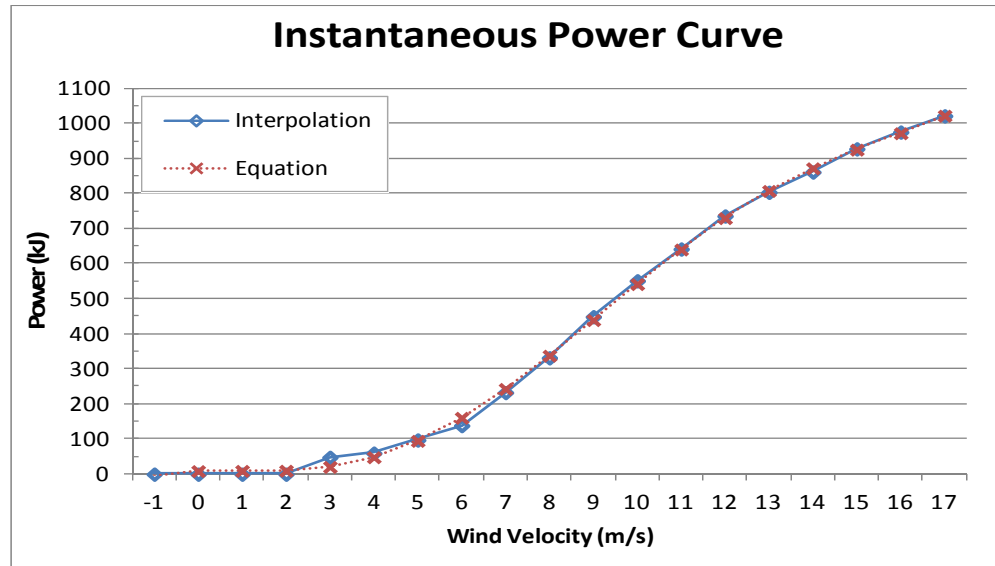


Figure 7.2: Fitted Power Curve for Wind Turbine.

Our second model for deriving the instantaneous power uses perturbation theory to derive wind power formulation in terms of statistical parameters. Wind power generated is proportional to the Velocity cubed with a cut-in and cut-off wind velocity. This can be expressed as

$$P = \begin{cases} 0 & \text{for } V \leq V_{\text{cut-in}} \\ \frac{1}{2} \rho V^3 & \text{for } V_{\text{cut-in}} \leq V \leq V_{\text{cut-off}} \\ 0 & \text{for } V \geq V_{\text{cut-off}} \end{cases} \quad (7.3)$$

where  $\rho$ ,  $V_{\text{cut-in}}$ , and  $V_{\text{cut-off}}$  are constants

Let  $E(P)$  be the expected value of power therefore:

$$E(P) = \frac{1}{2} \rho E(V^3) \quad (7.4)$$

In order to find out the pdf of wind power, we use perturbation theory on wind speed as  $V = \bar{V} + V'$  where  $V$  is the instantaneous wind speed,  $\bar{V}$  is the mean wind speed and  $V'$  is the perturbation term (small quantity) therefore:

$$E(V') = 0 \text{ (mean)} \quad (7.5)$$

$$\begin{aligned}
 Var V &= E(\bar{V} + V')^2 - [E(\bar{V} + V')]^2 \\
 &= E(\bar{V}^2) + 2E(\bar{V} \cdot V') + E(V'^2) - [E(\bar{V}) + E(V')]^2 \\
 &= E(\bar{V}^2) + 2E(\bar{V} \cdot V') + E(V'^2) \\
 &\quad - [E(\bar{V})]^2 - 2E(\bar{V})(V') - [E(V')]^2 \\
 &= \bar{V}^2 + 2\bar{V}E(V') + E(V'^2) - \bar{V}^2 \\
 &= E(V'^2) - [E(V')]^2 = Var(V')
 \end{aligned} \tag{7.6}$$

We now obtain the expression for expected value of power,

$$\begin{aligned}
 E(P) &= \frac{1}{2}\rho[E^3(V) + 3E(V)(V'^2) + E(V'^3)] \\
 &= \frac{1}{2}\rho[E^3(V) + 3E(V)E(V'^2)]
 \end{aligned} \tag{7.7}$$

(neglecting higher order forms)

$$Var(P) = E(P^2) - [E(P)]^2 \quad from Eqn. (3) \tag{7.8}$$

From Eqn. (1),

$$\begin{aligned}
 P &= \frac{1}{2}\rho(\bar{V} + V')^3 \\
 \therefore P^2 &= \frac{1}{4}\rho^2(\bar{V} + V')^6 \\
 \therefore E(P^2) &= \frac{1}{4}\rho^2 E \left[ \bar{V}^6 + 6\bar{V}^5V' + 15\bar{V}^4V'^2 + 20\bar{V}^3V'^3 + 15\bar{V}^2V'^4 + 6\bar{V}V'^5 + V'^6 \right] \\
 &= \frac{1}{4}\rho^2 \left[ [EV]^6 + 15(EV)^4E(V'^2) + 20(EV)^3E(V'^3) + 15(EV)^2E(V'^4) + 6EV(EV'^5) + E(V'^6) \right]
 \end{aligned} \tag{7.9}$$

$$[E(P)]^2 = \frac{1}{4} \rho^2 \begin{bmatrix} E^6 V + E^6 (V'^3) + 6E^4(V)E(V')^2 \\ + 2(E(V))^3 E(V'^3) + 6E(V)E(V'^2)E(V'^3) \\ + 9(E(V))^2 (E(V'^2))^2 \end{bmatrix} \quad (7.10)$$

$$Var(P) = \frac{1}{4} \rho^2 \begin{bmatrix} 9(E^4(V))^4 E(V'^2) + 15E^2(V)E(V'^4) \\ -9(E^2(V))^2 (E(V'))^2 - (E(V'^3))^2 \\ -2(E(V))^3 E(V'^3) \\ -6E(V)E(V'^2)E(V'^3) + E(V'^6) \end{bmatrix} \quad (7.11)$$

Wind power expression in terms of parameters of the Weibull pdf of the velocity

$$Var(P) = \frac{1}{4} \rho^2 [9[e(V)]^4 E(V'^2) - 9(E(V))^2 (E(V')^2)] \quad (simplified) \quad (7.12)$$

So we need  $E(V')$  ...  $k = 2$

Since the pdf of wind is Weibull (see Equation (7.1))

$$E(V^k) = a^k \Gamma\left(1 + \frac{k}{b}\right) \quad \Gamma(x) \sim \text{Gamma function} \quad (7.13)$$

$$E(V) = a \Gamma\left(1 + \frac{1}{b}\right) \quad k = 1 \quad (7.14)$$

$$\begin{aligned} Var(V) &= a^2 \left[ \Gamma\left(1 + \frac{2}{b}\right) - \left[ \Gamma\left(1 + \frac{1}{b}\right) \right]^2 \right] \quad k = 2 \\ \therefore E(V'^2) &= a^2 \left[ \Gamma\left(1 + \frac{2}{b}\right) - \left[ \Gamma\left(1 + \frac{1}{b}\right) \right]^2 \right] \end{aligned} \quad (7.15)$$

From (7.5), (7.14), and (7.15).

$$\begin{aligned}
 E(P) &= \frac{1}{2} \rho \left[ a^3 \left\{ \Gamma \left( 1 + \frac{1}{b} \right) \right\}^3 + 3a\Gamma \left( 1 + \frac{1}{b} \right) \left\{ \begin{array}{l} a^2 \Gamma \left( 1 + \frac{2}{b} \right) \\ -a^2 \left( \Gamma \left( 1 + \frac{1}{b} \right) \right)^2 \end{array} \right\} \right] \\
 &= \frac{1}{2} \rho \left[ a^3 \left\{ \Gamma \left( 1 + \frac{1}{b} \right) \right\}^3 + 3a^3 \Gamma \left( 1 + \frac{1}{b} \right) \Gamma \left( 1 + \frac{2}{b} \right) - 3a^3 \left\{ \Gamma \left( 1 + \frac{1}{b} \right) \right\}^3 \right]
 \end{aligned} \quad (7.16)$$

adding and subtracting ( $V^{13}$ ) finally

$$E(P) = \frac{1}{2} \rho a^3 \Gamma \left( 1 + \frac{3}{b} \right) \quad (7.17)$$

Hence,

$$E(P) = \frac{1}{2} \rho E(V^3) = E \left( \frac{\rho}{2} V^3 \right) \quad (7.18)$$

Moreover, after algebraic manipulation, we get from Equation (7.15)

$$Var(P) = \frac{1}{4} \rho a^6 \left[ \Gamma \left( 1 + \frac{6}{b} \right) - \left[ \Gamma \left( 1 + \frac{3}{b} \right) \right]^2 \right] \quad (7.19)$$

Now

$$\begin{aligned}
 Var(V^3) &= E(V^6) - [E(V^3)]^2 a^6 \Gamma \left( 1 + \frac{6}{b} \right) \\
 &\quad - \left[ a^3 \Gamma \left( 1 + \frac{3}{b} \right) \right]^2 a^6 \left[ \Gamma \left( 1 + \frac{6}{b} \right) - \left[ \Gamma \left( 1 + \frac{3}{b} \right) \right]^2 \right] \\
 \therefore Var(P) &= \frac{1}{4} \rho^2 Var(V^3) = Var \left( \frac{\rho}{2} V^3 \right)
 \end{aligned} \quad (7.20)$$

Thus we conclude that the wind power pdf can be approximated as a Weibull distribution with random variable  $\frac{\rho}{2} V^3$ , where  $V$  represents the random variable for wind speed.

## 7.4 Reliability Analysis

In considering a standalone AP solely dependent on wind power (without battery), a basic probabilistic reliability index is the loss of load expectation (LOLE). A loss of load occurs whenever the system load ( $L$ ) level exceeds the capability of the generating capacity ( $C$ ) of the wind turbine [69]. The LOLE index is based on the probability of the power generating system being inadequate to meet the demand at a given time or the loss of load probability (LOLP). We first use our one year hourly samples of wind speeds to obtain 365 capacity values for each hour/ use the log-logistic capacity pdf to generate 365 capacity values for each hour and compare it with the load at that hour, thus hours of outage are obtained by:

$$Outage_t = \sum_{i=1}^I p(C_i < L_i) \quad (7.21)$$

where the outage for an hour  $t$  is 1 on day  $i$  if the capacity is less than the load and 0 otherwise averaged over a total of  $I = 365$  days. The loss of load probability can therefore be obtained by:

$$LOLP_t = \frac{Outage_t}{I} \quad (7.22)$$

The LOLE obtained for our year hourly samples thus presents the expected number of hours during which the load will not be met in that year is a summation of all the hourly outages is obtained by:

$$LOLE = \sum_{t=1}^T (Outage_t) \quad (7.23)$$

To understand the capacity the wind energy failed to provide in the duration of study or in a given 24 hour period we determine the loss of energy

expectation (LOEE) and the expected demand not served (EDNS) respectively. The LOEE gives the value of unmet demand while the EDNS is another risk index that is calculated as the product of the state probability and the amount of load shortage in the system. Both the LOEE and EDNS are derived from the unmet demand for each hourly ( $i$ ) sample expressed as:

$$Unmet\ Demand_i = \begin{cases} L_i - C_i, & C_i < L_i \\ 0, & C_i \geq L_i \end{cases} \quad (7.24)$$

The loss of energy expectation (LOEE) for the whole year is a summation of unmet demand over a 24 hr period ( $T$ ) for each day ( $i$ ) in the year (I=365) :

$$LOEE = \sum_{t=1}^T \left\{ \sum_{i=1}^I (Unmet\ Demand_i) \right\} \quad (7.25)$$

The EDNS for each hour can be calculated by averaging the unmet demand over 365 days for each hour:

$$EDNS_t = \sum_{t=1}^T \left\{ LOLP_t \sum_{i=1}^I (Unmet\ Demand_i) \right\} \quad (7.26)$$

The EDNS over a 24 hour period is thus an average of the hourly EDNS or:

$$EDNS = \frac{1}{T} \sum_{t=1}^T \{EDNS_t\} \quad (7.27)$$

The time for which the load is not supplied by the system in a 24 hour period is the expected energy not supplied and is given by:

$$EENS = EDNS \times T \quad (7.28)$$

The energy index of reliability (EIR) is then given by:

$$EIR = 1 - \frac{EENS}{E_0} \quad (7.29)$$

## 7.5 Performance Evaluation

---

where  $E_0$  is the energy demand of the system over the 24 hour period under consideration. The energy index of unavailability can also be obtained by:

$$EIU = \frac{LOEE}{E_0} \quad (7.30)$$

Finally the forced outage rate can be calculated from the mean time to repair (MTTR) and mean time before failure (MTBF) by the following equation:

$$FOR = \frac{MTTR}{MTBF + MTTR} \quad (7.31)$$

where the MTBF is the average UP time or time the system spends with enough energy to serve the load while the MTTR is the average Down time, or time the system spends with insufficient energy as illustrated in Figure 7.3. The mean times can be derived from the probability density functions of the failure and recovery times generated for a capacity and load values samples or function generated values.

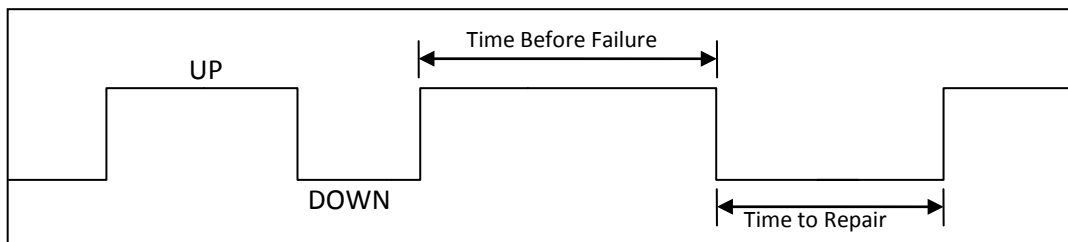
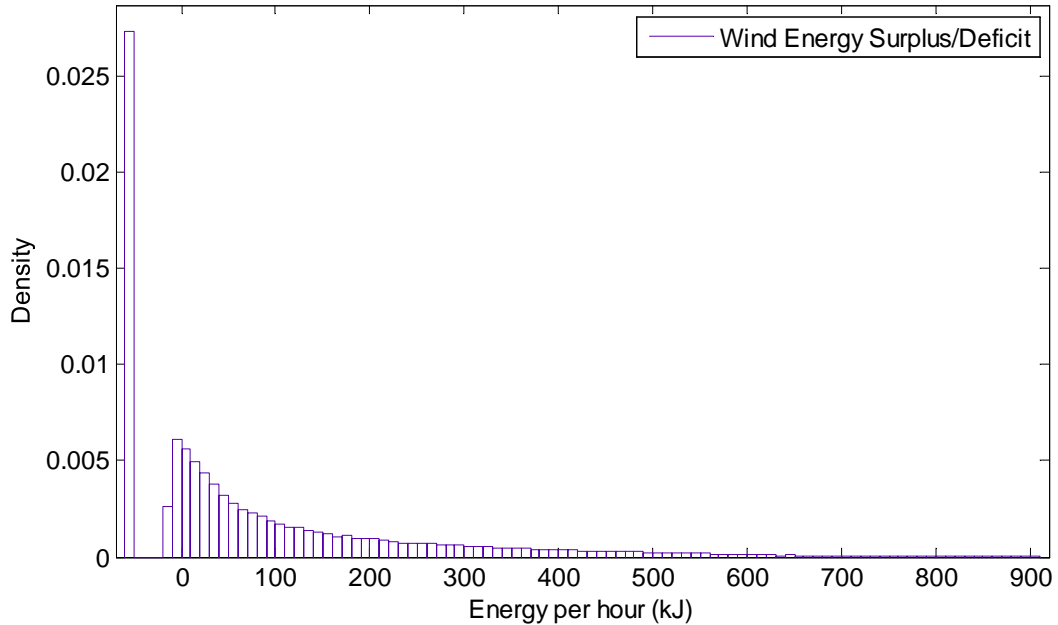


Figure 7.3: MTTR and MTBF estimation from system UP/Down time

## 7.5 Performance Evaluation

Various reliability indices have been used to analyse the system, however in addition, an understanding of the energy surplus and deficiency states is required to derive a battery size for the system. First we show the results of a battery analysis to determine a suitable battery capacity for the system. This is followed by analytic results of reliability indices and a comparison of the standalone system with and without a battery.



**Figure 7.4: PDF of hourly energy surplus/deficit.**

It is evident from Figure 7.4 that there is a significant amount of times where the energy is insufficient for the road side unit. Going back to the Weibull pdf in Figure 7.1, it can be seen that the majority of wind speeds lie in the low speed section of the pdf. This in effect causes the system to have a high outage rate with low magnitude energy deficiency 36.1% of the time as determined from the area under the curve lower than the 0 kJ which indicates a deficiency. The heavy tailed Weibull characteristic however, enables a significant amount of energy to be at a higher magnitude of energy surplus in the other 64.9% of the remaining instances. The surplus states occur nearly twice as much as deficit states and tend to be at higher magnitudes indicating a significant amount of energy can be stored for later use. Also note that no energy surplus occurs beyond 910 kJ due to the wind cut-off requirement for the turbine and the minimum energy requirement in any hour. With such high surplus energy magnitudes occurring more often than deficits the persistent behaviour of cumulative energy in the system as

time progresses is a continuous increase. Since the system is not grid-connected therefore does not enable a smart system whereby surplus electricity generated can be sold back to the power company, such surplus in the system can be disregarded. Considering a limit to battery capacity and a need of minimizing the battery size for easier deployment of the system, determining an appropriate battery size for the system requires an analysis to show the outage with varying battery sizes. Using a 60Ah 12V deep cycle battery with an 80% depth of charge (DOD) [111] the outage rate is reduced from 37% to as low as 1%. The decrease in outage hours as the capacity is increased as seen in Figure 7.5 follows an exponential decline. Since there are marginal benefits beyond a 60Ah battery we have decided to analyse the reliability with a 60Ah sized battery.

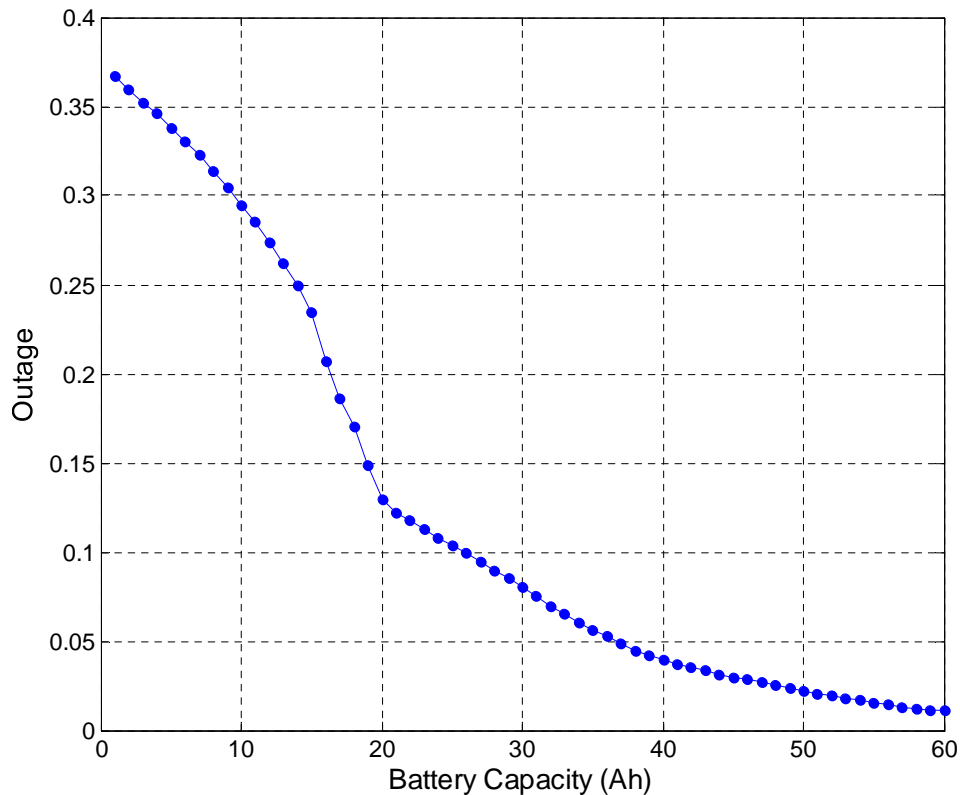


**Figure 7.5: System outage reduction with increased battery capacity.**

## 7.5 Performance Evaluation

---

The LOLP and EDNS with and without the use of a battery for each hour are shown in the Figure 7.6. The LOLP for a system without a battery remains between 26% and 40% during the whole day following the vehicular traffic profile with relatively lower LOLPs at early morning and late night hours. The LOLP in the case with a battery on the other hand maintained zero LOLP in the early hours until 6 am and reached a 0.05% peak in the evening rush hour periods. Both the LOLPs followed the vehicular traffic profile because increased vehicular density resulted in higher energy requirements at the RSU subsequently rendering the wind provided energy insufficient. A similar case is exhibited with the EDNS where the system without battery sustains a much higher demand not being served with around 0.5 kJ not being met in the early mornings and up to 1.6 kJ in the evening rush hour periods. The system setup with a battery on the other hand provided enough energy most of the day with a peak EDNS lower than 0.02 kJ in the rush hour periods. The EENS in the 24 hr period for the system without a battery was up to 76.17 kWh while the battery enabled the EENS to be reduced to 0.32 kWh.

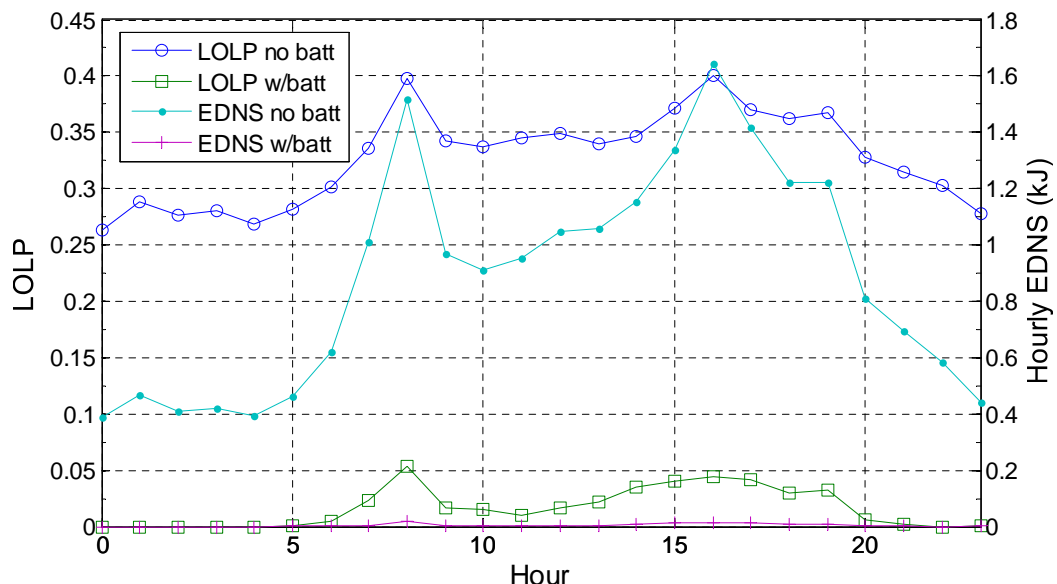
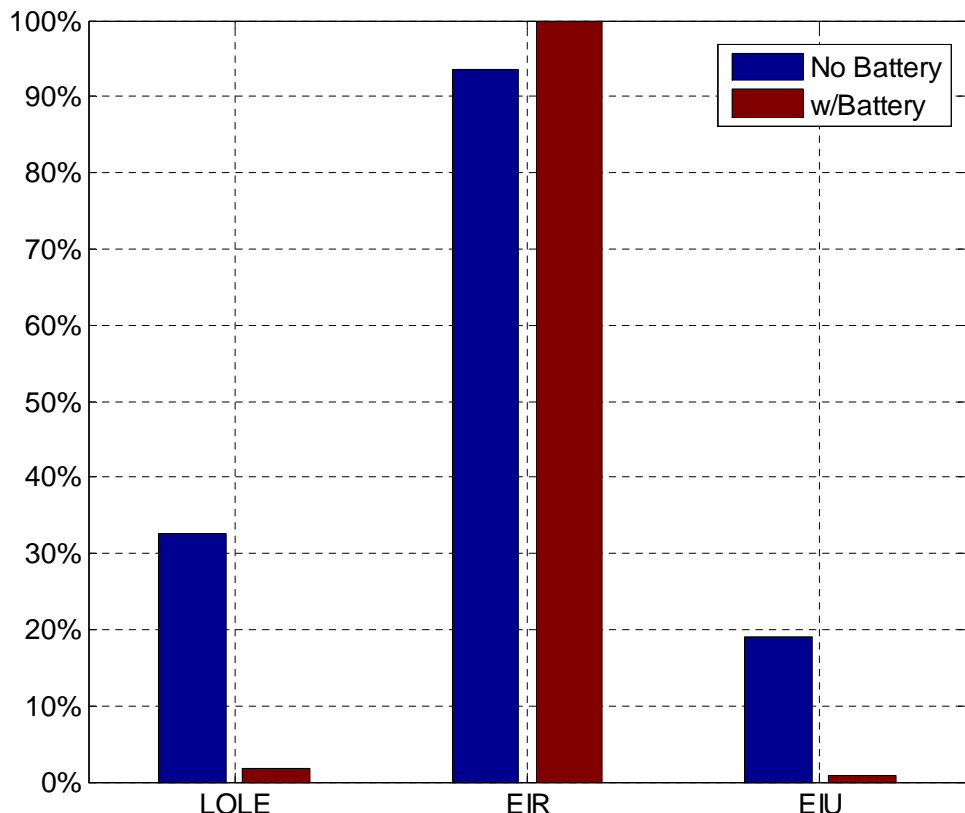


Figure 7.6: Hourly LOLP and EDNS with and without a battery.

## 7.5 Performance Evaluation

---

The overall system performance depicted in Figure 7.7 was analysed using the LOLE, EIR, and EIU. Looking at a 5 year study period the LOLE for the system without a battery is 32.7% which is close to the probability of a deficiency obtained from the pdf in Figure 7.4. This is expected since the loss of load will be due to an energy deficiency thus the probability of such energy deficiency without a battery will be the LOLE. Using a battery reduced the LOLE down to 1.64%. The EIR system without a battery subsequently displayed a low index (93.52%) of availability compared to the 99.97% availability with a battery equipped. The unavailability index therefore reached 19% in the first system while the battery equipped system was unavailable only 0.78% of the times.



**Figure 7.7: Overall system reliability.**

To make gain, a deeper understanding of the various energy reliability indices is needed together with a confirmation of their accuracy and their effect on system reliability. Figure 7.8 shows the survival function as the number of hours the system (with and without battery) can go beyond without a power loss. Both setups will last more than 3 hours with 100% certainty. Without a battery the RSU only has a 0.1% chance of making it beyond a full day (24 hours) while a battery gives a much higher probability of 0.32. Furthermore, constant average wind speeds can enable the battery equipped RSU to function continuously with a 0.1 probability going beyond 200 hours with a maximum MTBF of more than 76 days.

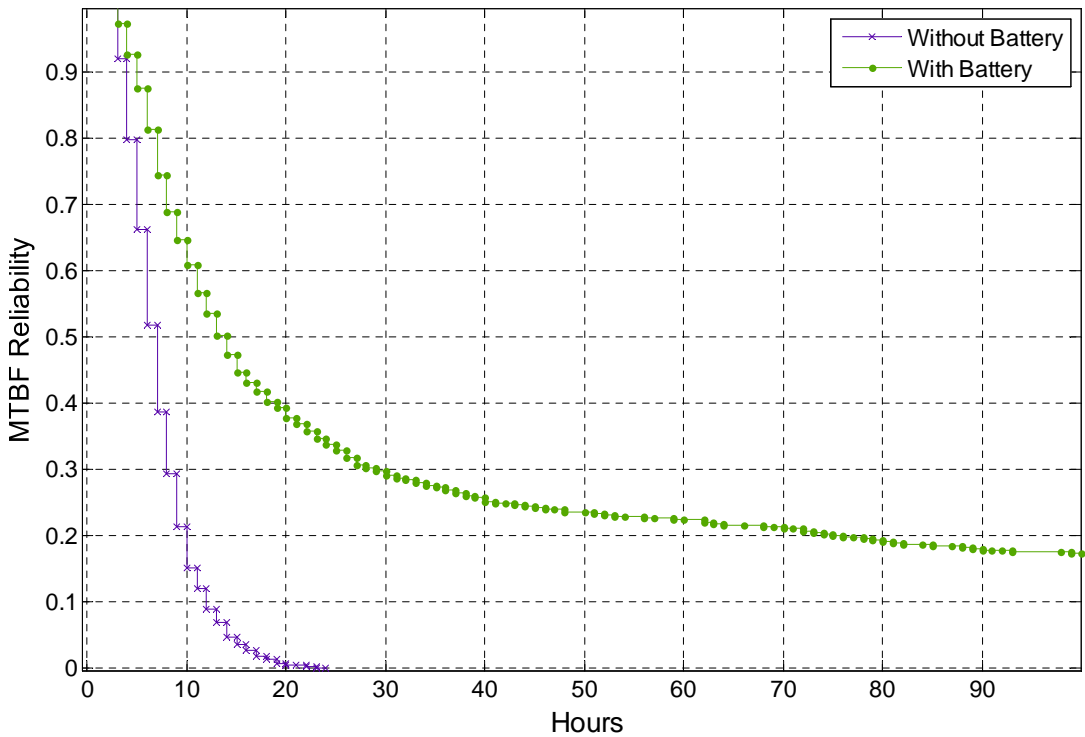


**Figure 7.8: MTBF survivor function.**

The MTTR gives an idea of how long the outages last. Both setups with and without a battery showed very similar trends in recovery times with the battery equipped RSU performing only very slightly better than a system without energy storage. This is because the recovery of the system is mainly

## 7.5 Performance Evaluation

---

dependent on the wind speed rather than the storage of energy. Looking at Figure 7.9 the probability of the system being repaired within the hour is around 0.34 for both systems. Both systems recovered from failure within 12 hours with a 0.99 probability.

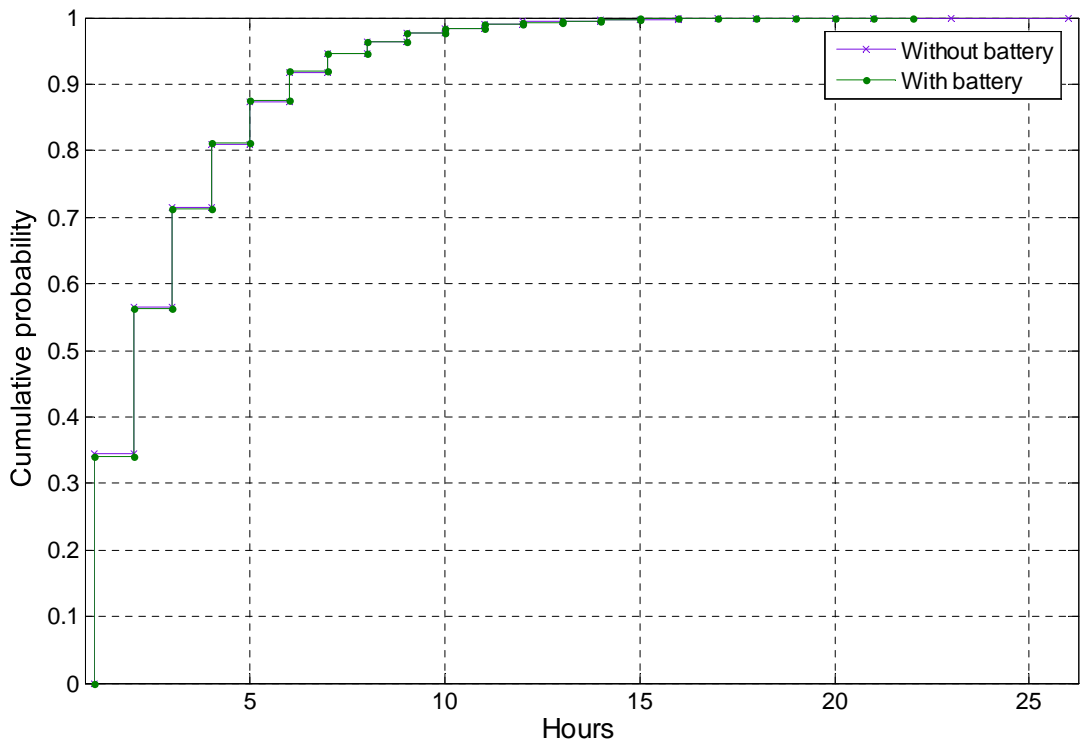


**Figure 7.9: MTTR Cumulative Probability.**

Finally the MTTR and MTBF can be used to determine the FOR (Equation (7.31)). Table 8.2 below shows the MTTR, MTBF, and FOR for the system with and without a battery.

System	MTBF	MTTR	FOR (%)
Without battery	7.41	2.93	28.3
With battery	61.9	2.93	4.5

**Table 7.2: System Reliability**

### 7.6 Summary

To analyse the reliability of a standalone wind powered RSU, the validity of the Weibull distribution for wind speeds was verified at the proposed motorway deployment location. The Weibull distribution has enabled two methods of obtaining hourly expected generated power values. The first method used the power curve from a wind turbine specification sheet along with Weibull wind speeds while the second method applied perturbation theory and the Weibull distribution. Both methods obtained the same reliability index results. Using the statistical expected values of wind energies for each hour, and the load energy requirements, a pdf illustrating the energy surplus and deficiency of the system has been obtained. A five year period simulation of wind energy supply and load energy consumption was performed to determine the effects of various battery capacities on outage rate. Various reliability indices are determined given a chosen battery capacity of 60 Ah. The system performance with a battery significantly improved, reducing the outage rate of RSU down from 28.3% to 4.5%. Though such an improvement can be considered suitable for leisure and other non-critical communication applications, vehicular safety presents high availability requirements requiring 99.999% availability which cannot be guaranteed with only renewable energy. Therefore renewable energies should be used in conjunction with non-renewable sources to ensure high availability.

---

## 8 Conclusions and Future Work

Studying the challenges associated with deploying vehicular networks, this thesis outlined a few state-of-the-art methodologies that obtain precise performance metrics for energy efficient motorway vehicular networks, ensuring a level of realism by using realistic measurements as input to the simulations and analyses. The study primarily addresses the performance trade-off in vehicular environments to minimise energy consumption and realise low carbon footprint deployments. The thesis investigates the effects of user mobility on wireless communication in a motorway vehicular environment which is subsequently used for various QoS aware and energy aware medium access control (MAC) and routing protocols. A novel architecture which enables enhanced energy efficient schemes and the use of renewable energy is proposed. Finally operational scenarios with renewable energy are proposed followed by a reliability analysis for such a system.

### 8.1 Summary

A real vehicular mobility profile is used to determine the energy consumption of the routing protocols considered. To determine the effects of hop numbers and hop lengths on the energy consumption, shortest and most forward hop V2V schemes were simulated to route a packet through a 5 km motorway stretch to a base station. This is followed by an optimisation

## 8.1 Summary

---

technique to determine the optimal hops and hop lengths. The hop lengths were then applied to the cumulative distribution function of inter-vehicular spacing to determine the achievable connectivity with the chosen protocol parameters. A centralised communication system with full connectivity is subsequently analysed by comparing the 802.11p MAC protocol and a modified packet reservation multiple access (MPRMA) protocol. Both schemes are simulated to determine and investigate their performance in terms of QoS and energy consumption. Having investigated both V2V and centralised V2R communications, the limitations of both schemes necessitated the use of road side units to act as low energy relay nodes and maintain connectivity on the motorway. To maximise energy savings at the road side units (RSUs) in a motorway vehicular-to-roadside (V2R) network, we introduce a reactive sleep strategy namely adaptive sleep cycles. An analytical model for the RSU with adaptive sleep cycles is proposed and developed using G/G/1/K vacation queuing where real vehicular traffic profile and packet size measurements are utilised. Instead of the traditional use of traffic shaping for QoS improvement, we proposed their use in a different context. We introduced two types of traffic shaping techniques (time and length-based traffic shaping) to extend the uninterrupted sleep duration and hence minimise the adaptive sleep cycle overheads (associated with wake-up and sleep operations) thereby maximising the energy savings. Finally to reduce the carbon footprint of RSU deployments we introduced the use of renewable sources of energy. The use of wind power was proposed and therefore the RSUs act as standalone entities. Real vehicular traffic profiles, reported data traffic measurements and reported wind measurements have been utilised to perform this study. The performance was analysed in

## **8.2 Key Findings**

---

several test cases and an operational scenario was suggested. It was deemed necessary to further scrutinise such standalone system availability when the intermittent nature of wind is considered. A wind energy model was therefore created to analyse the available wind energy and determine the level of reliability that can be achieved by the RSU. Statistical analysis was used to determine the Weibull parameters of the wind distribution. Furthermore, two methods were used to derive the wind generated power from instantaneous wind speed distributions. The first used the Weibull wind speed distribution along with the power curve of a suitable wind turbine to generate random hourly available energy. The second method employed perturbation theory to derive the statistical value of the expected power with Weibull distributed wind speeds. Using both of these methods, reliability indices were investigated and a suitable battery size was determined for reliable operation.

## **8.2 Key Findings**

- Shortest hop routing minimised the propagation distances decreasing the transmission energy consumption but reduced the gains in energy efficiency as a result of the increased number of hops which increase the network wide reception energy. Linear programming optimisation showed transmission with maximised propagation distance to be the most effective.
- The energy efficient most forward hop scheme offered 99% connectivity at moderate to high vehicular traffic with 80% connectivity at low vehicular traffic in a motorway. The probability

## 8.2 Key Findings

---

of connectivity was then improved with energy efficient relay nodes (RSUs) that can ensure connectivity at all hours of the day.

- The 802.11p MAC protocol's channel contention mechanism was found to be the debilitating factor degrading the performance of 802.11p. In addition the requirement for handshaking procedures limited the goodput of the protocol causing high delay and packet dropping in high traffic hours.
- The listen before talk mechanism of the 802.11p protocol resulted in high energy expenditure as vehicles constantly sensed the medium to determine availability. The M-PRMA protocol on the other hand worked efficiently enabled by a centralised architecture that reserves and coordinates transmission periods.
- With time-based and length-based traffic shaping techniques, average transmission energy savings of 84% and 77% are achieved respectively at the RSU while maintaining the end to-end packet blocking probability within 5% and the end-to-end average packet delay below 20 ms, meeting the requirements of voice, video and data, and green communication.
- Both analytical and simulation results reveal that with the introduction of sleep cycles and a very small battery (124 mAh), these RSUs are able to support quality of service (QoS) for video-related applications at each hour of the day in a motorway vehicular environment while increasing the energy efficiency up to 32%.
- A battery size of 60 Ah was able to bring the outage rate of the RSU from 28.3% to 4.5%

### 8.3 Future Work

This thesis has covered a specialised area in wireless communications key in the evolution towards heterogeneous integrated networks in 5G. Thus, it has opened many paths for possible expansions and future work.

1. The energy efficient routing studied can be merged with appropriate medium access protocols to provide an all-inclusive performance measure of a network. This can further lead to determining how a sleep cycle scheme can be employed to enable vehicles to save energy when not transmitting and not intending to relay packets. Such sleep cycles will undoubtedly require more sophisticated routing algorithms to make nodes aware of when they can switch to a low power mode.
2. The merging of various topics in this thesis can lead to the study of an extended motorway network which investigates a combination of V2V and V2R communications. The stand-alone renewable RSUs utilising sleep cycles studied in Chapter 7 can be used in conjunction with the optimised ad-hoc routing discussed in Chapter 5 to produce an intermittent RSU placement scheme which limits the number of deployments and thus overall network energy consumption.
3. Finally the intermittent nature of wind energy opens prospects with the design of innovative rate adaptive MAC protocols. Rate adaptive MAC protocols in the literature have been investigated with the aim of mitigating physical channel impairments. In an energy efficient case however, the MAC protocol can lower the

transmission rate in order to transmit at lower powers that match the available instantaneous power obtained from renewable sources of energy.

4. Finally experimental validation of the analytic and simulation results in this thesis is a very useful extension.

---

## References

- [1] GSMA, "Connected Car Forecast: Global Connected Car Market to Grow Threefold Within Five Years," GSMA2013.
- [2] P. Papadimitratos, A. La Fortelle, K. Evenssen, R. Brignolo, and S. Cosenza, "Vehicular communication systems: Enabling technologies, applications, and future outlook on intelligent transportation," *Communications Magazine, IEEE*, vol. 47, pp. 84-95, 2009.
- [3] H. Shah, "Road lengths in Great Britain: 2011," Department for Transport2012.
- [4] J. Grove, "Vehicle licensing statistics: quarter 3 2012," Department for TransportDecember 2012 2012.
- [5] G. Karagiannis, O. Altintas, E. Ekici, G. Heijenk, B. Jarupan, K. Lin, et al., "Vehicular Networking: A Survey and Tutorial on Requirements, Architectures, Challenges, Standards and Solutions," *Communications Surveys & Tutorials, IEEE*, vol. 13, pp. 584-616, 2011.
- [6] H. Moustafa, S. M. Senouci, and M. Jerbi, "Introduction to Vehicular Networks," *Vehicular Networks: Techniques, Standards and Applications*, 2009.
- [7] Z. Y. Rawashdeh and S. M. Mahmud, "Communications in Vehicular Networks," in *Mobile Ad-Hoc Networks: Applications*, X. Wang, Ed., ed, 2011.
- [8] GSMA. (2013, June 2013). *GPM Programme Overview*. Available: <http://www.gsma.com/mobilefordevelopment/programmes/green-power-for-mobile/programme-overview>
- [9] F. Richter, A. J. Fehske, and G. P. Fettweis, "Energy Efficiency Aspects of Base Station Deployment Strategies for Cellular Networks," in *Vehicular Technology Conference Fall (VTC 2009-Fall), 2009 IEEE 70th*, 2009, pp. 1-5.
- [10] J. Matos, A. Oliveira, T. Meireles, N. Ferreira, P. Mar, J. Fonseca, et al., "Emergent Vehicular Communications: Applications, Standards and Implementation."
- [11] M. Shulman and R. Deering, "Vehicle safety communications in the United States," US Department of Transport2007.
- [12] R. Meraihi, S. M. Senouci, D. E. Meddour, and M. Jerbi, "Vehicle-to-Vehicle Communications: Applications and Perspectives," *Wireless Ad Hoc and Sensor Networks*, pp. 285-308.
- [13] M. Jerbi, S. M. Senouci, Y. G. Doudane, and M. Cherif, *Vehicular Communications Networks: Current Trends and Challenges*: IGI Global, 2010.
- [14] P. Ranjan and K. K. Ahirwar, "Comparative study of vanet and manet routing protocols," in *Proceedings of the International Conference on Advanced Computing and Communication Technologies (ACCT 2011)*, 2011.

- 
- [15] H. Menouar, F. Filali, and M. Lenardi, "A survey and qualitative analysis of mac protocols for vehicular ad hoc networks," *Wireless Communications, IEEE*, vol. 13, pp. 30-35, 2006.
  - [16] J. B. Kenney, "Dedicated Short-Range Communications (DSRC) Standards in the United States," *Proceedings of the IEEE*, vol. 99, pp. 1162-1182, 2011.
  - [17] R. Uzcategui and G. Acosta-Marum, "Wave: A tutorial," *Communications Magazine, IEEE*, vol. 47, pp. 126-133, 2009.
  - [18] S. Eichler, "Performance Evaluation of the IEEE 802.11p WAVE Communication Standard," in *Vehicular Technology Conference, 2007. VTC-2007 Fall. 2007 IEEE 66th*, 2007, pp. 2199-2203.
  - [19] Q. Ni, L. Romdhani, and T. Turletti, "A survey of QoS enhancements for IEEE 802.11 wireless LAN: Research Articles," *Wirel. Commun. Mob. Comput.*, vol. 4, pp. 547-566, 2004.
  - [20] S. Kumar, V. S. Raghavan, and J. Deng, "Medium Access Control protocols for ad hoc wireless networks: A survey," *Ad Hoc Networks*, vol. 4, pp. 326-358, 5 2006.
  - [21] A. C. V. Gummalla and J. O. Limb, "Wireless medium access control protocols," *Communications Surveys & Tutorials, IEEE*, vol. 3, pp. 2-15, 2000.
  - [22] T. Razafindralambo and F. Valois, "Performance evaluation of backoff algorithms in 802.11 ad-hoc networks," presented at the Proceedings of the 3rd ACM international workshop on Performance evaluation of wireless ad hoc, sensor and ubiquitous networks, Terromolinos, Spain, 2006.
  - [23] G. Boudour, C. Teyssie, and Z. Mammeri, "Scheduling-Based Reservation MAC Protocol for Bandwidth and Delay Optimization in Wireless Mesh Networks," in *Networking and Communications, 2008. WIMOB '08. IEEE International Conference on Wireless and Mobile Computing*, 2008, pp. 272-277.
  - [24] S. K. Sarkar, T. G. Basavaraju, and C. Puttamatadappa, *Ad Hoc Mobile Wireless Networks: Principles, Protocols and Applications*: Auerbach Publications, 2007.
  - [25] J. Mo, H. W. So, and J. Walrand, "Comparison of multi-channel MAC protocols," presented at the Proceedings of the 8th ACM international symposium on Modeling, analysis and simulation of wireless and mobile systems, Montréal, Quebec, Canada, 2005.
  - [26] R. R. Choudhury, X. Yang, R. Ramanathan, and N. H. Vaidya, "Using directional antennas for medium access control in ad hoc networks," presented at the Proceedings of the 8th annual international conference on Mobile computing and networking, Atlanta, Georgia, USA, 2002.
  - [27] M. J. Miller, "Cross-Layer Desings for Energy-Saving Sensor and Ad-Hoc Networks," Ph.D, Computer Science, University of Illinois at Urbana-Champaign, 2005.
  - [28] L. Haratcherev, M. Fiorito, and C. Balageas, "Low-Power Sleep Mode and Out-Of-Band Wake-Up for Indoor Access Points," in *GLOBECOM Workshops, 2009 IEEE*, 2009, pp. 1-6.
  - [29] W. Wei, V. Srinivasan, and C. Kee-Chaing, "Power Control for Distributed MAC Protocols in Wireless Ad Hoc Networks," *Mobile Computing, IEEE Transactions on*, vol. 7, pp. 1169-1183, 2008.

- 
- [30] E.-S. Jung and N. H. Vaidya, "A power control MAC protocol for ad hoc networks," presented at the Proceedings of the 8th annual international conference on Mobile computing and networking, Atlanta, Georgia, USA, 2002.
  - [31] B. Vinod, "Exponential Queues with Server Vacations," *The Journal of the Operational Research Society*, vol. 37, pp. 1007-1014, 1986.
  - [32] W. Kumar, B. R. Qazi, S. Bhattacharya, and J. M. H. Elmirghani, "A Vacation-based Performance Analysis of an Energy-Efficient Motorway Vehicular Communication System," *submitted to IEEE Transactions on Vehicular Technology*, May 2013 2013.
  - [33] W. Kumar, S. Bhattacharya, B. R. Qazi, and J. M. H. Elmirghani, "An energy efficient double cluster head routing scheme for motorway vehicular networks," in *Communications (ICC), 2012 IEEE International Conference on*, 2012, pp. 141-146.
  - [34] X. Wu, S. Wu, H. Sun, and L. Li, "Dynamic slot allocation multiple access protocol for wireless ATM networks," in *Communications, 1997. ICC '97 Montreal, Towards the Knowledge Millennium. 1997 IEEE International Conference on*, 1997, pp. 1560-1565 vol.3.
  - [35] P. Kolios, V. Friderikos, and K. Papadaki, "Ultra Low Energy Store-Carry and Forward Relaying within the Cell," in *Vehicular Technology Conference Fall (VTC 2009-Fall), 2009 IEEE 70th*, 2009, pp. 1-5.
  - [36] W. Shan-Hung, C. Chung-Min, and C. Ming-Syan, "An Asymmetric and Asynchronous Energy Conservation Protocol for Vehicular Networks," *Mobile Computing, IEEE Transactions on*, vol. 9, pp. 98-111, 2010.
  - [37] H. Chih-Shun and T. Yu-Chee, "Cluster-based semi-asynchronous power-saving protocols for multi-hop ad hoc networks," in *Communications, 2005. ICC 2005. 2005 IEEE International Conference on*, 2005, pp. 3166-3170 Vol. 5.
  - [38] N. Li, Y. Xu, and S.-I. Xie, "A power-saving protocol for ad hoc networks," in *Wireless Communications, Networking and Mobile Computing, 2005. Proceedings. 2005 International Conference on*, 2005, pp. 808-811.
  - [39] W. Fisher, M. Suchara, and J. Rexford, "Greening backbone networks: reducing energy consumption by shutting off cables in bundled links," presented at the Proceedings of the first ACM SIGCOMM workshop on Green networking, New Delhi, India, 2010.
  - [40] M. Gupta and S. Singh, "Greening of the internet," presented at the Proceedings of the 2003 conference on Applications, technologies, architectures, and protocols for computer communications, Karlsruhe, Germany, 2003.
  - [41] S. Zhou, J. Gong, Z. Yang, Z. Niu, and P. Yang, "Green mobile access network with dynamic base station energy saving," in *ACM MobiCom*, 2009, pp. 10-12.
  - [42] G. Narlikar, S. Bhaumik, S. Chattopadhyay, and S. Kanugovi, "Green, energy-efficient network re-organization," *Alcatel-Lucent India*, 2011.
  - [43] Z. Kun and L. Husheng, "Achieving Energy Efficiency via Drowsy Transmission in Cognitive Radio," in *Global Telecommunications Conference (GLOBECOM 2010), 2010 IEEE*, 2010, pp. 1-6.
  - [44] M. Masonta, Y. Haddad, L. De Nardis, A. Kliks, and O. Holland, "Energy efficiency in future wireless networks: Cognitive radio

- 
- standardization requirements," in *Computer Aided Modeling and Design of Communication Links and Networks (CAMAD), 2012 IEEE 17th International Workshop on*, 2012, pp. 31-35.
- [45] K. Akkaya and M. Younis, "A survey on routing protocols for wireless sensor networks," *Ad Hoc Networks*, vol. 3, pp. 325-349, May 2005 2005.
- [46] S. E. Elayoubi, L. Saker, and T. Chahed, "Optimal control for base station sleep mode in energy efficient radio access networks," in *INFOCOM, 2011 Proceedings IEEE*, 2011, pp. 106-110.
- [47] A. A. Hammad, G. H. Badawy, T. D. Todd, A. A. Sayegh, and Z. Dongmei, "Traffic Scheduling for Energy Sustainable Vehicular Infrastructure," in *Global Telecommunications Conference (GLOBECOM 2010), 2010 IEEE*, 2010, pp. 1-6.
- [48] N. Tuan-Duc, V.-N. Quoc-Bao, V. Minh-Thanh, and M. Linh, "Energy efficient cooperative communication techniques for Intelligent Transport System," in *Advanced Technologies for Communications (ATC), 2011 International Conference on*, 2011, pp. 76-80.
- [49] F. Zou, J. Zhong, W. Wu, D.-Z. Du, and J. Lee, "Energy-efficient roadside unit scheduling for maintaining connectivity in vehicle ad-hoc network," presented at the Proceedings of the 5th International Conference on Ubiquitous Information Management and Communication, Seoul, Korea, 2011.
- [50] J. Toutouh and E. Alba, "An efficient routing protocol for green communications in vehicular ad-hoc networks," presented at the Proceedings of the 13th annual conference companion on Genetic and evolutionary computation, Dublin, Ireland, 2011.
- [51] J. Toutouh and E. Alba, "Green OLSR in VANETs with differential evolution," presented at the Proceedings of the fourteenth international conference on Genetic and evolutionary computation conference companion, Philadelphia, Pennsylvania, USA, 2012.
- [52] J. Toutouh, S. Nesmachnow, and E. Alba, "Evolutionary power-aware routing in VANETs using Monte-Carlo simulation," in *High Performance Computing and Simulation (HPCS), 2012 International Conference on*, 2012, pp. 119-125.
- [53] F. Wei and J. M. H. Elmirghani, "Green ICT: Energy Efficiency in a Motorway Model," in *Next Generation Mobile Applications, Services and Technologies, 2009. NGMAST '09. Third International Conference on*, 2009, pp. 389-394.
- [54] Z. Hasan, H. Boostanimehr, and V. K. Bhargava, "Green Cellular Networks: A Survey, Some Research Issues and Challenges," *Communications Surveys & Tutorials, IEEE*, vol. 13, pp. 524-540, 2011.
- [55] L. Chiaraviglio, D. Ciullo, G. Koutitas, M. Meo, and L. Tassiulas, "Energy-efficient planning and management of cellular networks," in *Wireless On-demand Network Systems and Services (WONS), 2012 9th Annual Conference on*, 2012, pp. 159-166.
- [56] W. Wei-Te, Y. Ya-Ju, and P. Ai-Chun, "Decentralized energy-efficient base station operation for green cellular networks," in *Global Communications Conference (GLOBECOM), 2012 IEEE*, 2012, pp. 5194-5200.

- 
- [57] R. Baines. *Femtocells - Reducing Power Consumption in Mobile Networks*. Available: [http://low-powerdesign.com/article\\_baines\\_092811.htm](http://low-powerdesign.com/article_baines_092811.htm).
  - [58] O. Arnold, F. Richter, G. Fettweis, and O. Blume, "Power consumption modeling of different base station types in heterogeneous cellular networks," in *Future Network and Mobile Summit, 2010*, 2010, pp. 1-8.
  - [59] T. D. Todd, A. A. Sayegh, M. N. Smadi, and Z. Dongmei, "The need for access point power saving in solar powered WLAN mesh networks," *Network, IEEE*, vol. 22, pp. 4-10, 2008.
  - [60] W. Li-Chun and S. Rangapillai, "A survey on green 5G cellular networks," in *Signal Processing and Communications (SPCOM), 2012 International Conference on*, 2012, pp. 1-5.
  - [61] P. Hu, R. Karki, and R. Billinton, "Reliability evaluation of generating systems containing wind power and energy storage," *Generation, Transmission & Distribution, IET*, vol. 3, pp. 783-791, 2009.
  - [62] J. R. Centre. Solar Irradiation and GIS [Online].
  - [63] R. Billinton and Bagen, "A sequential simulation method for the generating capacity adequacy evaluation of small stand-alone wind energy conversion systems," in *Electrical and Computer Engineering, 2002. IEEE CCECE 2002. Canadian Conference on*, 2002, pp. 72-77 vol.1.
  - [64] L. Ming-Shun, C. Chung-Liang, L. Wei-jen, and W. Li, "Combining the Wind Power Generation System With Energy Storage Equipment," *Industry Applications, IEEE Transactions on*, vol. 45, pp. 2109-2115, 2009.
  - [65] M. Shaaban and M. Usman, "Risk Assessment of Wind Generation Dispatch Using Monte Carlo Simulation," *International Journal of Smart Grid and Clean Energy*, vol. 2, pp. 258-263, May 2013 2013.
  - [66] D. G. Robinson, D. J. Arent, and L. Johnson, "Impact of Distributed Energy Resources on the Reliability of Critical Telecommunications Facilities," in *Telecommunications Energy Conference, 2006. INTELEC '06. 28th Annual International*, 2006, pp. 1-7.
  - [67] A. Keane, M. Milligan, C. J. Dent, B. Hasche, C. D'Annunzio, K. Dragoon, et al., "Capacity Value of Wind Power," *Power Systems, IEEE Transactions on*, vol. 26, pp. 564-572, 2011.
  - [68] P. S. Georgilakis and Y. A. Katsigiannis, "Reliability and economic evaluation of small autonomous power systems containing only renewable energy sources," *Renewable Energy*, vol. 34, pp. 65-70, 1// 2009.
  - [69] A. Jain, R. Balasubramanian, and S. C. Tripathy, "Reliability analysis of wind embedded power generation system for Indian Scenario," *International Journal of Engineering, Science and Technology*, vol. 3, pp. 93-99, 2011.
  - [70] M. Krasich, "How to estimate and use MTTF/MTBF would the real MTBF please stand up?," in *Reliability and Maintainability Symposium, 2009. RAMS 2009. Annual*, 2009, pp. 353-359.
  - [71] C. Oggerino, *High Availability Network Fundamentals*: Cisco Press, 2001.
  - [72] M. Fiore, J. Harri, F. Filali, and C. Bonnet, "Understanding Vehicular Mobility in Network Simulation," in *Mobile Adhoc and Sensor*

- 
- Systems, 2007. MASS 2007. IEEE International Conference on, 2007*, pp. 1-6.
- [73] A. Ghazy and T. Ozkul, "Design and simulation of an artificially intelligent VANET for solving traffic congestion," in *Mechatronics and its Applications, 2009. ISMA '09. 6th International Symposium on*, 2009, pp. 1-6.
- [74] J. Harri, F. Filali, and C. Bonnet, "Mobility models for vehicular ad hoc networks: a survey and taxonomy," *Communications Surveys & Tutorials, IEEE*, vol. 11, pp. 19-41, 2009.
- [75] M. Fiore, J. Harri, F. Filali, and C. Bonnet, "Vehicular Mobility Simulation for VANETs," in *Simulation Symposium, 2007. ANSS '07. 40th Annual*, 2007, pp. 301-309.
- [76] C. Sommer and F. Dressler, "Progressing toward realistic mobility models in VANET simulations," *Communications Magazine, IEEE*, vol. 46, pp. 132-137, 2008.
- [77] H. Wu, "Analysis and design of vehicular networks," Ph.D. Thesis, Georgia Institute of Technology, Georgia, USA, 2005.
- [78] M. Rudack, M. Meincke, and M. Lott, "On the dynamics of ad-hoc networks for intervehicle communications," *International Conference on Wireless Networks (ICWN'02)*, 2002.
- [79] W. Leutzbach, *Introduction to the Theory of Traffic Flow*. Berlin: Springer, 1988.
- [80] A. D. May, *Traffic Flow Fundamentals*: Prentic-Hall Inc, 1990.
- [81] D. L. Gerlough, "Traffic flow theory: a monograph," *Transportation Research Board, Washington* 1975.
- [82] B. R. Qazi, H. Alshaer, and J. M. H. Elmirghani, "Analysis and Design of a MAC Protocol and Vehicular Traffic Simulator for Multimedia Communication on Motorways," *Vehicular Technology, IEEE Transactions on*, vol. 59, pp. 734-741, 2010.
- [83] Z. W., Y. Chen, Y. Yang, X. Wang, Y. Zhang, X. Hong, et al., "Multi-Hop Connectivity Probability in Infrastructure-Based Vehicular Networks," *Selected Areas in Communications, IEEE Journal on*, vol. 30, pp. 740-747, 2012.
- [84] B. R. Qazi, H. Alshaer, and J. M. H. Elmirghani, "Development of a Motorway Simulator for Vehicular Multimedia Communications," in *Vehicular Technology Conference, 2008. VTC 2008-Fall. IEEE 68th*, 2008, pp. 1-5.
- [85] L. M. Feeney and M. Nilsson, "Investigating the energy consumption of a wireless network interface in an ad hoc networking environment," in *INFOCOM 2001. Twentieth Annual Joint Conference of the IEEE Computer and Communications Societies. Proceedings. IEEE*, 2001, pp. 1548-1557 vol.3.
- [86] HP, "A-802.11a/b/g Access Point Series," ed.
- [87] S. T. S. Chia, "1.7 GHz propagation measurements for highway microcells," *Electronics Letters*, vol. 26, pp. 1279-1280, 1990.
- [88] B. J. Singh, K. K. Aggarwal, and S. Kumar, "Characterization of the Propagation Environment by Field Measurements," *Institution of Engineers India Part Et Electronics and Telecommunications Engineering Division*, vol. 88, pp. 22-25, 2007.
- [89] L. Cheng, B. E. Henty, B. Fan, F, and D. D. Stancil, "Highway and rural propagation channel modeling for vehicle-to-vehicle

- 
- communications at 5.9 GHz," in *Antennas and Propagation Society International Symposium, 2008. AP-S 2008. IEEE*, 2008, pp. 1-4.
- [90] S. Dickey, D. J., H. C. L., and S. R., "ITS band roadside to vehicle communications in a highway setting," *California Department of Transportation University of California Berkeley Institute of Transportation Studies Partners for Advanced Transit Highways*, 2010.
- [91] C. Han, M. Dianati, R. Tafazolli, and R. Kernchen, "Throughput Analysis of the IEEE 802.11p Enhanced Distributed Channel Access Function in Vehicular Environment," presented at the Vehicular Technology Conference, 2010.
- [92] W. R. Heinzelman, A. Chandrakasan, and H. Balakrishnan, "Energy-efficient communication protocol for wireless microsensor networks," in *System Sciences, 2000. Proceedings of the 33rd Annual Hawaii International Conference on*, 2000, p. 10 pp. vol.2.
- [93] C. Fraleigh, S. Moon, B. Lyles, C. Cotton, M. Khan, D. Moll, et al., "Packet-level traffic measurements from the Sprint IP backbone," *Network, IEEE*, vol. 17, pp. 6-16, 2003.
- [94] I. P802.11p/D7.0, "Draft for wireless access in vehicular environments (WAVE)," ed.
- [95] Kapsch, "Smarter Vehicles, Safer Roads MCNU R1551," K. T. Inc, Ed., ed, 2008.
- [96] J. M. Smith, "Optimal design and performance modelling of M/G/1/K queueing systems," *Mathematical and Computer Modelling*, vol. 39, pp. 1049-1081, 2004.
- [97] F. R. B. Cruz, A. R. Duarte, and W. T. V., "Buffer allocation in general single-server queueing networks," *Computers and Operations Research*, vol. 35, pp. 3581-3598, November 2008 2008.
- [98] CurveExpert, ed, 2013.
- [99] S. K. Bose, *An Introduction to Queueing Systems*: Kluwer Academic/Plenum Publishers, 2002.
- [100] W. Kumar, A. Muhtar, B. R. Qazi, and J. M. H. Elmirghani, "Energy and QoS Evaluation for a V2R Network," in *Global Telecommunications Conference (GLOBECOM 2011), 2011 IEEE*, 2011, pp. 1-5.
- [101] G. M. Masters, *Renewable and Efficient Electric Power Systems*: Wiley-Interscience Inc, 2004.
- [102] UK Air Information Resource [Online]. Available: <http://uk-air.defra.gov.uk/>
- [103] S. G. Soriga, "ITS-G5 and Mobile Wimax Perfomance in Vehicle-To-Infracstructure Communications," *U.P.B. Sci. Bull*, vol. 74, pp. 143-156, 2012.
- [104] A. Networks, "Aruba AP-85FX and AP-85LX Access Points," ed.
- [105] P. Action. (August 2012). *Wind Electricity Generation*. Available: [http://practicalaction.org/docs/technical\\_information\\_service/wind\\_electricity\\_generation.pdf](http://practicalaction.org/docs/technical_information_service/wind_electricity_generation.pdf)
- [106] C. Honsberg and S. Bowden, "PVCDROM," ed, 2012.
- [107] N. H. Fuengwarodsakul, "Retrofitting a used car with hybrid electric propulsion system," in *Electrical Engineering/Electronics, Computer, Telecommunications and Information Technology, 2009. ECTI-CON 2009. 6th International Conference on*, 2009, pp. 114-117.

- 
- [108] S. A. Akdağ and A. Dinler, "A new method to estimate Weibull parameters for wind energy applications," *Energy Conversion and Management*, vol. 50, pp. 1761-1766, 7// 2009.
  - [109] S. A. Ahmed and H. O. Mahammed, "A Statistical Analysis of Wind Power Density Based on the Weibull and Ralyeigh models of "Penjwen Region" Sulaimani/ Iraq," *Jordan Journal of Mechanical and Industrial Engineering*, vol. 6, pp. 135-140, April 2012 2012.
  - [110] "Wren Micro-Turbine," in *Online*, S. G. T. Ltd, Ed., ed, 2007.
  - [111] "Approved Draft Recommended Practice for Sizing Lead-Acid Batteries for Stand-Alone Photovoltaic (PV) Systems," *IEEE Approved Std P1013/D10, Oct 2006*, 2007.
  - [112] K. Ayyappan and P. Danajayan, "Propagation Model For Highway In Mobile Communication System," *Ubiquitous Computing and Communication Journal*, vol. 3.
  - [113] M. Takai, J. Martin, and R. Bagrodia, "Effects of wireless physical layer modeling in mobile ad hoc networks," presented at the Proceedings of the 2nd ACM international symposium on Mobile ad hoc networking & computing, Long Beach, CA, USA, 2001.
  - [114] C. Tai-Po and S. Rappaport Stephen, "Generalized fixed channel assignment in microcellular communication systems," *Vehicular Technology, IEEE Transactions on*, vol. 43, pp. 713-721, 1994.
  - [115] M. K. Simon and M. S. Alouini, "Digital Communications Over Fading Channels (M.K. Simon and M.S. Alouini; 2005) [Book Review]," *Information Theory, IEEE Transactions on*, vol. 54, pp. 3369-3370, 2008.
  - [116] A. Goldsmith, *Wireless Communications*: Cambridge University Press, 2005.
  - [117] R. Prasad, A. Kegel, and O. L. van Linden, "Performance evaluation of microcellular systems with shadowed Rician/Rayleigh faded multiple co-channel interferers," in *Vehicular Technology Conference, 1992, IEEE 42nd*, 1992, pp. 427-430 vol.1.

---

# **Appendix A**

## **A.1 Modelling the Physical Layer**

The received signal strength or the measurement of power present in the received radio signal is a key deciding factor in enabling a reception and maintaining signal quality at the receiver, coupled typically with the noise and interference levels. The received signal is however affected by several qualities of the physical layer. It is therefore important to consider radio propagation when designing communication networks because the physical layer dictates signal coverage, and the achievable data rates. For this reason the study of the physical layer has led to various propagation models that enable an accurate characterisation of the radio channels in order to obtain realistic design assumptions for communication networks. Propagation models can be address two main characteristics of the channel: Path loss and fading [112, 113].

### **8.3.1.1. PATH LOSS**

The first study of path loss aims to predict signal strength between the transmitter and receiver based on the separation distance. Path loss is an average loss of power by the signal as it propagates through the channel. This model in effect determines the coverage area of the transmitter. It is mainly affected by the distance between the transmitter and receiver, and

objects that obstruct the signal along the path and antenna heights at the transmitter and receiver [112].

### 8.3.1.2. FADING

The second set of propagation models characterise the rapid fluctuations in received signals that result in fading. Fading occurs due to node and/or objects in the channel mobility which causes the signal to traverse different paths when going from the transmitter to the receiver with the vector summation of the multipath signals leading to space-time nulls. Another type of fading occurs when obstacles affect the wave propagation causing shadow fading [113].

### 8.3.1.3. SIGNAL-TO-INTERFERENCE RATIO (SIR)

Noise and interference from adjacent base stations must also be considered. A signal-to-interference ratio (SIR) is therefore used to quantify the signal quality. Mobile units receive interference from all base stations in the vicinity which use the same channel [114]. This SIR is one of the main factors that influence channel availability and allocation when considering a cluster or array of base stations in a cellular network.

## A.2 Propagation Model for V2R Communications

In a motorway environment, the mean received power at a distance  $d$ ,  $P_r(d)$  can be predicted using a deterministic propagation model. Furthermore, the fading and shadowing effects on the received signal can be combined and hence the received power can be expressed by a composite Gamma-log-normal distribution [115], given by

$$f_G(g) = \int_0^\infty \left(\frac{m}{z}\right) \frac{g^{m-1}}{\Gamma(m)} \exp\left(-\frac{m}{z}g\right) \times \frac{\xi}{z\sqrt{2\pi[\sigma_d]_{dB}}} \exp\left(-\frac{(10\log_{10} z - [\mu_z]_{dB})^2}{2[\sigma_d^2]_{dB}}\right) dz \quad (\text{A.1})$$

where  $\xi = 10/\ln 10$ ,  $[\mu_z]_{dB} = [P_r(d)]_{dB}$  is the mean of  $z$  in dB,  $[\sigma_d]_{dB}$  is the shadowing deviation of  $z_{dB}$ ,  $m = \frac{K^2+2K+1}{2K+1}$  is the distribution parameter and  $K$  is the Rician factor [115].

The composite Gamma-log-normal distribution can be approximated by a log-normal distribution with mean and standard deviation

$$[\mu_{l\_new}]_{dB} = [P_r(d)]_{dB} + \xi[\psi(m) - \ln(m)] \quad (\text{A.2})$$

$$[\sigma_{d\_new}]_{dB} = \sqrt{[\sigma_d^2]_{dB} + \xi^2 \zeta(2, m)} \quad (\text{A.3})$$

where  $\psi(m)$  is the Euler psi function and  $\zeta(\cdot, \cdot)$  is Riemaan's zeta function. Thus the outage probability can be expressed as

$$P_{out} = 1 - \left[ 0.5 \operatorname{erfc} \left( \frac{[P_{th}]_{dB} - [\mu_{l_{new}}]_{dB}}{\sqrt{2}[\sigma_{d_{new}}]_{dB}} \right) \right] \quad (\text{A.4})$$

where  $\operatorname{erfc}(\cdot)$  is the complementary error function and  $[P_{th}]_{dB}$  is the receiver threshold power in dB[116].

According to 802.11p [90], for centralised communication, the maximum allowed transmit power ( $P_t$ ) in service channel 174 is 33 dB<sub>m</sub> and in this work we have considered 30 dB<sub>m</sub> which is in line with the standard specification. In this appendix, BSs with antenna heights ( $h_b$ ) of 10 m with 3 dBi [86] gains and vehicle antenna heights ( $h_v$ ) of 1.5 m with 0 dBi gains are taken into account with an operating frequency of 5.9 GHz. A flat fading channel, which remains constant during a packet transmission, is assumed

during transmission. The probability of outage ( $P_{out}$ ) with different receiver threshold power ( $P_{th}$ ) setups (which accommodates different data rates) is shown in Figure A.1. Increasing the data rate, the outage increases, hence the communication range for an acceptable ( $P_{out}$ ) decreases. A  $P_{out} \leq 0.002$  can be achieved for all packets with a  $P_{th} = -90 dB_m$  (i.e.  $dr = 6 Mbps$ , which is typical in 802.11p standard) with a communication range of 800m [90].

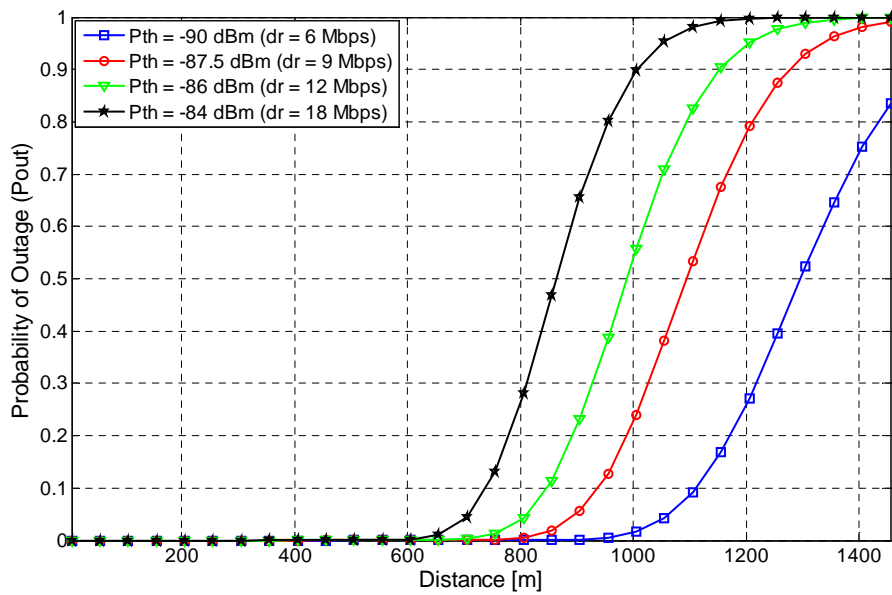


**Figure A.1: Probability of outage ( $P_{out}$ ) for V2R systems**

The break point distance ( $d_b$ ) can be calculated as

$$d_b = \frac{(4h_b h_v)}{\lambda} = 1200m. \quad (\text{A.5})$$

As  $d_b$  is greater than the maximum communication range (800m), it is reasonable to consider a single slope model with  $\nu = 3.4$  and  $[\sigma]_{dB} = 0.46dB$  [87] to calculate the mean received power. Since in a motorway environment the small scale fading is not severe as in urban areas, we have considered

$[K]_{dB} = 11dB$  (i.e.  $m \cong 7$ ) to model this type of fading hence  $[\sigma_{d\_new}]_{dB} = 1.76dB$ .

### A.3 Propagation Model For V2V Communications

For inter-vehicle communication (IVC) however, mostly a line-of sight signal is not present, hence the signal envelope follows a Rayleigh distribution [81] and the received power has an exponential distribution given by

$$f_P(p) = \begin{cases} \frac{1}{2\sigma_{rms}^2} \exp\left(-\frac{|p|}{2\sigma_{rms}^2}\right) & (p \geq 0) \\ 0 & (p < 0) \end{cases} \quad (\text{A.6})$$

where  $\sigma_{rms}$  is the root mean square value (rms) of the received signal amplitude, and  $\sigma^2$  is the time-averaged power of the received signal.

The mean received power can be predicted with deterministic propagation models, such as free space (FS), two-ray ground and path loss [81]. According to field measurements [88, 115, 117], the path loss model is more suitable to predict the mean received power in a motorway environment and is given by:

$$P_r(d) = P_r(d_{ref}) \left( \frac{d_{ref}}{d} \right)^{\nu} \quad (\text{A.7})$$

where  $P_r(d_{ref})$  is the reference power obtained with Friis (FS) formula and  $P_r(d)$  is the mean received power at a distance  $d$  [81]. The received signal has large-scale fading effects due to multiple reflections (shadowing). Hence, the received power can be described with log-normal pdf given by:

$$f_L(l, \mu, \sigma_d) = \begin{cases} \frac{1}{l\sqrt{2\pi\sigma_d}} \exp\left(-\frac{(\ln l - \mu)^2}{2\sigma_d^2}\right) & (l \geq 0) \\ 0 & (l < 0) \end{cases} \quad (\text{A.8})$$

where  $\mu = P_r(d)$  and  $\sigma_d$  is the shadowing deviation [81]. The combined path loss and shadowed model is:

$$[P_r(d)]_{dB} = [P_r(d_{ref})]_{dB} + 10\nu \log\left(\frac{d_{ref}}{d}\right) + X \quad (\text{A.9})$$

where  $X$  is a Gaussian random variable with 0 mean and  $\sigma_d$  standard deviation (in dB) [81]. The power received with equation (A.9) is used as average power in equations (A.6) for V2V communication systems. Hence, for motorway vehicular networks, a combined attenuation, shadowing and fading model is used. To determine the receiver power threshold, we have performed Matlab simulations based on the above model. We have considered  $P_t = 20$  dBm and practical values of antenna gains from [89]. The practical measurements from [88] are utilised to model radio wave propagation characteristics.

The break point,  $(d_b)$ , is 177 m for IVC with antenna height of 1.5 m and gain of 17.5 dB for each vehicle.. From [88] a two slope model (with  $\nu_1 = 2$ ,  $\nu_2 = 3.4$  ,  $\sigma_1 = 2.5$  dB and  $\sigma_2 = 0.9$  dB ) is considered to characterise propagation for V2V communication.

Simulating the received power for a centralised and V2V communication respectively, with (i) attenuation, (ii) attenuation and shadowing, and (iii) attenuation, shadowing and fading, the effects of shadowing were determined to be not severe for V2R communication due to the very limited multiple reflections in this environment.